

X-Ray and Vibrational Spectroscopy of Sulfate in Earth Materials

Satish C. B. Myneni

*Department of Geosciences
Princeton University
Princeton, New Jersey 08544
and*

*Earth Sciences Division
Ernest Orlando Lawrence Berkeley National Laboratory
Berkeley, California 94720*

INTRODUCTION

Sulfate is one of the most abundant inorganic ligands in the lithosphere and hydrosphere. It plays a major role in mediating mineral dissolution and precipitation, crystal growth, mineral–water and air–water interfacial reactions, aerosol chemistry and global climate, and biogeochemical cycling of several elements including inorganic and organic toxic contaminants. For several years, macroscopic methods and thermodynamic models have been used in understanding and predicting the geochemistry of sulfate in a variety of systems. As shown by several recent studies, molecular chemistry of chemical species cannot be identified by the macroscopic methods alone (Sposito 1990, Brown et al. 1999). Although researchers have been using different spectroscopic methods (especially infrared spectroscopy, IR) for examining sulfate molecular chemistry, sulfate in geologic materials has not been probed as extensively as some of the other oxoanions, such as chromate, selenate and arsenate. Details of different spectroscopic methods and their applications in geochemical studies are discussed by Hawthorne (1988).

The molecular properties of sulfate, such as coordination environment (types of connecting atoms, their number and bond distances), electronic state, and symmetry, dictate how sulfate reacts in a geochemical system. Several electronic states exist in a molecule, with each electronic state containing several vibrational states, and each vibrational state containing several rotational states (Fig. 1). The energies and probabilities of transitions between different electronic, vibrational, or rotational states can be measured and used in the identification of molecules and their chemical states. However, transitions among all of these states in a molecule are not feasible and the molecule symmetry determines whether a particular transition is allowed or forbidden (Cotton 1971). A variety of electron, X-ray, and optical spectroscopic methods can be used in studying the core (innermost) and valence (outermost) electronic transitions, and infrared and Raman spectroscopic methods can be used to obtain information on the vibrational transitions. All of these methods provide complementary information on the structural environment of sulfate. Information on sulfate coordination can also be obtained indirectly using the sulfate-complexed ion or molecules that are sensitive to light in the visible region, such as Fe^{3+} in iron sulfates (Rossman 1975, Huang et al. 2000). Rotational modes and their applications to studying sulfates are not discussed, as they have not been used in probing sulfates in geological materials.

In many cases, samples must be modified or placed in an environment different from their original conditions to enable exploration of sulfate molecular behavior using certain spectroscopic methods. As discussed later, information from such ex-situ methods may not represent the true coordination environment of sulfate. Hence, researchers should be

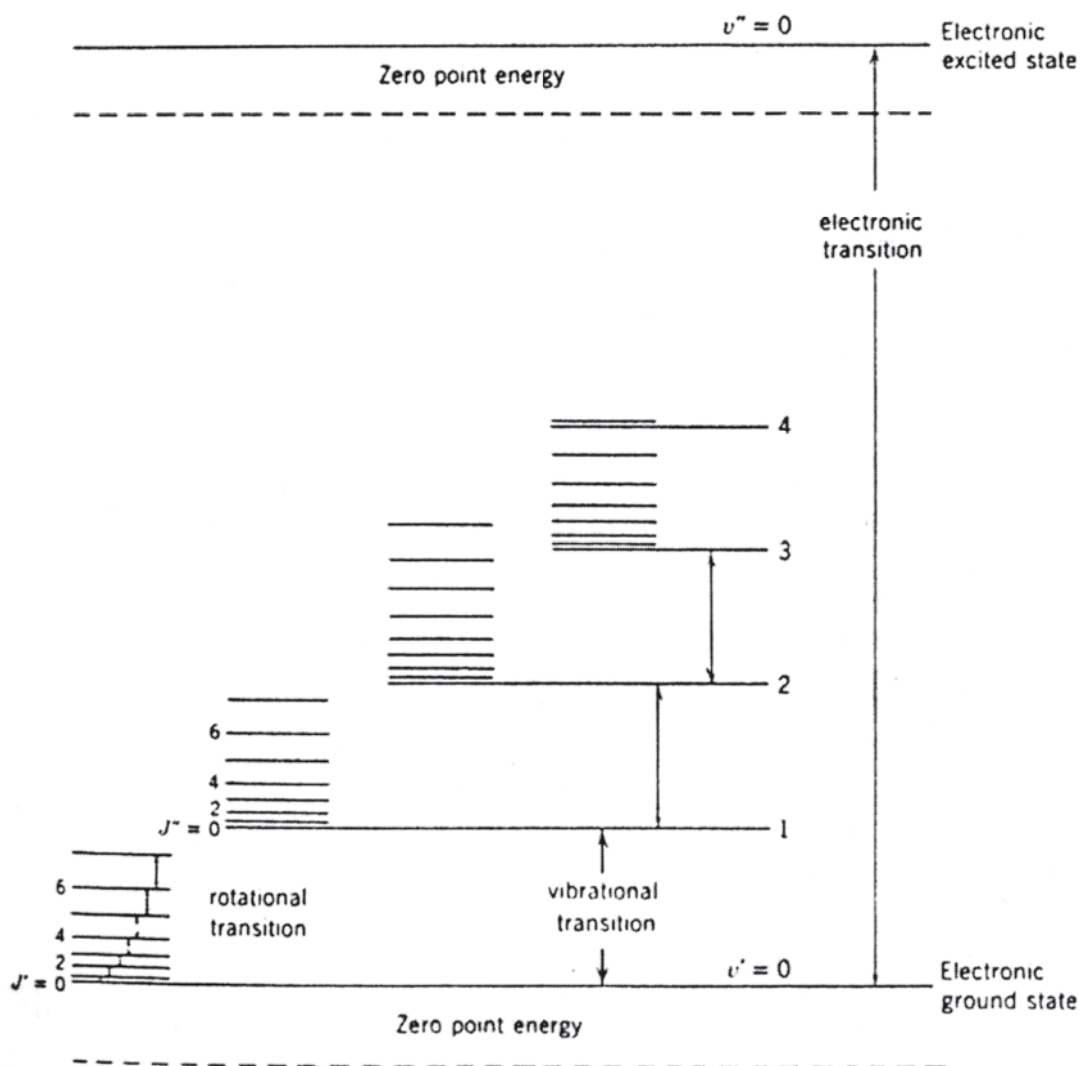


Figure 1. Energy levels of a diatomic molecule (modified from Nakamoto 1984). The letters 'J' and 'v' represent rotational and vibrational quantum numbers, respectively, and the superscripts i, ii, ... represent different energy levels. The energy differences between the adjacent rotational intervals increases as J increases, and the energy differences between vibrational intervals decreases as v increases. The vibrational fine structure is also evident in the electronic spectra of several diatomic molecules.

cautious in choosing the appropriate set of spectroscopic methods for their investigation. In addition, several complementary techniques must be used to obtain complete information on the coordination environment of sulfate in heterogeneous matrices.

This chapter is focused primarily on X-ray absorption and vibrational spectroscopic methods, as these methods are widely used in exploring the chemistry of sulfate in geological materials. These methods can also be used to obtain *in situ* information on geological samples in their native state. Structural identification of crystalline sulfate minerals using X-ray diffraction is discussed by Hawthorne et al. (Chapter 1, this volume), and hence this method is not considered here, except for its applications in studying liquids. Also provided here is information on other spectroscopic methods that can be used to probe sulfate minerals directly, yielding information complementary to the above techniques.

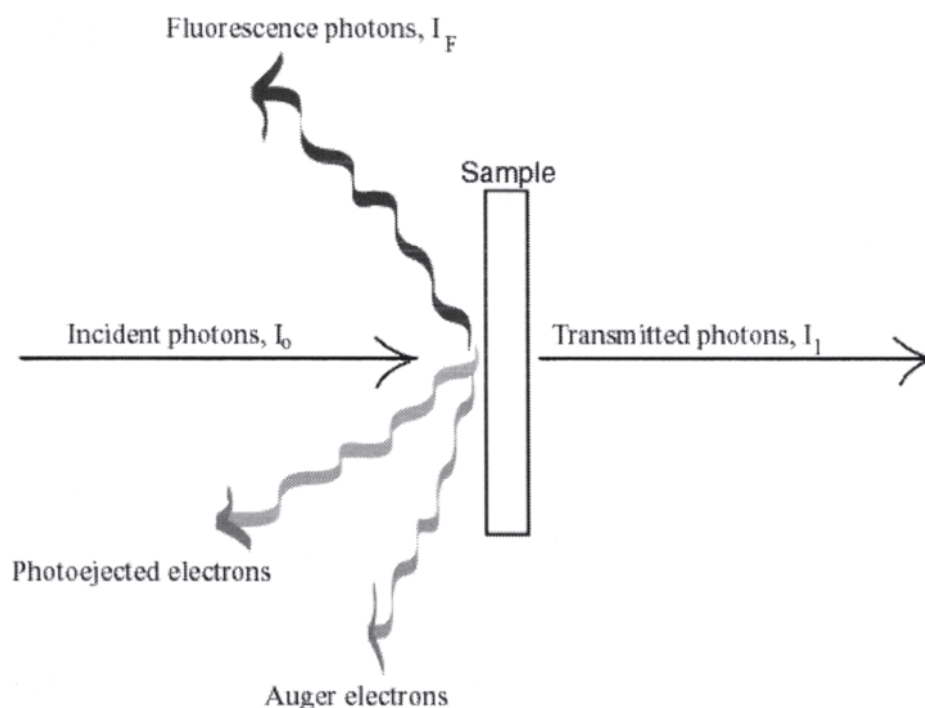


Figure 2. X-ray interactions with sample. X-ray spectra of sample are collected by placing ion chambers or detectors at different locations around the sample to detect X-ray photons or electrons (modified after Brown et al. 1988). For example, the ratio of I_F to I_0 gives the X-ray absorption spectrum in fluorescence detection mode. The samples must be placed in vacuum to examine the photo-ejected or Auger electrons.

X-RAY SPECTROSCOPY

The chemical behavior of molecules is determined by their electronic structure. Information on the energy levels and symmetries of the occupied and unoccupied molecular orbitals, where electrons reside in a molecule, is critical for predicting the molecular chemistry. A combination of X-Ray spectroscopic techniques can offer this unique information about molecules present in a variety of structural environments. These techniques are based on detecting: (1) absorption of X-rays by samples (X-ray absorption spectroscopy), (2) emitted fluorescence photons from samples (X-ray emission spectroscopy), and (3) ejected photoelectrons from the core or valence levels of X-ray-absorbing atoms in samples (X-ray photoelectron spectroscopy) (Fig. 2). These X-ray methods can be used for studying all electronic states or the electronic transitions of sulfate by selecting suitable energy. All of the above mentioned methods can be used for studying samples under *in situ* conditions, but photoelectron spectroscopy is applicable to samples in high vacuum (recent developments allow measurements under a few torrs of pressure, as is discussed later). Because of different selection rules for different electronic transitions and processes, these methods offer complementary information on the molecular orbital structure of sulfate. In addition, different depth and spatial sensitivities can be achieved in samples by using suitable sample geometry, and by choosing the right photon energy and X-ray spectroscopic method. Detailed discussions of these methods and their applications to geological systems (italicized citations) are available in the following reviews:

X-ray absorption spectroscopy Stern 1974, Lytle et al. 1982, Teo 1986, Konings-berger and Prins 1988, Hawthorne 1988, Stöhr 1992, Schulze et al. 1999, Brown et al. 1999.

X-ray photoelectron spectroscopy: Baker and Betteridge 1972, Briggs 1977, Briggs and Seah 1983, Hawthorne 1988, Hochella 1988, Hochella and White 1990, Perry 1990, Brown et al. 1999.

A brief introduction to these methods and a review of their application to studies on sulfate geochemistry are presented in this chapter. The primary focus is on X-ray absorption spectroscopy because it has been used extensively for studying minerals. To the author's knowledge, there are no published reports on the molecular chemistry of sulfate in geological samples using X-ray emission or Auger electrons, and hence these are not discussed. However, studies of dilute heterogeneous geological samples in ambient conditions are feasible now using these methods and high-brightness synchrotron X-ray sources.

X-ray absorption spectroscopy (XAS)

The XAS technique has been used widely in the past 15 years to examine the oxidation state and coordination environment of a variety of geochemical species in minerals and at their surfaces, and in soils and aqueous solutions at dilute concentrations. This technique is element-specific and, with some exceptions, has low interference from the sample matrix. Samples can be examined under a wide range of conditions (temperature, pressure, and water content) using this technique. The detection limits are on the order of $<10^{-6}$ μM concentration, especially for heavy elements. Interested readers are referred to Waychunas and Brown (1984), Waychunas (1986), Calas and Manceau (1986), Brown et al. (1988), Brown (1990), Schulze et al. (1999), and Brown et al. (1999) and articles cited therein for details on XAS studies of geological samples.

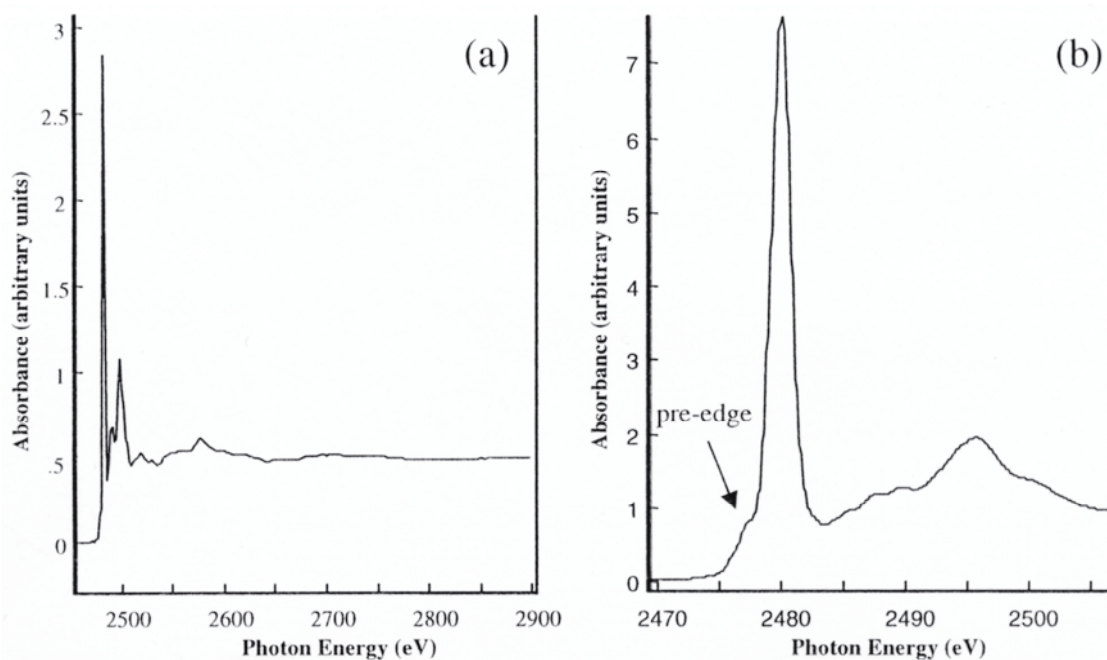


Figure 3. X-ray absorption spectrum of sulfate: (a) EXAFS spectrum of S in alunite; (b) XANES spectrum of S in ferric sulfate (Myneni, unpublished data). The pre-edge region of the XANES spectrum that represents transitions from $1s \rightarrow 3p$ orbitals (hybridized with metal $3d$ orbitals) are shown in (b).

Photo interactions with matter: XANES & EXAFS spectroscopy When high-energy X-rays are absorbed by a molecule, the innermost electrons from the $1s$, $2s$, $2p$, etc. orbitals of the X-ray-absorbing atom (absorber) are ejected into unoccupied molecular orbitals and continuum state of a molecule (Figs. 3, 4). Such transitions occur

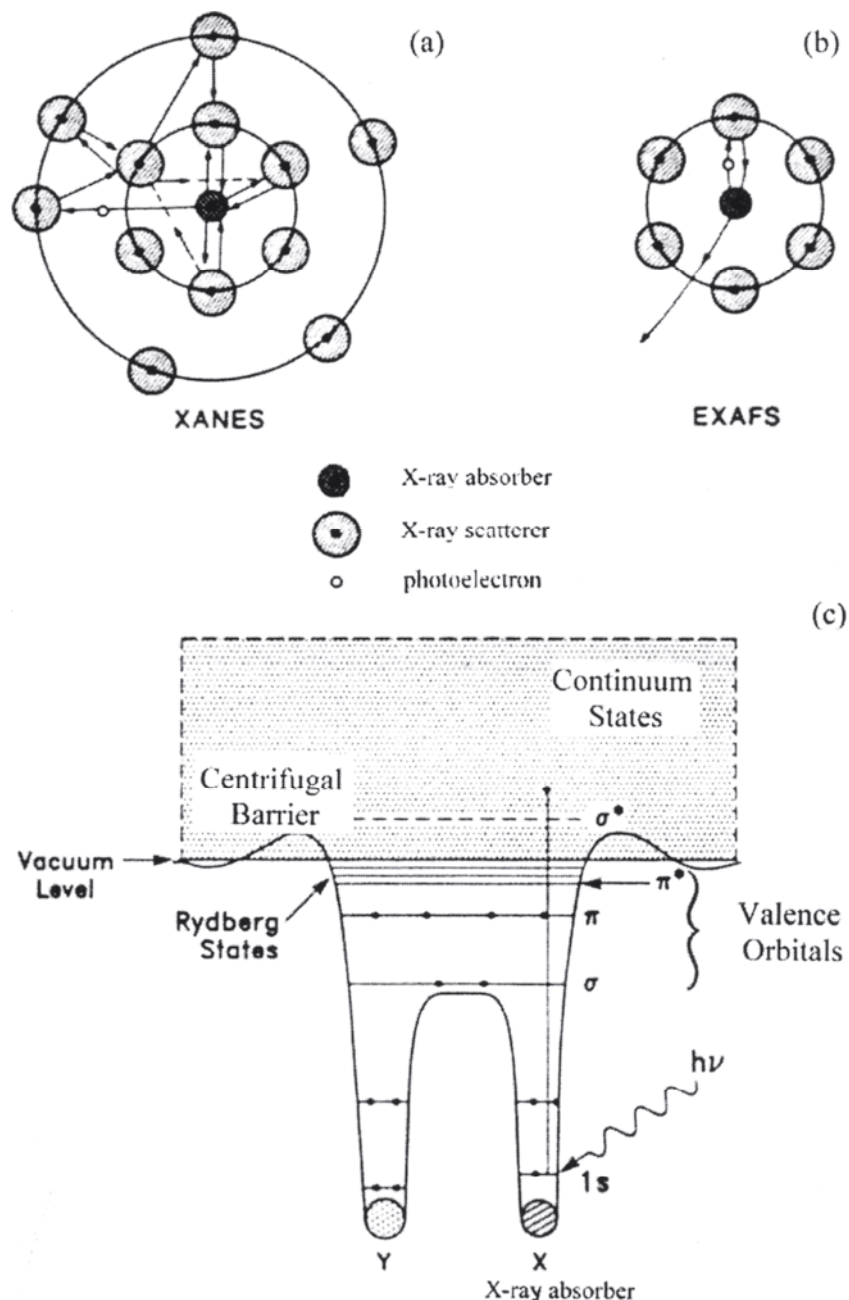


Figure 4. The XANES and EXAFS regions of XAS spectra are explained by multiple and single scattering of photoelectrons by the neighboring atoms of the absorber, respectively (a, b; modified after Brown et al. 1988). The XANES spectrum can also be explained by the electronic transitions from the core hole to the unoccupied or partly filled orbitals. For example the electronic transitions in a diatomic molecule, such as CO is shown in 'c'. The symbols, σ and π , and σ^* and π^* , represent the occupied and unoccupied molecular orbitals, respectively (modified from Stöhr 1992).

with the highest probability when the energy of incident X-ray photons is equal to the binding energy of core electrons of the absorber. In an X-ray absorption spectrum (absorption plotted as a function of incident X-ray energy), such transitions produce a sharp peak, which is commonly referred to as the white line or absorption edge. However, the electronic transitions have low probabilities on either side of the absorption edge. Localized electronic transitions from the core hole to vacant or partly filled atomic

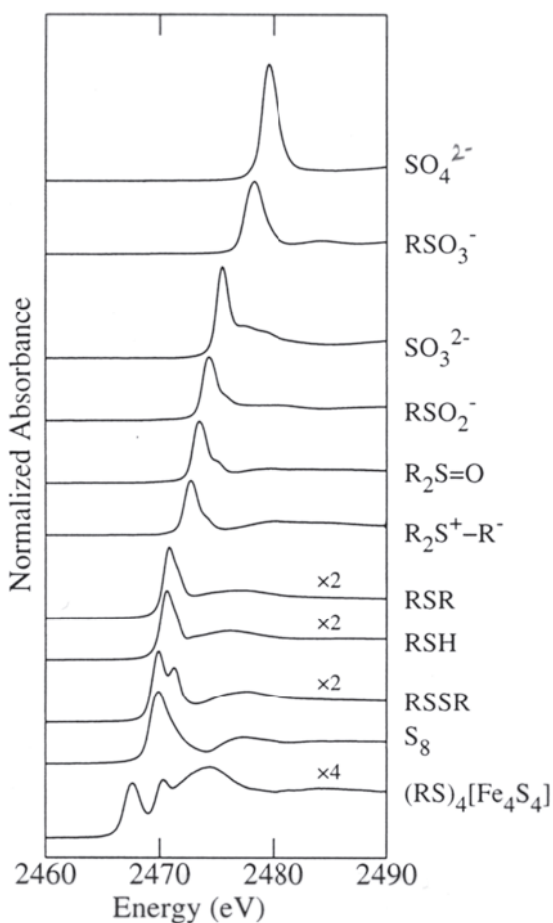


Figure 5. XANES spectra of different inorganic and organic sulfur compounds, and 'R' represents an organic molecule. Spectra of other relevant compounds are also shown in Figure 6. (modified from Pickering et al. 1998)

explain the XANES spectra, and are used by researchers to calculate the XANES spectra theoretically from the atomic coordinates. The EXAFS part of the spectrum has been traditionally explained using single and multiple scattering of the released photoelectron by neighboring atoms of the absorber (Sayers et al. 1970, Stern 1974, Sayers 1975, Lee and Pendry 1975, Stöhr 1984, Rehr et al. 1994, Natoli 1995, Rehr and Albers 2000). Currently, the scattering theories are used by researchers to analyze the EXAFS spectra theoretically.

The XANES and EXAFS spectra contain significant chemical information about the X-ray absorber (Teo 1986, Brown et al. 1988, Stöhr 1992). The XANES region can provide information on the oxidation state and coordination environment of the absorber. The energy of the absorption edge is dependent on the oxidation state of the absorber, which is manifested by the type of ligand or metal to which the absorber is bonded, and by the energy levels of the unoccupied molecular orbitals of the absorber. For instance, the absorption edge of 1s electrons (also referred to as the K absorption edge, as in K-, L, and M-electronic states in atoms) shifts to high-energy and its intensity increases with an increase in the oxidation state of the absorber (Figs. 5, 6). In addition, the intensity of the edge is affected by the absorber coordination environment and the extent of mixing of atomic orbitals and their symmetry in a molecule (e.g. *s-p* mixing, details discussed later;

and molecular orbitals can occur at energies lower than the absorption edge, thereby causing peaks in the absorption spectrum (referred to as the pre-edge; Brown et al. 1988). The spectroscopy that deals with near- and pre-edge part of X-ray absorption spectrum is referred to as X-ray absorption near-edge structure spectroscopy (XANES). Some researchers use 'NEXAFS' (near-edge X-ray absorption fine-structure spectroscopy) to refer to the same energy region of the X-ray absorption spectrum. As the incident photon energy is increased well above the absorption edge, the electronic transitions occur with lower probability and the released photoelectrons from the core hole interact with, and are scattered by, the atoms surrounding the absorber. This process produces oscillatory structure in the X-ray absorption spectrum, which is commonly referred to as the extended X-ray absorption fine structure (EXAFS) spectrum (typically includes features ~50eV above the absorption edge; Fig. 3).

The spectral features in the XANES region can be explained by the localized electronic transitions within the atom, and also by the multiple scattering of released photoelectrons by the atoms surrounding the absorber (Fig. 4). With certain differences, both of these theories can

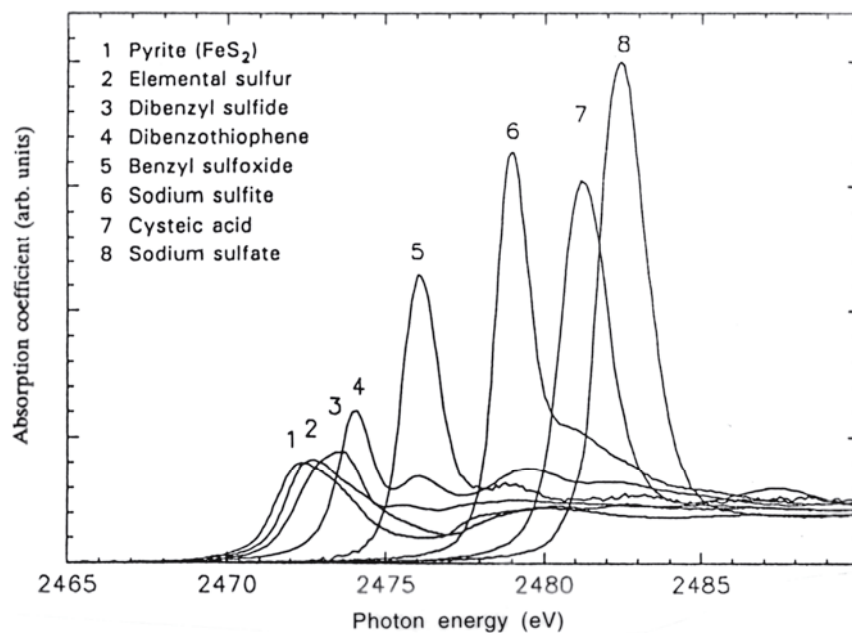
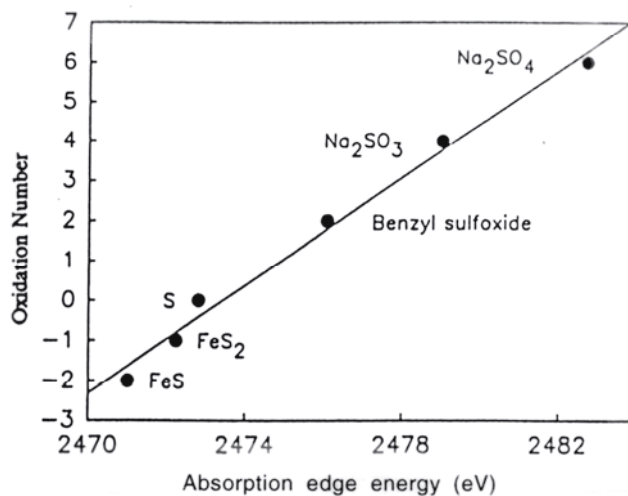


Figure 6. XANES spectra of sulfur compounds, showing the relationship between the spectral intensities and energies and the oxidation state of sulfur (modified from Vairavamurthy et al. 1994). The spectra shown here are complementary to those shown in Figure 5.



Teo 1986, Brown et al. 1988, Stöhr 1992). The EXAFS region is sensitive to absorber-backscatterer distances (frequency of oscillations increases with an increase in bond distance), the number of backscatterers (EXAFS amplitude increases with an increase in the number of backscatterers), and the atomic number of backscatterers (changes both amplitude and frequency). A detailed discussion of the L absorption edges is presented later in this chapter.

The XANES and EXAFS spectra of unknown samples can be analyzed by comparing their spectra with known spectra of structurally well-defined compounds, or by using either the single and multiple scattering theory or density functional theory (for the XANES region) for the hypothesized structures of molecules and clusters. Different computer programs have been developed for performing these theoretical calculations and interested readers are referred to special volumes published on X-ray spectroscopy (*Physica B*, 1995, v 208,209; *Journal de Physique IV*, 1997, v 7; and references therein). Experimental XAS studies can be conducted with laboratory X-ray sources, but it is difficult to obtain high photon flux and tunable monochromatic beams. Synchrotron X-ray sources permit spectral collection on a relatively short time and at high-energy resolution on extremely dilute samples. A list of synchrotron sources and their energy

limitations is provided in several review articles on synchrotron research (e.g. Brown et al. 1988). An update on some of these facilities in which X-ray spectroscopic studies of sulfur compounds have been conducted is provided in Table 1.

XAS at the sulfur K absorption edge The strong absorption of X-ray photons by air in the soft X-ray region (low-energy X-rays) makes XAS studies at the S absorption edge (2472 eV, Vaughan 1986) more complicated than collecting the heavy element absorption edges in the hard X-ray region (high-energy X-rays), which are routinely performed on geological samples. Low fluorescence yields of light elements in the soft X-ray region also limit the detection of S to the order of millimolar concentrations. For these reasons, EXAFS spectroscopic studies were not conducted at the S absorption edge on dilute samples, and most previous XAS studies of S were limited to the edge region and to samples in vacuum conditions. However, with the availability of high-flux and high-brightness beams at synchrotron X-ray sources (e.g. ALS, APS; Table 1) and multi-element solid-state detectors, EXAFS studies on dilute samples under ambient conditions are now possible. As well, several research groups have recently built experimental chambers for studying aqueous, wet, and biological samples by enclosing the X-ray beam path and sample compartment in He gas. Such experimental chambers are common at the SSRL and the ALS for routine XAS studies at the S absorption edge (Table 1, Fig. 7). Several reports are published on experimentation with XAS using hard X-rays. However, a short discussion on experimental facilities and spectral collection is presented here because XAS studies at the S-absorption edge are different from routine hard X-ray methods.

The X-ray absorption spectra are collected directly by monitoring the energy-dependent sample transmission and electron yield, or indirectly by examining changes in sample fluorescence (which is directly proportional to the sample absorbance for dilute samples). Of these, the electron-yield methods are more surface sensitive and are limited to sampling in vacuum conditions (Teo 1986, Brown et al. 1988, Stöhr 1992). Transmission methods are commonly used for concentrated samples, and the X-ray absorption spectra are collected by using ionization chambers behind the sample chamber (Fig. 7). The sample fluorescence can be monitored using ionization chambers, photodiodes, and energy-resolvable solid-state detectors. For examining dilute samples, the solid-state detectors are well-suited because the background sample fluorescence and scattered radiation can be eliminated by collecting the sample fluorescence only (provided that the detector has an energy resolution sufficient to separate fluorescence and scattered photons). The XAS data can also be collected by measuring the photoelectron-induced ionization of gas (e.g. He) present in the sample chamber (similar to electron yield), but this method is not as surface sensitive as are the direct electron yield methods. The surface sensitivity of flat samples can also be enhanced by examining the samples in grazing incidence mode (Brown et al. 1988).

Transmission XAS studies of S-containing samples can only be conducted on thin films because the X-rays can penetrate $<10 \mu\text{m}$ at 2472 eV. Although the fluorescence yield is small at the sulfur K absorption edge ($<10\%$), fluorescence detection is the most commonly used method for studying dilute samples (Vaughan 1986, Brown et al. 1988). With the help of currently available fluorescence detectors, such as the Lytle detector (Lytle et al. 1984) and photodiodes, researchers have successfully examined sulfur at concentrations of a few hundred micromolar at the SSRL, and at millimolar concentrations at the NSLS. Because the fluorescence detectors are placed on the same side of the sample as the incident photon beam (Fig. 7), the sample thickness need not be maintained precisely. However, fluorescence detection schemes pose problems for studying concentrated samples because of self-absorption of fluorescence photons by the

Table 1. Synchrotron X-ray sources optimized for conducting X-ray spectroscopy on S-bearing samples

<i>Country</i>	<i>Synchrotron Light Source</i>	<i>Comments</i>
France	European Synchrotron Radiation Facility (ESRF) & other facilities	X-ray spectromicroscopy beamline ID-21 is optimized for conducting XAS of small samples and for spectromicroscopy studies. LURE also has the capabilities, but the beamlines are not optimized for S-XAS studies. EXAFS SA32 beamline at the super-SCQ synchrotron (Qrsay) also has the capabilities to conduct S-XAS.
Germany	ANKA BESSY	ANKA-XAS is optimized for XANES studies. In addition some of the beamlines at HASY Lab (Hamburg), and SYL1 at the Physics Institute of Bonn University can be used with minor modifications to the existing facilities KMC-2 is optimized for vacuum studies.
India	INDUS1	Some of the beamlines can be used for conducting XAS of S; however, the beamline information is currently not available.
Japan	Photon Factory, Springate	X-ray spectroscopy studies at the S-absorption edge have been conducted at these facilities; but information on these beamlines is not available.
Sweden	MAX Lab	I-811 is under construction and this facility can be used for conducting S-XAS studies on dilute samples.
Taiwan	Synchrotron Radiation Research Center	BL15B is optimized for S studies, and other beamlines such as SL 3B can also be used for S-XAS studies.
United Kingdom		Stations 3.4 and 6.3 can be used for studies in vacuum. Perhaps some of the other high-flux soft X-ray beamlines can be optimized for S XAS studies.
USA	Advanced Light Source (ALS), Berkeley, CA Advanced Photon Source (APS), Chicago, IL National Synchrotron Light Source (NSLS), Brookhaven, NY Center for Advanced Microstructures & Devices (CAMD) Baton Rouge, LA	Currently BL 9.3.1 and 6.3.1 are optimized for conducting XAS in vacuum. SXEER and Klien's chamber are optimized for studying S in aqueous samples and at the interfaces under ambient conditions. Spectromicroscopy studies with a spatial resolution of 0.8 μm can be performed on wet samples at beamline 10.3.1. With the help of SXEER, L-edge spectroscopy studies can be conducted under ambient conditions on several high-flux beamlines such as 7.0.1 and 8.0.1, and the bend-magnet beamlines 6.3.2 and 9.3.2 (for concentrated samples). STXM endstation at the beamline 7.0.1 can be used for spectromicroscopy studies at the L-edges of S (spatial resolution 0.1 μm). S-XAS studies can be conducted at several beamlines, and these are in developmental stages. Spectromicroscopy studies can be performed on samples of size $<0.1 \mu\text{m}$ at some of these beamlines. Currently no beamline is optimized to conduct S L-edge spectroscopy studies. X-19A and X-11B are optimized for conducting in-situ studies of S compounds in aqueous solutions or at interfaces. Such studies can also be conducted at other intermediate-energy beamlines after small modifications. S L-edges can be examined at the STXM beamline (X-1A). Port 5B is optimized for conducting S-NEXAFS of concentrated samples

Table 1, continued

Stanford Synchrotron Light Source (SSRL), Stanford, CA	High flux wiggler beamline, 6-2 is optimized for conducting XANES of S at submillimolar concentrations, and EXAFS of concentrated samples. Beamline 2-3, and wiggler beamlines can be used to examine S compounds at millimolar concentrations under ambient conditions, and 3.3 in vacuum
Synchrotron Radiation Center (SRC), Madison, WI	Ports 122 and 023 are optimized for vacuum studies

There are also synchrotron light sources either in planning stages, in construction, or operational in Brazil, China, Korea, Russia, and Thailand, but no information is available. A third-generation source is being built in Canada (Canadian Light Source). Although the storage ring at Aarhus, Denmark (ASTRIO) is optimized for soft X-ray studies, it has no beamlines to go to energy as high as S absorption edges. The sulfur L-edge can be examined at several beamlines at the above facilities, however, only few of them can be used to examine aqueous samples.

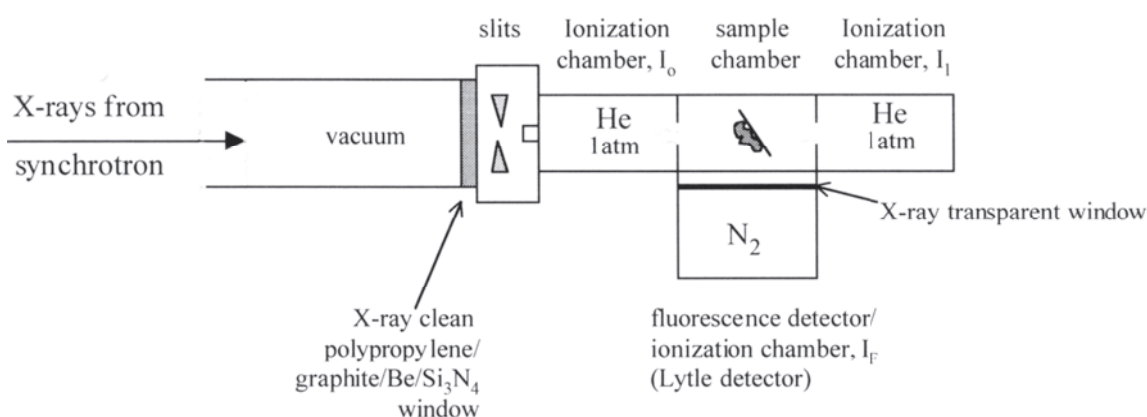


Figure 7. Schematic diagram showing the sample and the sample-detector geometry for collecting the XAS spectra of S under ambient conditions. Helium is used in the beam path and in the sample chamber to prevent photon absorption by air. Nitrogen is used in the ion chambers to capture the fluorescence or transmitted photons.

sample. Hence concentrated samples are diluted with KBr or BN, or thin sample smears are used to minimize these effects. Several research groups have also used theoretical calculations for correcting the experimental spectrum of these self-absorption effects (Waldo et al. 1991, Vairavamurthy et al. 1994). Although electron yield and transmission methods can be used for collecting XAS data of concentrated samples, these methods can be affected by charging, and saturation, respectively (Brown et al. 1988).

Spectral resolution. The intrinsic spectral resolution of the absorption edge of any element is primarily determined by the lifetime of its core hole electrons (width of the core hole), which is approximately 0.4 eV for sulfur (Brown and Doniach 1980). Spectral resolution is also determined by the type of monochromator crystal that is used and by the size of the photon source (e.g. slit openings, or the vertical divergence of the beam). Commonly, a Si(111) double crystal monochromator is used for conducting the XAS of sulfur at several synchrotron facilities. Using Si(111) monochromator crystals and proper source size, the best achieved spectrometer resolution is around 0.5 eV at the sulfur absorption edge. Although other monochromator crystals, such as Ge(111) and InSb(111) can also be used, Si(111) crystals offer better energy resolution. The source size can significantly improve the spectral resolution for collimated beams (Brown et al. 1988). Better spectral resolution can be achieved by reducing the slit openings in the

spectrometer, although this severely reduces the photon flux to the sample. At third-generation synchrotron facilities, better spectral resolution is achievable because of the small source size and high photon flux.

Data c~~l~~ectin. X-ray absorption spectra can be collected using one of the detection schemes and a set of monochromator crystals as described above. An XANES spectrum typically begun several tens of eV below the absorption edge and extends up to 100-150 eV above the edge (with a step size of a few eV). At the absorption edge, samples are scanned with an edge step of 0.1 eV or less (e.g. Rompel et al. 1998, Frank et al. 1999). Although the best achievable spectral resolution is about 0.5 eV, small changes in the energy of the absorption edge (commonly less than 0.5 eV in chemically similar compounds) and the appearance of shoulders on the absorption edge (e.g. associated with metal complexation) can be detected easily with a smaller step size. For collecting the EXAFS spectra, step sizes of 1-3 eV are sufficient and the spectra must be collected up to several hundred eV above the absorption edge. Samples with a high Cl content can pose problems for long EXAFS scans because of the absorption edge around 2840 eV for Cl. As well, the monochromator has to be detuned over 90% (from maximum incident energy) below the sulfur absorption edge to examine samples with high Fe concentrations. This is done to minimize the third-order component of the incident beam, which has the energies of the Fe absorption edge.

Sulfur XAS data are usually calibrated by comparing with the absorption edge of elemental sulfur (2472 eV). However, as different research groups have used different energies for the absorption edge of elemental sulfur, care must be exercised when spectral comparisons between different reports are made. For example, the absorption edge of sulfur in sodium sulfate is reported to have different energy positions in this chapter, and these are not inherent to samples and data-collection schemes. This difference is present because different calibrations have been used by various research groups, and it is necessary to look at the original articles for the energy calibrations. Researchers often use sulfur compounds that exhibit absorption features sharper than elemental sulfur (e.g. thiosulfate and sulfate) for routine spectrometer calibration during data collection.

XAS ~~o~~ f ~~s~~ulfur ~~co~~mpds. The majority of XAS studies conducted on sulfur have focused on a variety of organo-sulfur compounds because of their role in biological systems (proteins, enzymes, cells) and their common occurrence in coals and petroleum hydrocarbons, and as humic substances in soil and sediment organic matter (Spiro et al. 1984, Gorbaty et al. 1990, Waldo et al. 1991, George et al. 1991, Vairavamurthy 1998, Pickering et al. 1998, Sarret et al. 1999). Relatively little work has been done on the XAS of sulfate and sulfide minerals, except for the studies done by Bancroft, Vairavamurthy, Waychunas, Myneni, and their research groups. The difficulties associated with collecting XANES and EXAFS spectra at the sulfur absorption edge, and poor availability of synchrotron facilities optimized for sulfur studies, have also contributed to the small number of sulfur-XAS studies. However, this is expected to change in the near future as several new facilities optimized for sulfur-XAS are under construction.

The energies of maximum absorbance for sulfur in different oxidation states is separated by several eV, and hence the X-ray spectra of sulfates can be distinguished from other sulfur compounds (Spiro et al. 1984, Frank et al. 1987, George and Gorbaty 1989, Waldo et al. 1991, Huffman et al. 1991, 1995; Morra et al. 1997, Vairavamurthy 1998, Xia et al. 1998, Pickering et al. 1998) (Figs. 5, 6). Various studies have indicated that the absorption edge shifts to higher-energy with an increase in the formal oxidation state of sulfur (Figs. 5, 6). As well, the intensity of the absorption edge increases with an increase in the sulfur oxidation state (Fig. 6), because the number of vacancies in the sulfur valence orbitals (primarily sulfur 3p character) increases (Waldo et al. 1991,

Vairavamurthy 1998, Pickering et al. 1998). This effect is also commonly found in the X-ray absorption spectra of other elements (Brown et al. 1988). The EXAFS spectroscopic investigation of different forms of sulfate was started only recently, and results have not yet been published. However, some published information is available on the EXAFS of amorphous sulfides (Warburton et al. 1992, Hibble et al. 1999, and references therein).

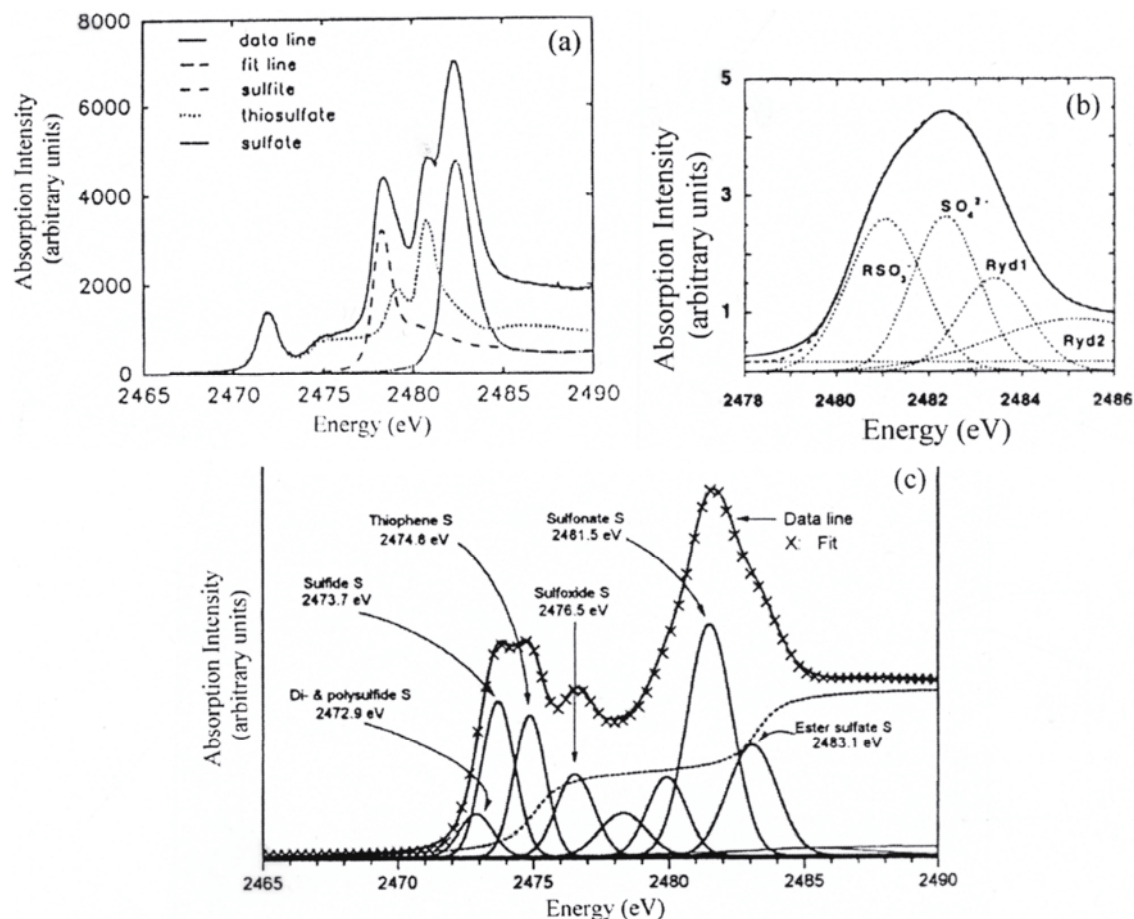


Figure 8. XANES spectral analysis of composite sample spectra containing a mixture of S compounds: (a) composite spectrum fit with a linear combination of sulfate, sulfite and thiosulfate spectra (modified from Vairavamurthy et al. 1994); (b) sulfur in blood cells of tunicate, *Ascidia ceratodes*, fit with a combination of several Gaussian profiles (modified from Frank et al. 1994); and (c) sulfur in humic substances fit with several Gaussian profiles after the spectral component of core hole to continuum transitions is subtracted from the XAS spectrum using an arc tangent function (modified from Vairavamurthy 1998).

Spral analysis. In samples containing more than one form of sulfur, the XANES spectra can be used to distinguish and to estimate the proportion of each form. Discrimination is possible because sulfur compounds in different oxidation states are separated by several eV, and significant spectral differences exist between compounds of similar form (Figs. 6, 8). Several different techniques are used to fit the XAS data of mixtures of sulfur compounds. Reviews of fitting procedures are provided by Hawthorne and Waychunas (1988), Waldo et al. (1991), George et al. (1991), Vairavamurthy et al. (1994), Frank et al. (1994), and Vairavamurthy (1998). One of the common methods is to fit the compound spectrum with a linear combination of individual component spectra of

different models. All of the model and sample spectra are normalized for their spectral intensities several eV above the absorption edge before they are fit with different components (Waldo et al. 1991, George et al. 1991, Vairavamurthy et al. 1994, Frank et al. 1994, Rompel et al. 1998) (Fig. 8). In another approach, the spectral contributions of the core hole excitations into the continuum are subtracted using an arctangent function (Fig. 8), and the remaining peaks ($1s \rightarrow 3p$) of the composite spectrum are fit with a mixture of Gaussian and Lorentzian peaks representing different forms of sulfur (Huffman et al. 1991, Vairavamurthy 1998, Xia et al. 1998). These methods are summarized by Vairavamurthy et al. (1994), and the problems with the fitting routines are discussed in detail by Hawthorne and Waychunas (1988) and by George and Steele (1995). Principal component analyses can be used to obtain information on the number and the probable type of components in the compound spectrum, and details are reported in several recent papers (George and Steele 1995, Wasserman et al. 1999, Ressler et al. 2000). All of these methods are useful for deconvoluting the compound spectrum of an unknown sample, provided that the sample consists of a mechanical mixture of pure compounds. This is a very important caveat in the XANES analysis.

Several researchers have used XAS as a fingerprinting technique to identify the presence of the different sulfur compounds in complex matrices, and other researchers, as mentioned above, have used a series of simple structural models to quantify the fractions of the different forms of sulfur. Although quantification is not absolute, XAS has provided important *in situ* information on the ratio of oxidized and reduced forms of sulfur in coals and humic substances of different origin, which no other non-destructive sampling method has been able to provide. However, quantification of different sulfur forms should be approached with caution because recent studies have shown that changes in protonation and coordination of the sulfur functional groups can cause significant changes in the sulfur spectrum (Frank et al. 1999, Myneni and Martinez, 1999, Myneni et al. 2000b). Hence a small list of structural models may not be sufficient for the accurate determination of a mixture of compounds and their concentrations in complex unknown samples (which may not be simple mechanical mixtures).

Several steps are involved in EXAFS analysis, and these include (in sequence): (1) subtraction of background from the sample X-ray absorption spectrum, (2) fitting a spline function to the X-ray absorption spectrum and extraction of EXAFS, (3) converting the energy of the EXAFS oscillations into the modulus of wave vector, k (\AA^{-1}) (4) computing the Fourier transform of EXAFS in distance-space, and fitting the Fourier transform or the EXAFS with the phase- and amplitude-functions derived theoretically or experimentally for different absorber-backscatterer pairs. Details of EXAFS analysis and its limitations are given by Teo (1986), Brown et al. (1988), and Rehr and Albers (2000).

XANES spectra of sulfate and tetrahedral transition. X-ray absorption spectra of sulfur-bearing salts were collected in the late 1960s and efforts were made to correlate the spectra with the electronic structure of sulfate and its bonding interactions (Nefedov and Formichev 1968). A comprehensive study of this kind was that of Sekiyama et al. (1986). The sulfate ion in tetrahedral (T_d) symmetry has primarily two unoccupied antibonding molecular orbitals: a_1^* of $3s$ character and t_2^* of $3p$ character. Sekiyama et al. (1986) have assigned the intense feature in the XANES spectrum of solid sodium sulfate to the $1s \rightarrow t_2^*$ orbitals (labeled as A in Fig. 9a lower part; spectral assignments in Table 2). The $1s \rightarrow a_1^*$ transitions are dipole-forbidden because of the s -character in a_1^* orbitals, and do not appear as intense features in the X-ray absorption spectrum. The high-energy features above the absorption edge (labeled as Band C in Fig. 9a, lower part) are assigned to the $1s \rightarrow$ unoccupied $3d$ -like e^* and t_2^* orbitals. Similar assignments were made for sulfate in

Table 2. Assignments of the absorption spectra of S K-edge of Na₂SO₄, Na₂SO₃, Na₂S₂O₃, and Na₂S₂O₅ (modified from Sekiyama et al. 1986). The alphabetical labels shown in the third column correspond to the spectral features marked in Figure 9.

<i>Mlele</i>	<i>Energy</i> (<i>e</i>)	<i>Labl</i>	<i>Transiti</i>
SO ₄ ²⁻	2479.9	A	S 1s → t ₂ *
	2488.7	B	d-type shape resonance
	2495.6	C	d-type shape resonance
SO ₄ ³⁻	2475.5	A	S 1s → e*
	2477.5	B	S 1s → a ₁ *
	2478.9	C	d-type shape resonance
	2487.6	D	d-type shape resonance
	2494.6	E	d-type shape resonance
S ₂ O ₃ ²⁻	2469.2	A	terminal S 1s → a ₁ * (terminal, central S 3pσ)
	2476.4	B	central S 1s → a ₁ * (terminal, central S 3pσ)
	2478.0	C	S 1s → e* (central, S 3pπ)
	2479.8	D	S 1s → a ₁ * (central S 3s and 3pπ)
	2483.2	E	d-type shape resonance
	2493.2	F	d-type shape resonance
S ₂ O ₅ ²⁻	2475.8	A	S 1s → 3p (-SO ₂)
	2480.2	B	S 1s → 3p (-SO ₃)
	2489.2	C	d-type shape resonance
	2495.9	D	d-type shape resonance

CuSO₄·5H₂O (Tyson et al. 1989). The t₂* orbitals are considered to be the bound-state orbitals because the energy for the 1s → t₂* transition is below the ionization potential. The high-energy broad feature is assigned to the 1s → continuum state transitions, as this feature is above the ionization potential. However, the transitions labeled at B and C in Fig. 9a (lower part) were not observed in the X-ray absorption spectrum of aqueous sulfate, but appear instead as one broad feature (discussed later in this chapter).

Changes in the symmetry of sulfate from T_d to C_{3v}, C_{2v}, or any other low-symmetry group associated with sulfate complexation, causes the splitting of the triply degenerate, unoccupied t₂* molecular orbitals into either a₁* and e*, or its degeneracy may be completely eliminated. The energy difference among these orbitals is modified primarily by the strength of bonding between sulfate and the complexing atoms (or the overlap of sulfate molecular orbitals with those of the complexing atom). Hence, information on the energy levels of molecular orbitals of sulfate and its complexes can be obtained directly from the XANES spectra. The X-ray absorption spectra of other structurally relevant sulfur compounds in different bonding environments are shown in Figure 9 and Table 2. The electronic transitions and spectral features of different oxoanions, such as SiO₄⁴⁻, PO₄³⁻, and ClO₄⁻, are expected to exhibit the same trends (Okude et al. 1999).

Theoretical studies to understand the molecular orbital structure of sulfates have not been conducted extensively when compared to other inorganic systems. The majority of the previous theoretical studies on sulfur have focused on organo-S compounds, such as

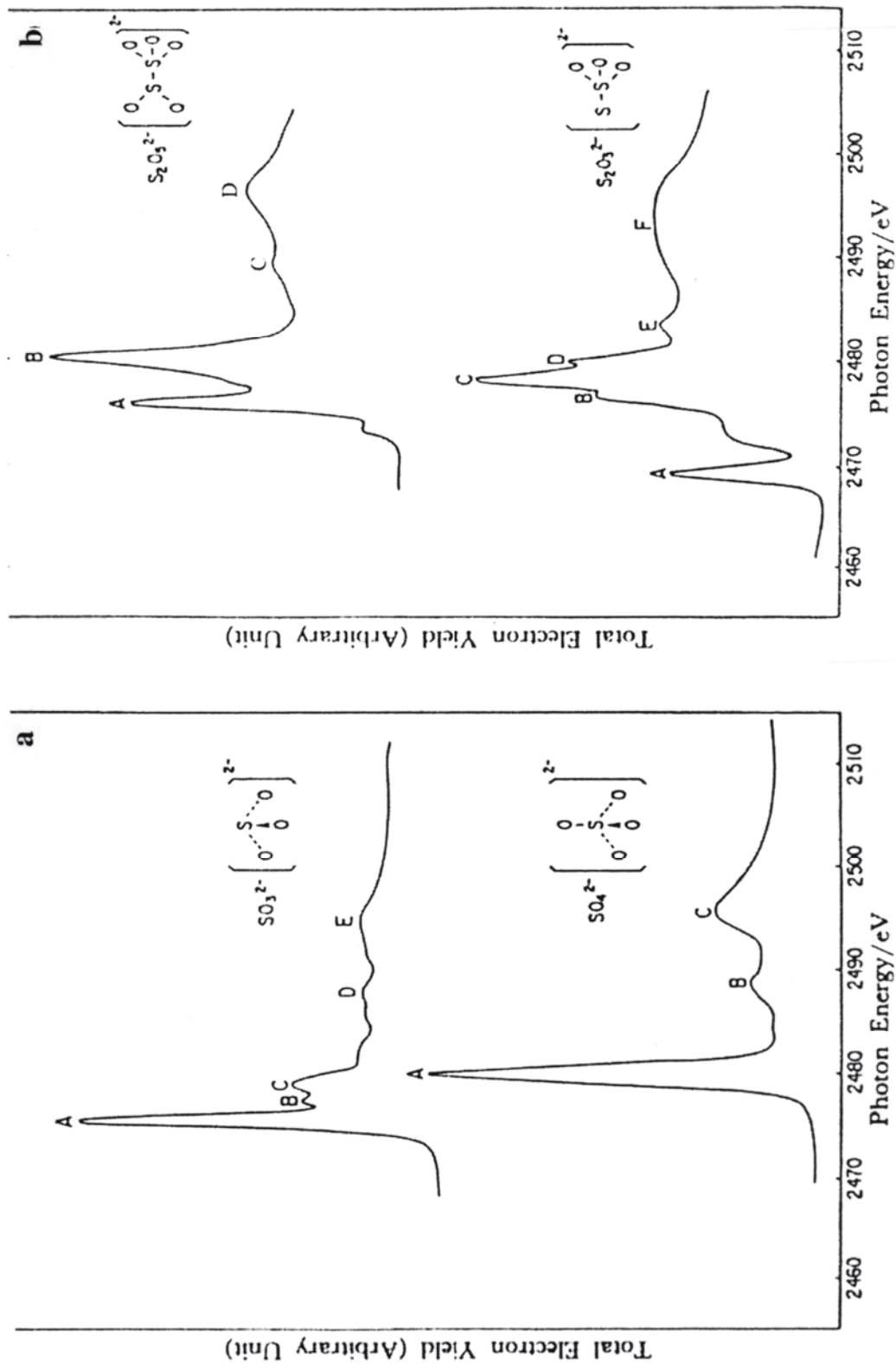


Figure 9. XANES spectra of sulfate and other closely related molecules (modified from Sekiyama et al. 1986). For spectral assignments, see Table 2.

cysteine and thiophene, using multiple scattering X-alpha (MS-X α), Hatree Fock static-exchange, and density functional theory (Hitchcock et al. 1986, Tyson et al. 1989, Mochizuke et al. 1999, Fernandez-Ramos et al. 2000). The theoretical MS-X α calculations of the XANES spectra of sulfate in different compounds reproduced the main absorption edge accurately, but not the other spectral features in the vicinity of the absorption edge (Tyson et al. 1989). Lindsay and Gibbs (1988, and references therein) examined the molecular orbital structures of different gas-phase sulfur-oxide molecules, including H₂SO₄, using the 6-31G** bases set. Their vibrational spectral calculations of these molecules were in excellent agreement with the experimental values. However, theoretical studies on solvated species are necessary to understand the influence of solvation on the molecular orbital structure of sulfates and their complexes, which can significantly help in the interpretation of the XANES spectra. Several research groups are currently working on these issues.

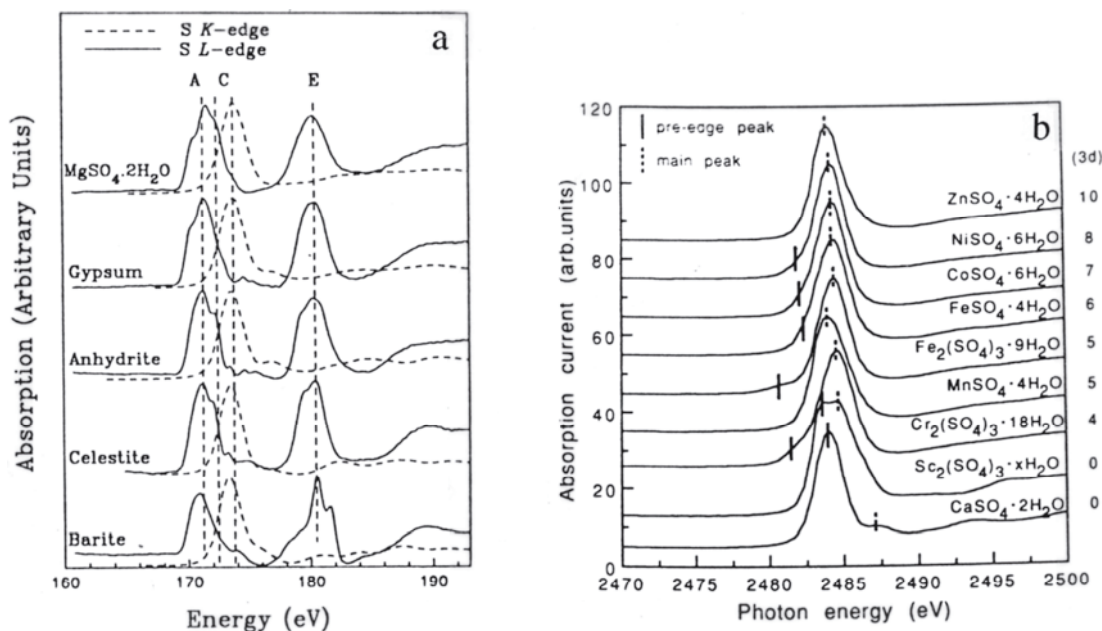


Figure 10. XANES spectra of alkaline earth and transition-metal sulfates: (a) alkaline earth sulfates. Both L-, and K-edge spectra are shown here. The assignments A, C, and E correspond to different L-edge transitions in sulfates (modified from Li et al. 1995); and (b) the pre-edge and absorption edge positions of different transition-metal sulfates (modified from Okude et al. 1999).

XAS sulfatein slids. XAS studies of sulfate minerals are not as common as those reported for sulfides. Detailed studies on the XANES spectra of alkaline-earth mineral sulfates (Li et al. 1995; Myneni, unpublished data), transition-metal sulfates including several ferric sulfate minerals (Li et al. 1995, Okude et al. 1999, Myneni et al. 2000b, Waychunas, unpublished data), and Al-sulfates (Myneni, unpublished data) were recently conducted using high-resolution spectrometers. Li et al. (1995) compared the K-, and L-edge XANES spectra of the sulfates of Mg (sanderite), Ca (gypsum, anhydrite), Sr (celestine) and Ba (barite), and observed that the K absorption edge is shifted to lower energy and the spectral features above the main absorption edge become more complex as the atomic number of the cation increases. These changes have been attributed to the stronger backscattering of the high-atomic-number elements beyond the first-shell coordination around sulfur (Fig. 10).

The XANES spectra of transition-metal sulfates indicate that the edge position, splitting in the absorption peak, and the energy of deconvoluted peaks are dependent on

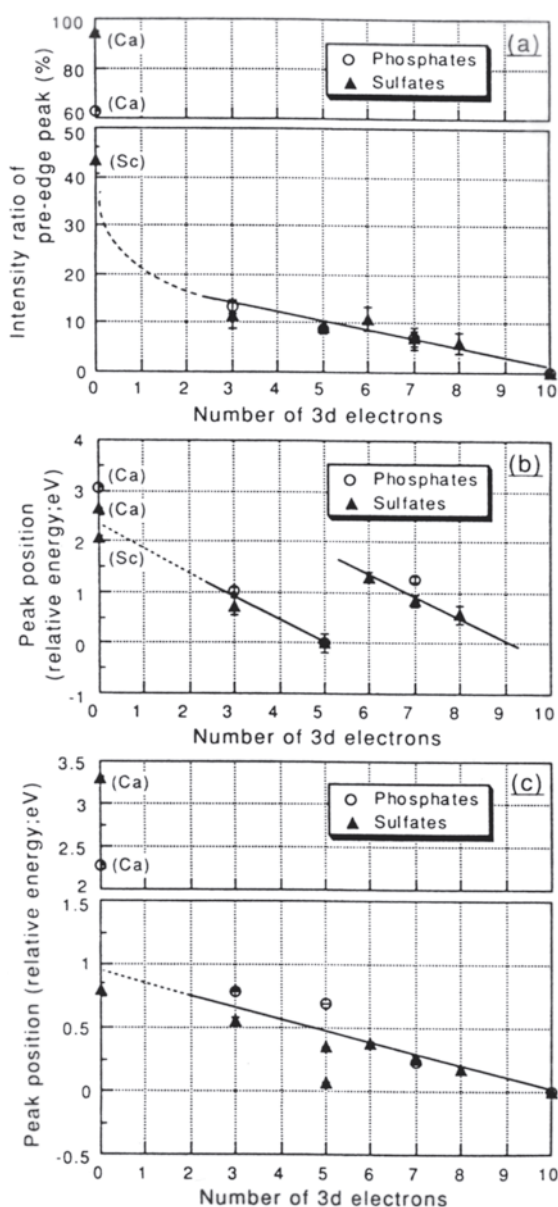


Figure 11. Correlations between spectral features of transition-metal sulfate and phosphates and the number of d electrons in the transition metal: (1) intensity ratio of the S pre-edge peak; (b) energy of pre-edge peak; and (c) energy of the absorption edge. (modified from Okude et al. 1999).

the number of d -electrons in the transition metal (Figs. 10-12). All of the transition-metal sulfates, with the exception of $\text{ZnSO}_4 \cdot 4\text{H}_2\text{O}$ (boyleite) show a pre-edge feature whose intensity decreases with an increase in the number of d -electrons (Fig. 10; Okude et al. 1999). The pre-edge peak overlaps the main absorption edge peak and does not appear as a distinct feature in spectra for some of the transition-metal sulfates (e.g. $\text{FeSO}_4 \cdot 7\text{H}_2\text{O}$, melanterite). An increase in the number of d electrons in the transition metal causes their pre-edge to shift to lower energies, with a gap between d^5 and d^6 metal sulfates (Figs. 11, 12). These results indicate that the pre-edge features in these spectra originate from the hybridization of metal $3d$ orbitals with sulfur $3p$ states (Shadle et al. 1995, Rose Williams et al. 1997, Okude et al. 1999). Mineral sulfides and transition-metal chloro salts also exhibit the same behavior (Shadle et al. 1995, Rose Williams et al. 1997, Wu et al. 1997).

Detailed XANES spectroscopic studies are in progress on the naturally occurring Fe-sulfate minerals common to acid mine drainage environments (Myneni and Alpers, unpublished data; Waychunas, unpublished data). These include minerals such as melanterite, jarosite, copiapite, coquimbite, römerite, rhomboclase, voltaite, and halotrichite, some of which are shown in Figure 12. The structure and chemical composition of these minerals are discussed by Hawthorne et al. (Chapter 1, this volume), and Jambor et al. (Chapter 6, this volume). These XANES studies of S in Fe-sulfates indicate that the spectra are sensitive to sulfate coordination to Fe polyhedra and the oxidation state of Fe.

There are primarily two effects associated with complexes of Fe: (1) shift in the absorption maximum to high-energy by about 0.5 eV, and (2) appearance of pre-edge features when compared to that of aqueous sulfate. These changes are noticed only where there is a direct linkage of sulfate group to the Fe polyhedra. The pre-edge feature in ferrous salts overlaps the sulfur absorption edge and appears as a low-energy shoulder (Figs. 11, 13). In addition, the pre-edge feature in Fe^{3+} sulfates is present at about 2 eV lower energy than that of the Fe^{2+} salt, halotrichite. Such shifts are also noticed in the K absorption spectra for Cl in Fe^{3+} - and Fe^{2+} -chloride and thiolate salts (Shadle et al. 1995, Rose Williams et al. 1997). Also, the pre-edge

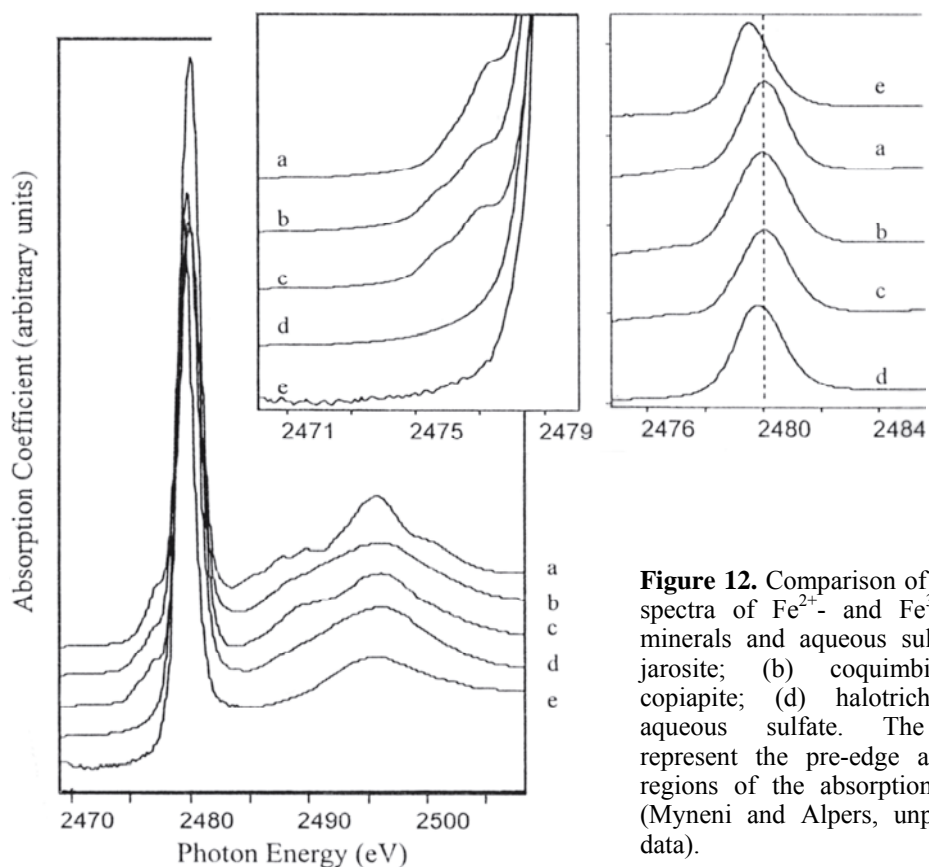


Figure 12. Comparison of XANES spectra of Fe^{2+} - and Fe^{3+} -sulfate minerals and aqueous sulfate: (a) jarosite; (b) coquimbite; (c) copiapite; (d) halotrichite; (e) aqueous sulfate. The insets represent the pre-edge and edge regions of the absorption spectra (Myneni and Alpers, unpublished data).

feature in Fe^{3+} salts has a doublet. The peaks in the doublet are separated by about 2.0 eV, with the highest energy feature 3.0 eV below the absorption maximum (Fig. 12). The energy of the pre-edge feature in Fe^{3+} -sulfate salts is also sensitive to the number of Fe polyhedra connected to each sulfate polyhedron. In coquimbite and copiapite, each sulfate group is connected to two Fe atoms, and in jarosite each sulfate is connected to three Fe atoms (Myneni et al. 2000b). Accordingly, coquimbite and copiapite exhibit pre-edge features at the same energy, approximately 0.5 eV below that of jarosite. However,



Figure 13. XANES spectra of sulfur in biogenic carbonates (modified from Pingitore et al. 1995). The spectral components just above the S absorption edge are shown.

these pre-edge features disappear when direct interactions between sulfate and the Fe^{3+} polyhedra are absent, or when H-bonds are present between Fe-coordinated water and sulfate, such as in ferric ammonium sulfate (Myneni et al. 2000b). Theoretical studies are necessary to understand the correlation between the changes in the energy levels of molecular orbitals and the change in the linkages in the Fe-sulfate polyhedra. In addition to these pre-edge features, electronic transitions to the continuum state, or the multiple scattering features 10-15 eV above the absorption edge, also vary with the sulfate coordination to cations (Fig. 12). Salts in which sulfate is not bound to any cations have smooth features (e.g. sulfate in aqueous solutions, ettringite, ferric ammonium alum) compared to those of the cation-complexed sulfates. Although Al sulfates, such as alunite, alunogen, basaluminite, and ettringite, follow the trends described above, these minerals do not exhibit any pre-edge features (Myneni unpublished data).

Using the XANES spectroscopy of S in modern and ancient corals, Pingitore et al. (1995) suggested that the form of sulfur in these samples is present almost exclusively as sulfate (Fig. 13). Spectral comparison of coral samples with those of Ca sulfates, such as anhydrite and gypsum, and sulfate in dolomite indicated that sulfate in biogenic carbonate samples is not present in the form of Ca sulfate minerals. Sulfate coordination is similar in all of the aragonite corals Pingitore et al. (1995) examined. Based on this information, they proposed that sulfate substitutes for carbonate in biogenic calcite, aragonite and dolomite and thus influences sulfate chemistry in oceans.

There are no published reports on the EXAFS spectroscopic studies of sulfate salts or sulfate minerals. Recently, EXAFS studies have been conducted to examine sulfate coordination in Fe^{3+} sulfates and Al hydroxy sulfates commonly found in acidic mine drainage environments, CaAl hydroxysulfates in cements, and sulfate complexes in aqueous solutions and at the mineral water interface (Waychunas, Myneni, unpublished data). Because several Al- and Fe hydroxysulfates are poorly crystalline (see Bigham and Nordstrom, this volume), EXAFS studies of sulfur in these materials are useful in understanding their structure and geochemistry.

XANES spectra of aqueous sulfates are reported by Vairavamurthy et al. (1994), Frank et al. (1994), and Myneni et al. (2000a); a detailed analysis of these spectra is presented by the last authors. Sulfate exists in T_d symmetry in aqueous solutions if the hydrated water is excluded from symmetry predictions (see later discussion on vibrational spectra). The XANES spectrum of aqueous SO_4^{2-} has a sharp absorption edge, corresponding to the $1s \rightarrow t_2^*$ transitions, and its energy is the same as that of solid Na- and K-sulfate salts (Figs. 12, 14). A broad feature 10 eV above the absorption edge in the XANES spectrum of SO_4^{2-} corresponds to continuum-state transitions. However, when SO_4^{2-} is complexed with protons or metals, the energy levels of molecular orbitals change and the degeneracy of orbitals is lost. Such changes in SO_4^{2-} coordination may significantly influence its XANES spectral features, and these are shown for sodium salts of SO_4^{2-} , HSO_4^- , COSO_3 (organo-sulfates), and $\text{S}_2\text{O}_8^{2-}$ (persulfate) in Figure 14. With the exception of sodium sulfate, the sulfate group in all other salts is bonded to a proton, carbon, or another oxygen, and accordingly the main absorption edge is split into two peaks. The amount of splitting varies with the type of atom connected to the sulfate group and it is highest in persulfate (Fig. 14).

Protonation of a sulfate polyhedron causes changes in the SO bond length, which increases from 1.473 Å in SO_4^{2-} (uncomplexed S–O) to 1.58 Å in HSO_4^- (SOH). The XANES spectrum of aqueous HSO_4^- ion (e.g. aqueous solutions of NaHSO_4) exhibits two overlapping features, which are separated by approximately 1.5 eV, with the peak maximum about 0.5 eV higher than that of aqueous sulfate (Frank et al. 1994, Myneni and Martinez, 1999). The shift to higher energy is caused by the splitting of triply

Figure 14. XANES spectra of sulfur in covalently bonded sulfate compounds. The sulfate spectrum shown at the top is that of sulfur in solid potassium sulfate. All other salts are Na salts (from Myneni and Martinez 1999).

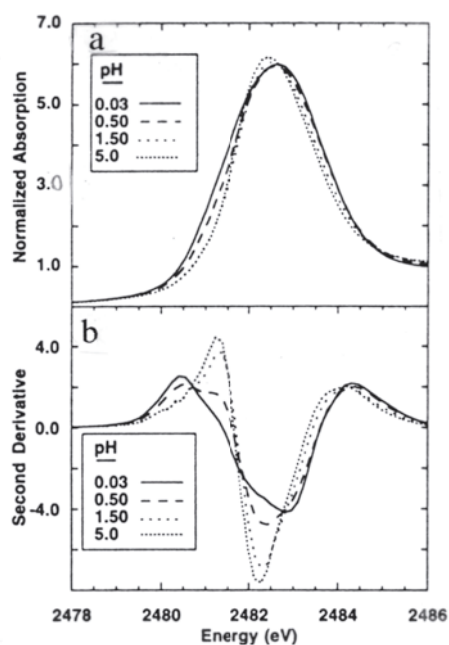
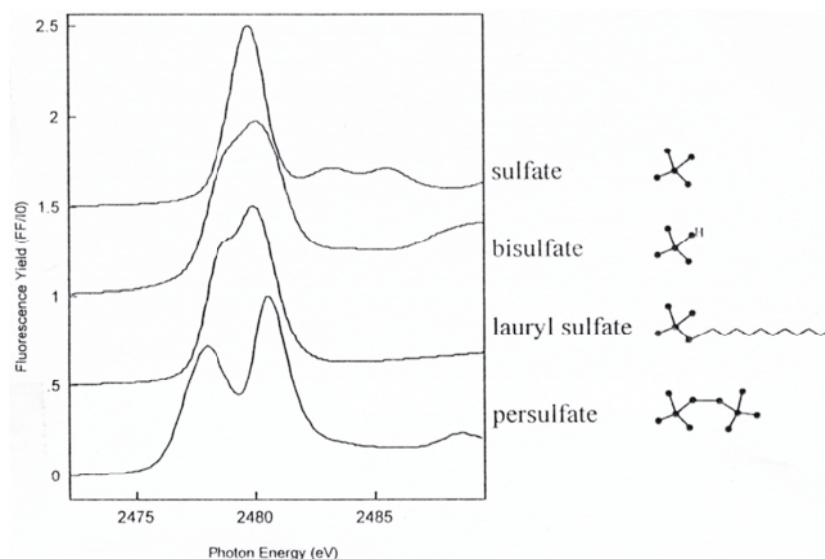


Figure 15. XANES spectra of sulfur in sulfate at different pH values: (a) raw XANES spectra; and (b) second derivative of spectra shown in (a) (modified from Frank et al. 1994).

degenerate t_2^* orbitals into a_2^* and e^* associated with the protonation of SO_4^{2-} (Figs. 14, 15). The two peaks of XANES spectrum correspond to electronic transitions to these two unoccupied states. It should be noted that these a_2^* orbitals have significant sulfur $3p$ character, and hence the $1s \rightarrow a_2^*$ transitions appear as an intense feature (in contrast to the $1s \rightarrow a_1^*$ transitions discussed above). The XANES spectra of organo-sulfates and metal-complexed sulfates are expected to show the same behavior and are discussed later in this chapter. Frank et al. (1994) titrated a solution of sulfuric acid to its second pK_a ($= -\log K_a \sim 1.0$, where K_a is the dissociation constant), and their results indicate that the XANES spectra are broader and the peak maximum shifts to higher energy by almost 0.5 eV as the protonation of sulfate increases in aqueous solutions (Fig. 15). The peak broadening is caused by the splitting of the absorption edge and the formation of HSO_4^- close to the second pK_a of sulfuric acid.

The spectroscopic studies of Frank et al (1994) on vanadium(III)-sulfate complexes in acid solutions showed that the absorption edge of aqueous sulfate becomes broader, with distinct low- and high-energy features (0.7 eV above the

peak maximum of aqueous SO_4^{2-}), as the concentration of vanadium(III) increases in aqueous sulfate solutions (1 M sulfate + dilute sulfuric acid, Fig. 16). Frank et al. (1994) assigned these spectral changes to the formation of a VSO_4^+ complex. Additions of Mn^{2+} and NH_4^+ ions to the same solutions (in the absence of vanadium) did not produce any changes in the XANES spectrum of SO_4^{2-} which indicate that the Mn^{2+} and NH_4^+ ions do not form inner-sphere complexes with SO_4^{2-} .

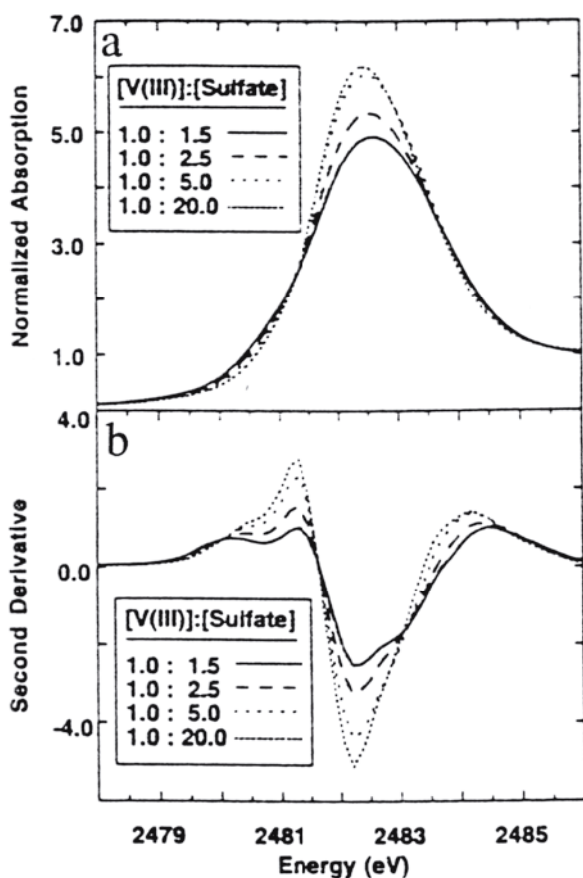


Figure 16. Sulfur XANES spectra of aqueous V(III)-sulfate solutions: (a) raw XANES spectra; (b): second derivative of spectra shown in (a) (modified from Frank et al. 1994).

spectroscopy are necessary to evaluate the Fe^{3+} complexes in dilute acidic sulfate solutions. When the pH of Fe^{3+} -containing solutions is increased, Fe oxides and sulfates precipitate from solution, and the nature of aqueous and colloidal Fe^{3+} -sulfate complexes can not be examined unambiguously above pH 4.0.

The above-mentioned studies indicate that the formation of aqueous sulfate complexes and their electronic structure can be studied directly using XAS spectroscopy. Such information on the electronic structure of sulfate, and its modifications associated with protonation and metal complexation, is useful for predicting the geochemistry of sulfate complexes and their redox reactions in aquatic systems.

XAS of organosulfates. Sulfate molecules bonded to C atoms in organic molecules, such as organo-sulfates and sulfate-esters, can exist at high concentrations in biological molecules and in the form of humus in soils and aquatic systems (Sposito 1989, Stevenson 1994). Organo-sulfates have been identified as one of the dominant functional groups in humic substances that were collected from different sources around the world (Morra et al. 1997, Vairavamurthy et al. 1997, Xia et al. 1998, Myneni and Martinez 1999). Because of the high aqueous solubility of organo-sulfates and their ability to form micelles, several of these compounds are used as cleaning agents in industrial and household applications. For these reasons, several organo-sulfates are commonly found in wastewater from industrial and residential areas. Organo-sulfur compounds, especially the oxidized forms of sulfur, play a major role in atmospheric chemistry and are also

Myneni et al. (2000a) examined sulfate complexation with Fe^{3+} ions in acid solutions. The X-ray absorption spectra of sulfur for mixtures of Na-sulfate and Fe^{3+} -chloride aqueous solutions (at different ratios and pH values) show a shift in the peak position of SO_4^{2-} to higher energy, and a small pre-edge feature appears when compared to that of aqueous sulfate. These features are similar to those reported earlier for Fe^{3+} -sulfate complexes in ferric sulfate salts discussed above (Myneni et al. 2000b). These studies indicate that Fe^{3+} forms complexes with sulfate in aqueous solutions, but do not distinguish monomeric- and polymeric- Fe^{3+} sulfate complexes (note that Fe^{3+} polymerizes in acidic solutions; Stumm and Morgan 1982, Masion et al. 1997, and references therein). Hence, the percentages of SO_4^{2-} bound to different Fe^{3+} forms and of free SO_4^{2-} in aqueous solutions are difficult to estimate from XAS studies alone. Although vibrational spectroscopic studies support the XAS observations, the question related to the percentage of free and complexed sulfate in aqueous solutions still remains (Hug 1997, Myneni et al. 2000b). Detailed XANES studies together with EXAFS

expected to represent a significant organic fraction in aerosol particles (Warneck 1988).

By using spectral deconvolution methods and the spectral features of structurally simple organo-sulfates, several organo-sulfates and sulfonates have been identified as the dominant oxidized forms of sulfur in soils and sediments (Figs. 8, 17). However, several of the previous studies were conducted at low resolution or failed to identify a low-

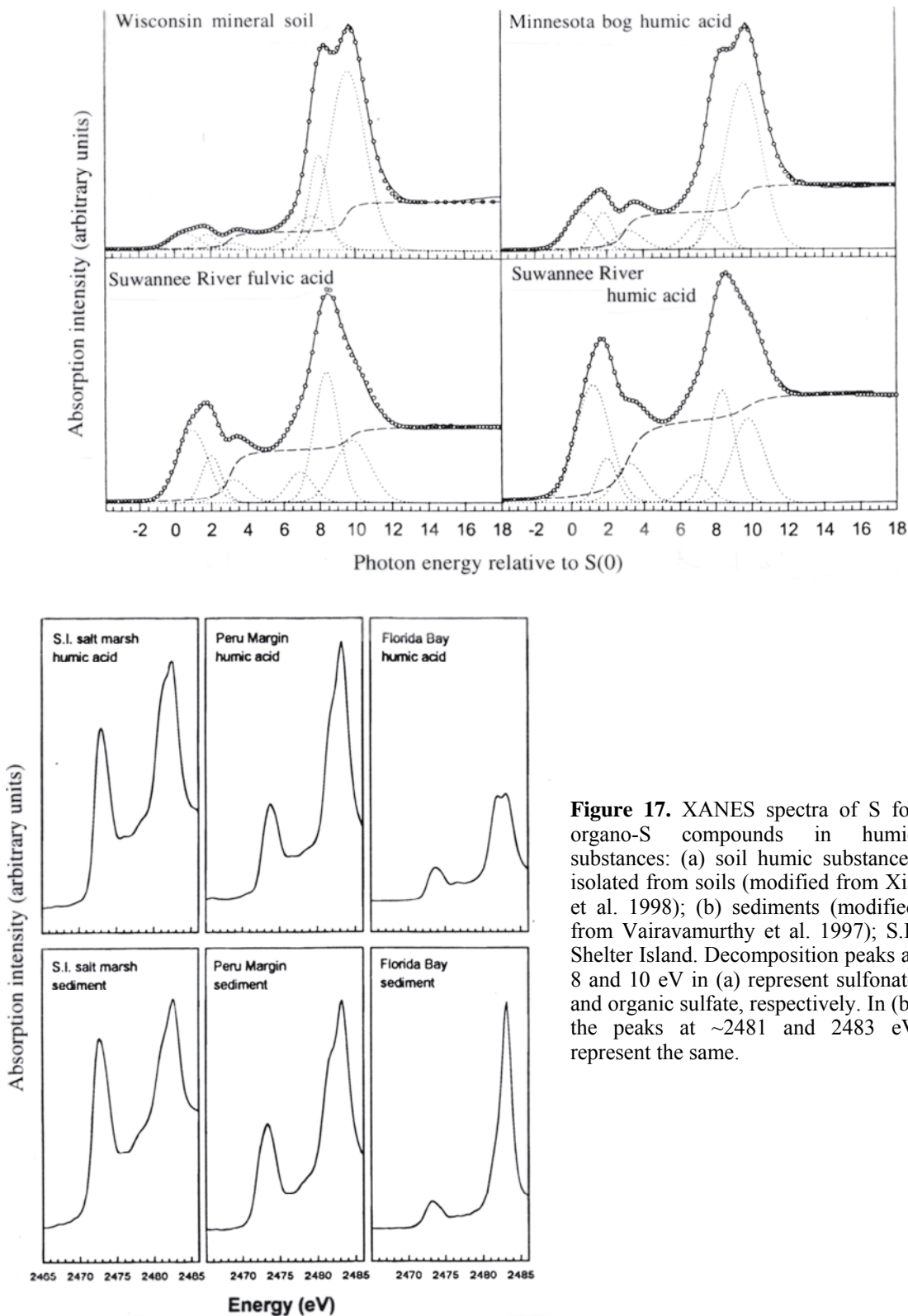


Figure 17. XANES spectra of S for organo-S compounds in humic substances: (a) soil humic substances isolated from soils (modified from Xia et al. 1998); (b) sediments (modified from Vairavamurthy et al. 1997); S.I.: Shelter Island. Decomposition peaks at 8 and 10 eV in (a) represent sulfonate and organic sulfate, respectively. In (b) the peaks at ~2481 and 2483 eV represent the same.

energy feature below the absorption edge of sulfate in organo-sulfates (Fig. 14). Myneni and Martinez (1999) reported that this feature arises from the bonding of the SO_4^{2-} group to a carbon atom. The XANES spectral features of organo-sulfates are similar to those of protonated sulfates, and the sulfur absorption edge is split into two distinct features (Fig. 17). Attachment of a carbon atom to one of the oxygen atoms of the sulfate group, as in $-\text{C}-\text{OSO}_3$ (e.g. lauryl sulfate) changes sulfate symmetry from T_d to C_{3v} , and the $1s \rightarrow t_2^*$ characteristic of uncomplexed SO_4^{2-} splits into $1s \rightarrow a_2^*$ and e^* in $-\text{C}-\text{OSO}_3$ (Fig. 14). Of particular interest is that the energies of the absorption edge of sulfonate and the low-energy feature in organo- SO_4^{2-} are similar. A detailed examination of several surfactant molecules, such as decyl sulfate, dodecyl sulfate, laureth sulfate, and dodecyl benzene sulfonic acid, also indicated splitting in the absorption edge of sulfur (Myneni, unpublished data). Hence, the low-energy feature (~ 2478 eV) adjacent to the sulfate peak in humic materials and coals, identified as sulfonate by previous researchers (Morra et al. 1997, Vairavamurthy et al. 1997, Xia et al. 1998), may not necessarily represent sulfonates entirely (Fig. 17). Although researchers used different chemical means (e.g. by treating the samples with Basalts, as barium trifluoroacetate) to separate sulfonate and organo-sulfate, they are not easily distinguishable using the X-ray absorption spectra alone.

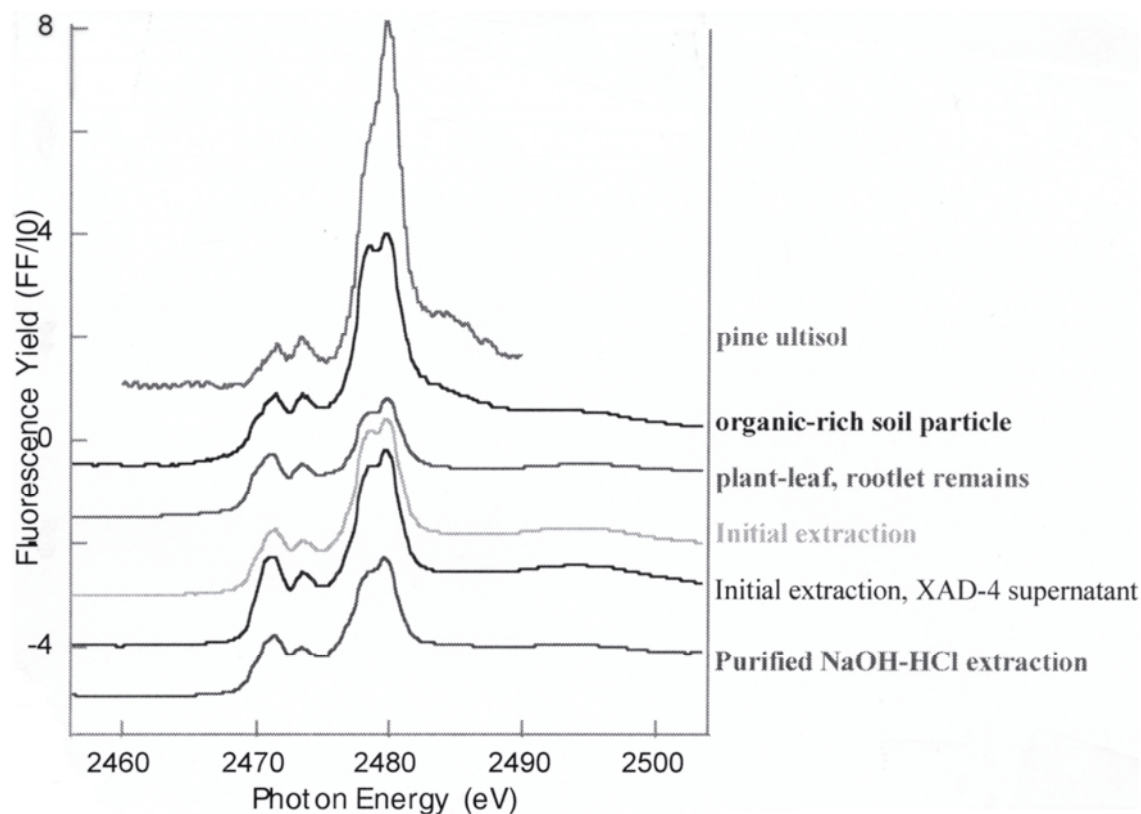


Figure 18. XANES spectra of sulfur in soil organic matter in Pine Ultisol, and different isolated humic substance fractions (from Myneni and Martinez 1999).

In contrast to isolated humic materials, fresh and undisturbed humic substances in soil exhibit different behavior for the ratio of oxidized to reduced sulfur species (Fig. 18). The Pine Ultisol from Puerto Rico (Myneni and Martinez 1999) showed that the percentage of the oxidized forms of sulfur is much higher than that of the reduced forms (Fig. 18). The XANES studies also indicated that the oxidized forms of sulfur (sulfonate, organo-sulfate, inorganic sulfates) are lost during the extraction of humic

substances from soils and that the isolated fraction preferentially retains the reduced-sulfur forms (Fig. 18; Myneni and Martinez 1999). The reported high concentrations of reduced-sulfur forms relative to sulfate and sulfonate in soils of oxidizing environments may be attributed to this preferential isolation.

XAS of sulfate at interface. When sulfate adsorbs on mineral surfaces, it can form (1) outer-sphere complexes, in which the sulfate and mineral surface interact through intermediate water molecules; and (2) inner-sphere complexes, in which sulfate bonds with cation polyhedra directly on mineral surfaces (Sposito 1994, Brown et al. 1999). The inner-sphere sulfate-cation complexes can be monodentate-mononuclear, monodentate-binuclear, bidentate-mononuclear, and bidentate-binuclear complexes. For several years, researchers have been using a variety of molecular methods to identify the types of complexes at the mineral-water interface and in aqueous solutions (Vaughan and Patrick 1995, Brown et al. 1999). The results indicate that the coordination chemistry of sulfate complexes on surfaces is not understood well, and is widely debated in the case of several mineral surfaces. Although XAS has been used successfully to resolve uncertainties for several complexes (Brown et al. 1999), only recently has this technique been used to study the coordination chemistry of sulfate at the interfaces (Myneni et al. 2000a). The vibrational spectroscopy portion of this chapter contains complementary information on sulfate reactions at interfaces.

Using XAS, Myneni et al. (2000b) have examined sulfate complexes on goethite, ferrihydrite, and hematite at different pH values and sulfate concentrations. These studies indicate that the XANES spectrum of S in sulfate adsorbed on goethite at pH > 3.5 is similar to that of aqueous SO_4^{2-} . When solution pH is <3.5, the adsorption maximum shifts to higher energy by about 0.2-0.3 eV and a pre-edge appears approximately 3 eV below the absorption edge. The pre-edge contains two overlapping features, and their energies are the same as those reported for coquimbite and copiapite (Fig. 19). These results indicated that SO_4^{2-} interacts primarily with goethite surfaces as outer-sphere and

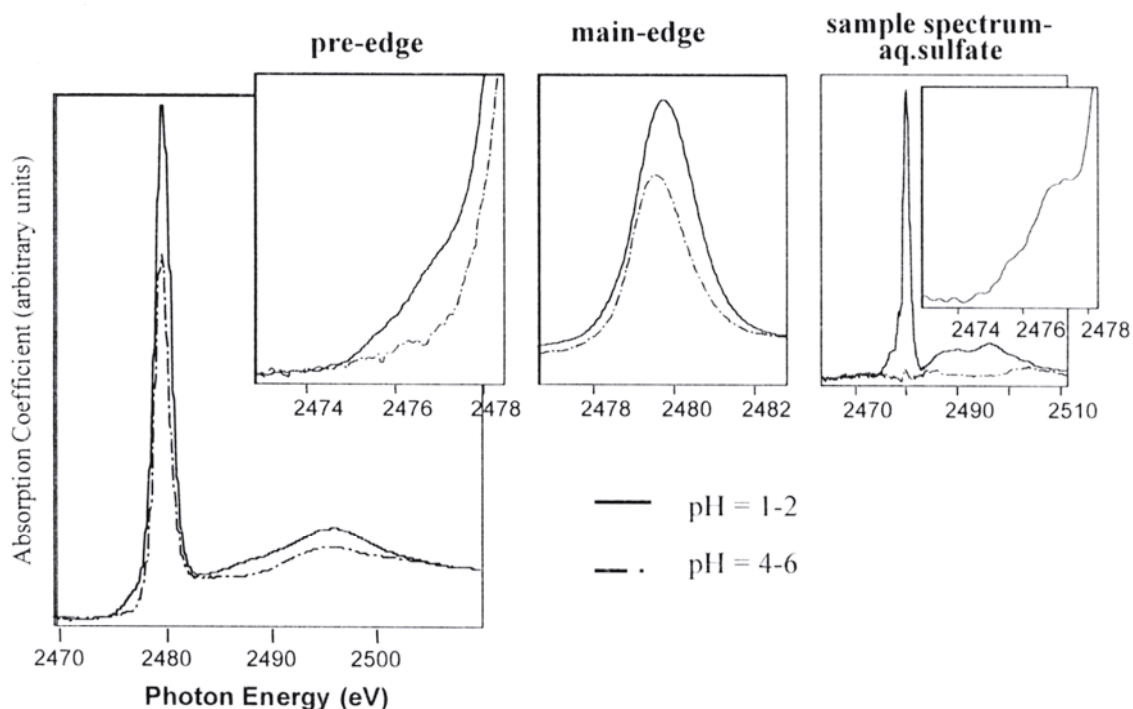


Figure 19. S-XANES spectra of sulfate sorbed on goethite at different pH values (from Myneni et al. 2000b, unpublished data).

H-bonded complexes at $\text{pH} > 3.5$. Below this pH , SO_4^{2-} forms both inner- and outer-sphere complexes on goethite surfaces. From partial least-squares fit of these sample spectra, the inner-sphere complexes were around 35% of total sorbed sulfate at $\text{pH} \sim 2.0$. Although evidence for inner-sphere complexes was not found at higher pH , their presence may not be ruled out completely, as their concentration may be too low to be detected with XAS. In contrast to goethite, sulfate adsorbed on hematite exhibits significant inner-sphere complexation at neutral pH (Myneni et al. 2000b). Although the energies of pre-edges of adsorbed SO_4^{2-} are similar to that reported for copiapite and coquimbite, a detailed investigation is necessary to understand the nature and origin of the pre-edge features and their sensitivity to the sulfate coordination. XANES studies have also been conducted to examine the interactions of sulfur oxide and its oxidation to sulfite and sulfate on several catalyst surfaces (Rodriguez et al. 1999a,b, and references therein).

X-ray absorption spectroscopy at the sulfur L-edge

Electronic transitions from $2s$ and $2p$ states ($2p_{1/2}$, $2p_{3/2}$) to unoccupied molecular orbitals, similar to XAS at the K-edge associated with $1s$ electrons, can also be studied. These transitions occur at 230.9, 163.6, 162.5 eV for elemental sulfur, these edges are termed L_1 , L_2 , and L_3 , respectively. The L_2 and L_3 edges are commonly studied in addition to the K-edge because of different selection rules for the electronic transitions. The features in the sulfur L_2 - and L_3 -edge spectra are assigned to the electronic transitions of sulfur from $2p$ to unoccupied $4s$ or $3d$ states. Both of these transitions are dipole allowed and produce significant structure in the L-edge spectra. In addition, the intrinsic core hole lifetime broadening is much smaller for L-edges than for K-edges, and this makes the spectral resolution better than 0.1 eV at the L-absorption edge of sulfur (Brown et al. 1988). Because the X-ray penetration into samples is very small at the L-absorption edge of sulfur (<100 nm in concentrated samples), very high surface sensitivity can be achieved using L-edge spectroscopy. Kasrai et al. (1996) indicated that sampling depth is around 5 nm at the L-edge, compared to 70 nm at the K absorption edge of sulfur in electron yield mode.

The synchrotron instrumentation used to examine L-edges is different from that used from K-edges. Until recently, L-edge spectroscopic studies were limited to vacuum conditions. Typically, diffraction gratings are used instead of monochromator crystals (as at the K-edges) for obtaining monochromatic light from synchrotrons. As the L-edge for S has extremely small fluorescence yield relative to its K-edge, the L-edge XAS studies are done in electron-yield mode. Stöhr (1992) gives more details on synchrotron experimentation at the L-edges (detection schemes, detectors, data collection). Several soft X-ray synchrotron facilities have beamlines that can provide photons at the L-absorption edge of S, but only few beamlines are optimized to do this under ambient conditions (Myneni et al. 2000a). The low fluorescence yield at the L-edges of S, and photon absorption by air in the soft X-ray region restrict the applications of L-edge spectroscopy to aqueous solutions and wet mineral and biological samples. However, recent developments at spectromicroscopy facilities at the ALS and NSLS (Table 1) allow L-edge spectroscopy studies on thin liquid films, mineral pastes, and biological samples under ambient conditions. Specialized beamline end-stations, such as the Soft X-ray Endstation for Environmental Research (SXEER) at the ALS, are optimized to examine dilute samples in electron- and fluorescence-yield modes and in transmission (Myneni et al. 2000a).

Sulfur L-edge spectra of a series of compounds indicate that the L-edges shift to higher energies with increase in the oxidation state (Fig. 20). Significant spectral differences also exist among chemical compounds that are closely related, especially for

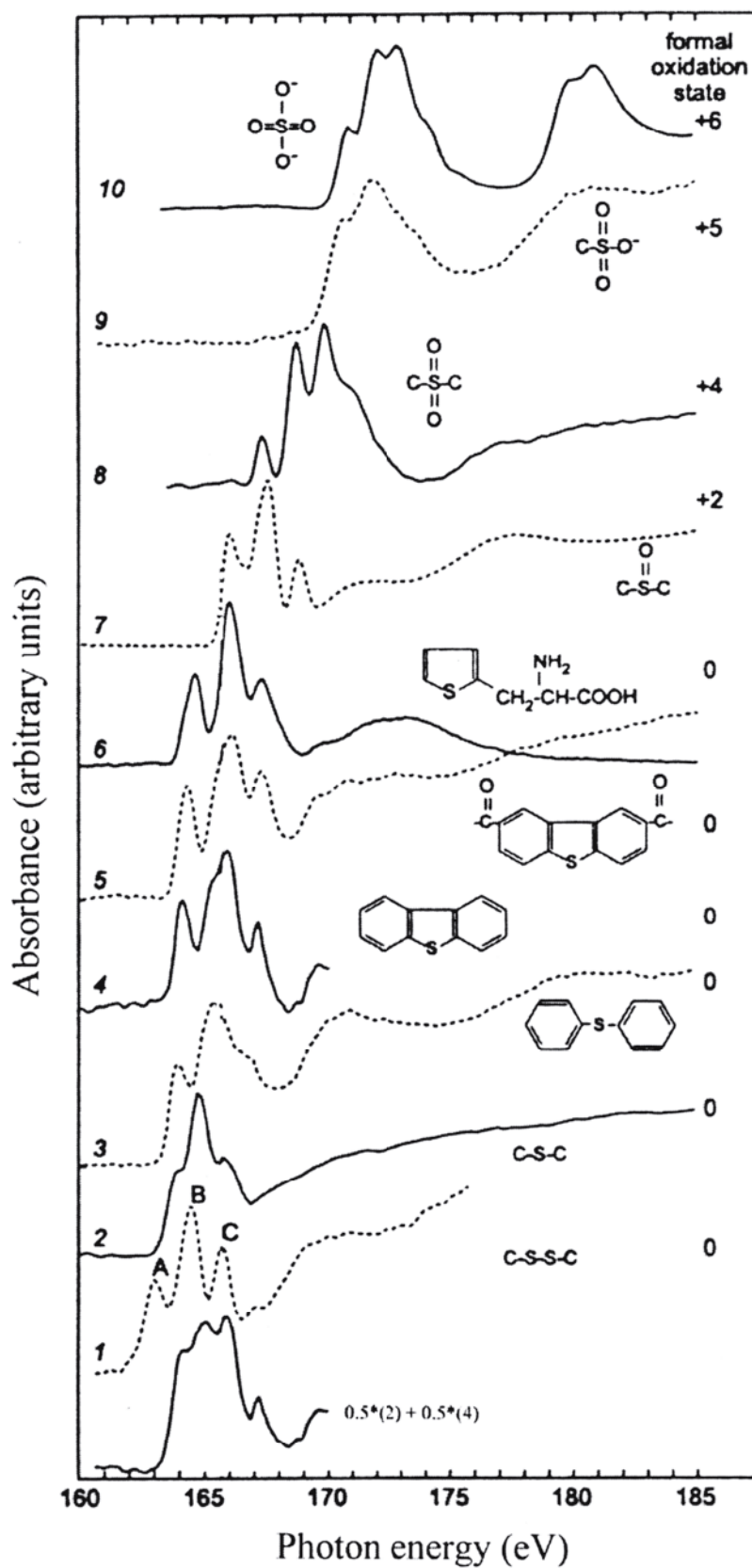


Figure 20. L-edge XANES spectra of S in different redox states and coordination environments (modified from Sarret et al. 1999). The bottom spectrum is a combination of spectra (2) and (4).

reduced-sulfur forms (Kasrai et al. 1994, Sarret et al. 1999). A majority of the previous sulfur L-edge studies were done on transition-metal sulfide minerals and on SO_x reactions on catalyst surfaces (Li et al. 1994, 1995, and references therein). The only study that has reported L-edge spectra of mineral sulfates was conducted by Li et al. (1995), who indicated that the L-edge spectra are highly sensitive to the local coordination of sulfates. In the case of alkaline-earth sulfate minerals, the L-edges shift to lower energies with an increase in the atomic number of the complexing atom (Fig. 20). In transition metal-sulfates, all have L-edges at 171.5 (±0.1) eV, except for MnSO₄ (171.8 eV; Li et al. 1995). To the author's knowledge, sulfur L-edge spectroscopic studies in aqueous samples have not been conducted. However, with the availability of the third-generation synchrotron sources, and end-stations optimized to examine samples under ambient conditions, new information is expected in the near future.

X-ray photoelectron spectroscopy

In X-ray photoelectron spectroscopy (XPS), the spectral properties of ejected photoelectrons from a photon-, or electron-absorbing atom are studied (Fig. 2). Although incident X-rays can penetrate much farther than electrons at the same incident energy, released photoelectrons have a much shorter mean-free path and hence XPS can detect only the photoelectrons from surface layers. XPS provides information on the density of occupied electronic states in an atom, and is complementary to the XAS techniques discussed above. When XPS is used as a core hole spectroscopy, the XPS spectra are characteristic of photon-absorbing atoms (as in XAS). XPS spectra also include information on the absorber coordination, as the coordinated atoms can modify the energy of the core hole electrons and the scattering of the released photoelectrons. Because the spectral properties of an electron are investigated in this method, these studies are conducted in high vacuum (~10⁻⁶ torr or less). However, the availability of high-flux bright X-rays sources at the third-generation synchrotron sources (e.g. the ALS) has led to the development of relatively high-pressure XPS chambers and differentially pumped sample chambers that operate at pressures of 5-10 torr (Ogletree et al. 2000). Some of the preliminary work on XPS of less volatile liquids at moderate pressures (~10⁻⁵ torr) was conducted by Siegbahn in the late 1970's. The interpretation of the XPS spectra of unknown compounds is typically done by comparing the sample spectra with those of known models. Libraries of XPS spectra of different compounds are available for comparison. However, the interpretation is difficult if the materials have open-shell ions.

Although XPS has not been used in studying mineral sulfates or their interfaces, it has been used for examining the surface chemistry of sulfides. The oxidation of SO_x and sulfate interactions with catalyst surfaces have also been investigated extensively using XPS (e.g. Jirsak et al. 1999, Rodriguez et al. 1999a,b; and references therein). These studies indicate that the 2*p* spectra of S in different oxidation states are separated by several eV; thus, the oxidation state and the bonding environment of different S groups can be identified easily using XPS. Watanabe et al. (1994) used XPS and Fourier transform infrared (FTIR) spectroscopic methods to examine sulfate interactions with surfaces of hematite and maghemite. The 2*p* spectra of S exhibit two overlapping features separated by approximately 2 eV (Fig. 21). The 2*p* spectrum of S in sulfate on maghemite (γ-Fe₂O₃) surfaces are 0.6 eV lower than on hematite (α-Fe₂O₃), which indicates differences in the sorption sites of these mineral surfaces (Fig. 21). Watanabe et al. (1994) attributed the doublet in the XPS spectra of sulfur to sulfate bonded to hematite and maghemite surfaces at two distinctly different sites, and suggested that these sites are less polar in the case of hematite when compared to those of maghemite.

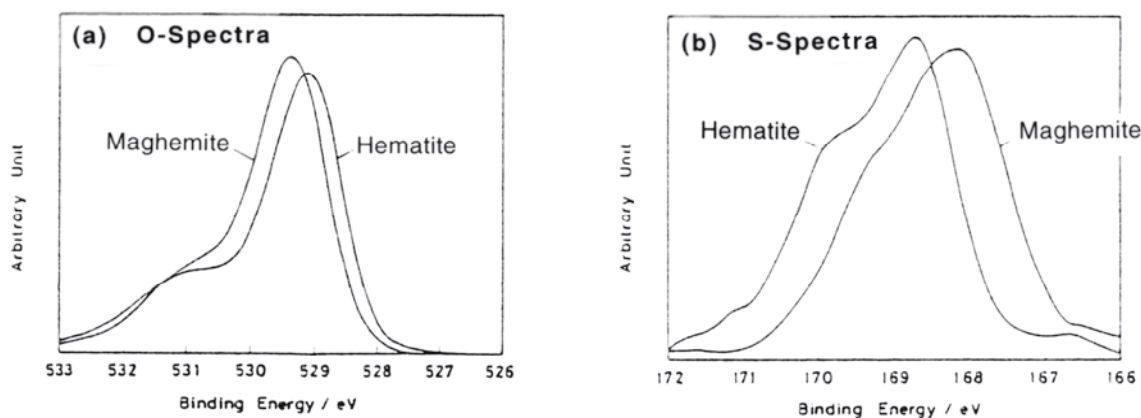


Figure 21. XPS spectra of sulfate sorbed on hematite and maghemite; (a) O 1s XPS spectra; (b) 2p XPS spectra of sulfur in sulfate (from Watanabe et al. 1994).

X-ray imaging and spectromicroscopy

Obtaining spatially resolved spectroscopic information selectively on different regions of interest in a heterogeneous sample and conducting microscopy based on chemical (or spectral) contrast of different regions of a heterogeneous sample are useful in the examination of spatial heterogeneity in geological samples (Schulze et al. 1999, Myers-Ilse et al. 2000). Such spectromicroscopy studies facilitate the examination of dilute samples and detailed micro-structures, which are otherwise not detectable by conventional molecular probes. Although spectromicroscopy studies of sulfur have not yet been reported for geological samples, the recent availability of these facilities at the third-generation synchrotron sources will help in the examination of a variety of samples of geological and biogeochemical significance. These facilities are operational for the sulfur L-edge spectromicroscopy at the ALS and NSLS, and are under construction for the sulfur K-edge spectromicroscopy at the ALS and APS (Table 1). The spectromicroscopy facilities are based on focusing the X-ray beam to spot sizes smaller than a micrometer using mirrors, or to better than 100 nm using zone-plate optics (Warwick et al. 1998). For studying the L-edges, the microscopes with zone-plate optics are the only available option. The detectors and other optics are the same as those discussed for XAS above.

Spectromicroscopy studies of heterogeneous samples can also be conducted using XPS, and these are well developed at the synchrotron sources (e.g. ALS). At the third-generation synchrotrons, spatial resolution better than one micrometer can be obtained on mineral surfaces. Researchers have been using the bright beams of the synchrotron sources to develop photoelectron emission microscopy (PEEM), to obtain a spectral resolution better than 50 nm (Anders et al. 1999). This is a photon-in, electron-out technique and is sensitive to surfaces. Research is in progress, and future developments in PEEM may improve the spatial resolution to better than 20 nm. Although these methods are relatively new, they have potential applications in studying the sulfate geochemistry of heterogeneous geological surfaces.

VIBRATIONAL SPECTROSCOPY

Vibrational spectroscopy was developed at the beginning of the 1900s and has been used ever since to study the structural properties of materials. Several books have been written on the theory and interpretation of vibrational spectroscopy, and on the fundamental vibrations of several molecules (e.g. Farmer 1974, Nakamoto 1986, Colthup et al. 1990, Ferraro and Nakamoto 1994, Suetaka 1995). Vibrational transitions in

Table 3. Comparisons of IR and Raman spectroscopy (modified from Fadini and Schnepel 1991)

<i>Parameter</i>	<i>IR spectroscopy</i>	<i>Raman spectroscopy</i>
Photon interactions	Absorption	Scattering
Vibrational excitations	Polychromatic IR radiation	Monochromatic radiation
Energy measurement	Absolute	Relative to excitation energy
Requirement for the activity of a vibration	Change in dipole moment, $\partial\mu/\partial Q \neq 0$	$\partial\alpha/\partial Q \neq 0$
Intensity of the bands	$I \propto (\partial\mu/\partial Q)^2$	$I \propto (\partial\alpha/\partial Q)^2$
Representation of the spectrum	Absorption, logarithmic 'downwards'	Scattering intensity, linear 'upwards'
Preferred technique for	Routine gas analysis	Aqueous solutions, single crystals, polymers

molecules can be studied using infrared (IR) and Raman spectroscopic methods, which are complementary. Together they provide complete information on vibrational transitions. The fundamental differences between these methods are shown in Table 3 and Figure 22.

In IR spectroscopy, molecules absorb photons when the energy of the incident light is equal to the energy difference between the vibrational ground state and the high-energy states. The probability of these transitions is higher when there is a change in the dipole moment of a molecule (Fig. 23). In Raman spectroscopy, vibrational transitions are examined by measuring light that is inelastically scattered by the sample. When high-energy light is incident on a molecule, a majority of it is scattered elastically (Rayleigh scattering) by the molecule. A small fraction (<0.001) of the incident light is scattered inelastically by the sample and causes small features in the energy spectrum of the scattered light. These transitions can represent either Stokes or anti-Stokes conditions (Fig. 22). Such vibrational transitions occur in Raman spectra when there is a change in the polarizability of molecules (Fig. 23).

The total number of vibrations in a molecule is $3n-6$, where n is the total number of atoms in a molecule ($3n-5$ for linear molecules). Although IR and Raman spectroscopic methods can provide information on the majority of vibrational transitions in a molecule, several transitions are not detected by either method. Selection rules are helpful in determining whether a vibrational transition is allowed or forbidden for either of these methods, and a detailed review of these is provided by Cotton (1971), Farmer (1974), Nakamoto (1986), Colthup et al. (1990), and in several books on molecular spectroscopy. Vibrational frequencies of a molecule are related to their bond strength and atomic masses, and the observed shifts in vibrational spectra represent changes in either of the two or in both of these variables. Changes in spectral intensity are related to the concentration of molecules with identical geometry, and to changes in molecule dipole moment (in the case of IR) or polarizability (in Raman spectroscopy). Applications of IR and Raman techniques to geological materials are discussed in detail by McMillan and Hess (1988), McMillan and Hofmeister (1988), and Johnston (1990).

Theoretical vibrational spectra can be calculated using quantum mechanics and semi-empirical methods (Stewart 1989a,b; Seeger et al. 1991, Tossell and Vaughan 1992). The calculated spectra are useful in identifying the experimental spectra of sulfate in different environments.

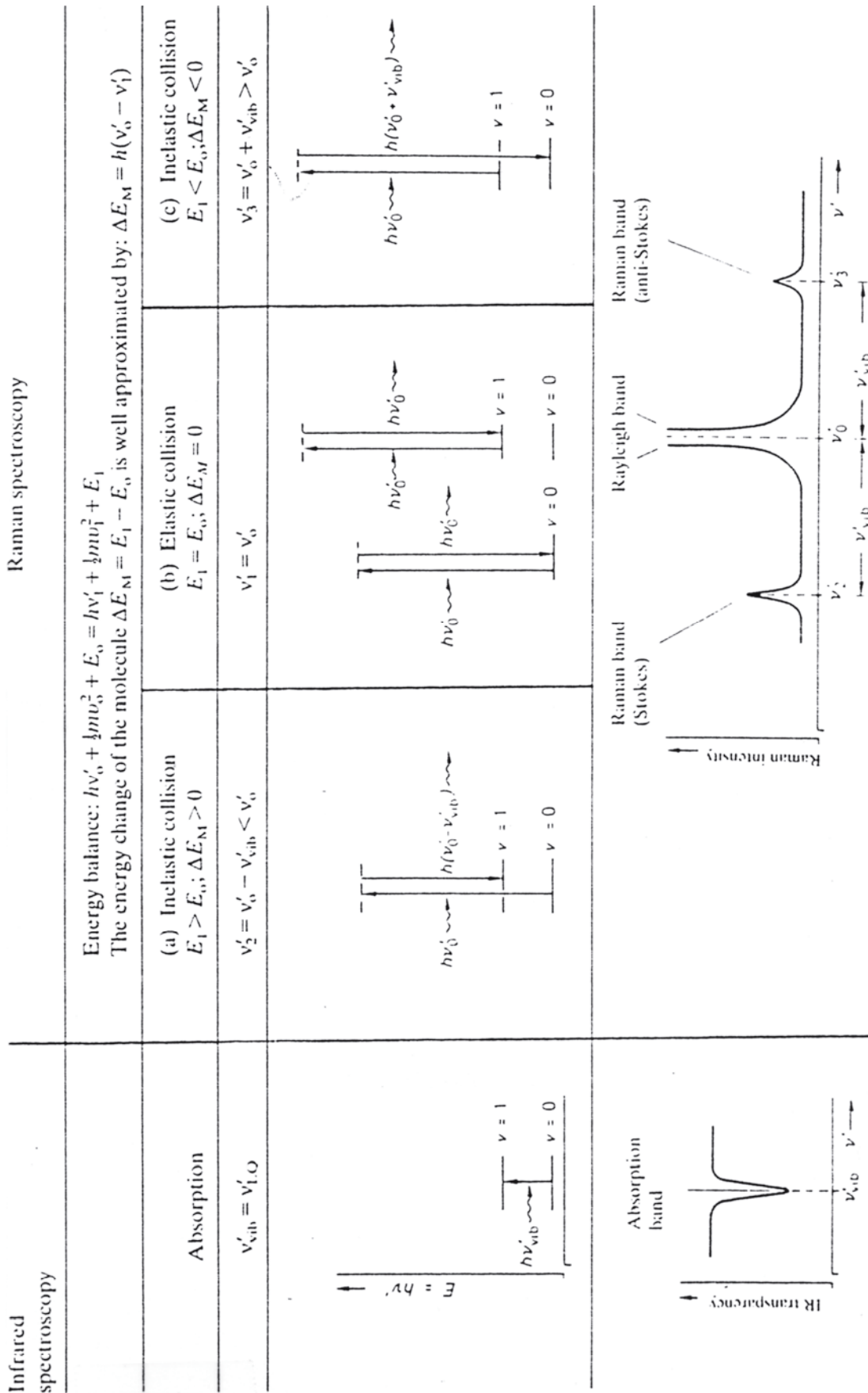


Figure 22. Vibrational transitions and the origin of vibrational spectra in infrared (IR) and Raman spectroscopy. $\nu = 0$ ground state, $\nu = 1$ first excited state (modified from Fadini and Schnepel 1989).

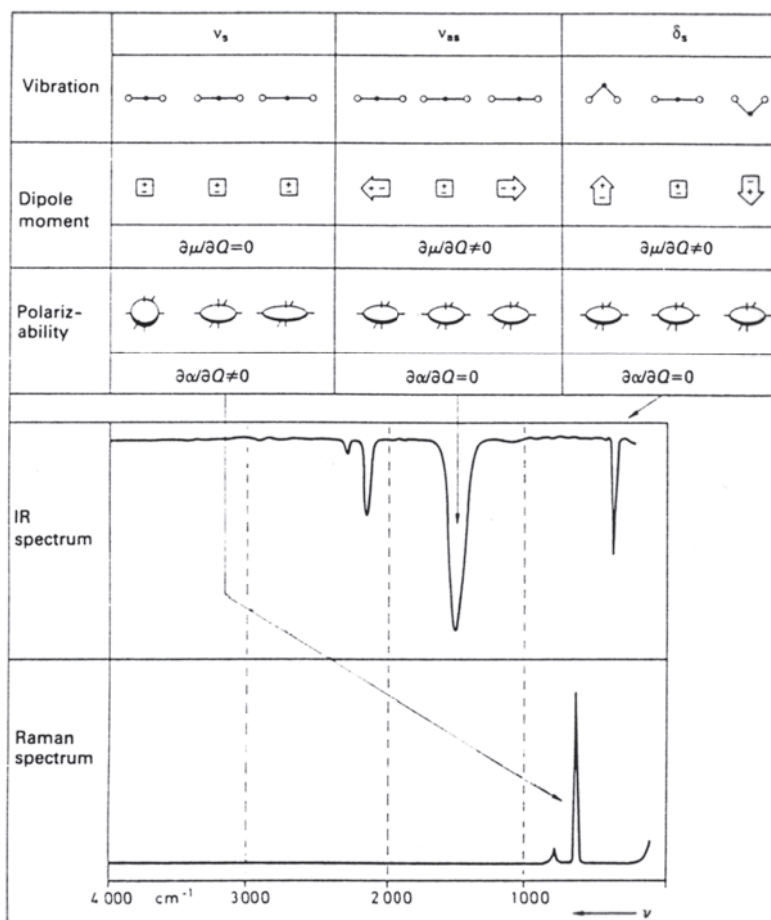


Figure 23. Raman and infrared spectra of CS_2 . Changes in molecule dipole moment and polarizability for each of the vibrations are also shown with their peak intensities in Raman and IR (from Fadini and Schnepel 1989).

Symmetry and vibrational modes of sulfate and its complexes

The vibrational spectral features, nomenclature and interpretation for arsenate is discussed in detail by Myneni et al. (1998b); parts of that discussion are presented here to clarify the spectral interpretation on sulfates. Sulfate is a tetrahedral (T_d) molecule with an average S–O bond length of 1.472 Å (Hawthorne et al. Chapter 1, this volume). Variation in solvation (coordination of water molecules at different oxygen atoms of sulfate), metal complexation, and protonation of sulfate can modify the S–O bond lengths, and cause changes in symmetry from T_d to either C_{3v}/C_3 (monodentate, corner-sharing), C_{2v}/C_2 (edge-sharing, bidentate binuclear), or C_1/C_s (corner-sharing, edge-sharing, bidentate binuclear, multidentate) (Table 4). Such changes in the bond length and the symmetry of sulfate molecules may shift the vibrational bands to different energies and cause the degenerate vibrations to become nondegenerate. Changes in the vibrational spectrum of sulfate associated with symmetry changes can be interpreted using group theory (Table 4; Cotton 1971, Farmer 1974, Nakamoto, 1986).

In the infrared region, SO_4^{2-} exhibits nine normal modes: and A_1 (symmetric stretch, ν_1), an E (symmetric bending, ν_2), and two F (asymmetric stretching and bending, ν_3 and ν_4 respectively); the symbols A_1 , E , and F correspond to non-, doubly-, and triply-degenerate vibrations, respectively. In physical chemistry and spectroscopy literature, both of these notations (A , E , F ; ν_1 , ν_2 , ...) are commonly used. The subscript (e.g. ν_1) is

Table 4. Normal modes of sulfate in different symmetries (modified from Farmer 1974)

<i>Site sym sulfate</i>	<i>Vibrational Mode & symclass</i>			<i>Activity</i>		<i>No of IR active bands</i>
	ν_1	ν_2	ν_3, ν_4	<i>R active only</i>	<i>IR and R active</i>	
T _d	A ₁	E	F ₂	A ₁ , E	F ₂	2
D _{2d}	A ₁	A ₁ +B ₁	B ₂ +E	A ₁ , B ₁	B ₂ , E	4
S ₄	A	A+B	B+E	A	B, E	5
D ₂	A	2A	B ₁ + B ₂ + B ₃	A	B ₁ , B ₂ , B ₃	6
C _{2v}	A ₁	A ₁ +A ₂	A ₁ + B ₁ + B ₂	A ₂	A ₁ , B ₁ , B ₂	8
C ₂	A	2A	A+2B	-	A, B	9
T	A	E	F	A, E	F	2
C _{3v}	A ₁	E	A ₁ +E	-	A ₁ , E	6
C ₃	A	E	A+E	-	A, E	6
C _s	A'	A'+ A''	C	-	2A', A''	9

used to distinguish different vibrations, and has no relation to the symmetry of a molecule. As the symbol 'v' has been used by several researches to represent stretching vibrations only, some of the interpretations in the literature may be confusing unless the notation is clearly specified. The bending vibrations occur at low wavenumbers where several molecules exhibit both vibrational and rotational modes and hence it is difficult to distinguish sulfate-bending vibrations from others in heterogeneous geological materials. Although several researchers have assigned different bands to bending vibrations of sulfate in complex matrices, readers should be cautious about these assignments and interpretations. For these reasons, only the stretching vibrations are focused in this Chapter, and the symbols ν_s and ν_{as} have been chosen to represent the symmetric and asymmetric stretching vibrations (Myneni et al. 1998b). The vibrating atom-pair has also been specified to avoid misinterpretations (e.g. ν_s of S–OH represents the symmetric stretching vibrations of the S–OH bond).

In association with changes in SO_4^{2-} symmetry and coordination, the A₁ band may shift to different wavenumbers, and the degenerate E and F modes may give rise to several new A₁, B₁, and/or E vibrations (Table 4). In many instances the apparent structural symmetry of SO_4^{2-} species in solutions, crystals, or in the vicinity of interfaces may not follow closely the above-described symmetry predictions. Such discrepancies may be caused by: (1) extensive H-bonding of the non-bonding O atoms of SO_4^{2-} with several H₂O molecules, (2) SO_4^{2-} polydentate complexation with cations, or (3) tilt of the SO_4^{2-} -complexed cation (or proton) away from the S–O–M axis (typically considered to be linear in symmetry analysis). For these reasons, the presence of high-symmetry species in samples may not be excluded if the vibrational spectra exhibit all SO_4^{2-}

fundamental vibrations. Similarly, the appearance of single, unsplit peaks for degenerate SO vibrations do not completely rule out the presence of low-symmetry species in the samples. The symmetry of an SO_4^{2-} group can be very low, in fact as low as C_1 , but not result in enough peak splitting to be identified. In summary, disparities between the symmetry predictions and experimental data are caused by the finite spectral resolution and our commonsense perspective on molecular symmetry. However, such deviations in apparent symmetry can be identified with chemical shift information from A_1 vibrational modes and peak splitting of degenerate vibrations.

For ions in crystals, the applications of site-symmetry and factor group analysis, and correlation methods can offer complete information on the vibrational spectra of the ions (Bhagavantam and Venkataraidu 1969, Fateley et al. 1971, Cotton 1971). These methods provide symmetry information for sulfate groups on the basis of their location and the local coordination inside the crystal. Interpretation of molecular spectra of aqueous solutions and interfaces is more complex than that of solids. In aqueous solutions, several sulfato complexes can exist at different concentrations, and the vibrational spectrum of an aqueous sample is a composite spectrum of all these complexes. The same is true for sulfato complexes on mineral surfaces, where a variety of surface complexes can exist, e.g. the outer-sphere, inner-sphere, and H-bonded complexes discussed above. Inner-sphere complexes can also exist in several forms (discussed above), and identification of these complexes from the vibrational spectra should be approached with caution. The selection rules for the vibrational transitions of surface complexes are also different when compared to those solutions and solids (Urban 1993, Suetaka 1995). A variety of outer- and inner-sphere complexes can also exist in aqueous solutions, and their identification and relative concentrations are difficult. The challenge in vibrational spectroscopy is to identify the molecular chemistry of these complexes from the energy shifts in ν_1 vibrations, and from the amount of splitting in degenerate vibrations (ν_2, ν_3, ν_4), which are directly related to the strength of SO_4^{2-} complexes.

Data collection and analysis

The methods of data collection for vibrational spectra from samples in different environments are well-developed and widely available. A variety of data-collection methods have been developed to obtain IR and Raman spectra of dilute species in aqueous solutions and solids, at mineralwater interfaces, and for spatial resolution of micrometer-size domains. A brief description of these methods is provided here; more detailed discussion of these methods is available in the references cited on IR and Raman spectroscopy.

Infrared spectroscopy Dry, solid samples can be examined in transmission, diffuse-reflection, and external-reflection modes. For examination in transmission and diffuse-reflection modes, the samples are commonly diluted with IR-transparent KBr or KCl. The diffuse-reflection and external-reflection methods are more surface-sensitive than the transmission methods (assuming that the species of interest is present on surfaces and in bulk). When extreme surface sensitivity is required for solids, a grazing incidence or external reflection method with a high angle of incidence-reflection (80°) is typically used. The surface sensitivity can also be varied by changing the angle of the incident beam (Harrick 1987). Liquid samples are examined in the transmission and attenuated-total-reflection (ATR) modes. For examining liquid samples that have different refractive indices and pH, several different ATR crystals are available (Harrick 1987; also refer to the Spectra-Tech web page, <http://www.spectratech.com>). The ATR cells are also used for collecting spectra of wet pastes, suspensions, and interfaces of colloids and fluids. Details of these methods are discussed by Farmer (1974), Nakamoto (1986), Harrick (1987), Ferraro and Nakamoto (1994), and Suetaka (1995). The optics of the infrared

spectrometer are different for different energy regimes (far-, mid-, near-IR), and suitable optics must be used to get the best sensitivity.

Raman spectroscopy Raman spectra of samples can be collected by exciting them at different wavelengths using different lasers, such as Kr⁺ (647.1 nm), He-Ne (632.8 nm), or Ar⁺ (488.0, 514.5 nm). Laser wavelength selection depends on the sample type and background fluorescence. Energy-tunable lasers have been developed recently, and these can be used to excite at any wavelength that is best suited for the sample.

Spectral analysis. Spectral identification of unknown samples can be conducted by comparing their spectra with those of several known compounds, or by conducting theoretical calculations. For identifying the fundamental vibrations, researchers typically use spectral libraries that are published by different groups, such as the Sadtler IR Digital Spectra Libraries, the American Society for Testing and Materials (ASTM) Database, and the Canadian Scientific Numerical Database Service (Search Program for IR Spectra, and several others). In practice, the normal modes of vibration of a chemical species cannot be identified unambiguously without examining a series of structural models having similar composition, or by conducting theoretical investigations. As discussed earlier, changes in bond strength of a molecule can cause significant shifts in its vibrational spectra, and prior knowledge is essential for identifying these changes and for distinguishing the spectral features of a molecule from the spectral features of other molecules.

The presence of molecules in different structural states with closely related spectral features in geological matrices might cause their vibrational spectra to be broad. Overlap of vibrations of molecules of interest with those of other molecules can also contribute to such broadening. For deconvoluting such composite spectra, researchers use spectral second derivatives and principal-component analysis for identifying the number of peaks, and then fit the composite spectrum with a mixture of Lorentzian and Gaussian peaks (Maddams 1980, Gillette et al. 1982, Hawthorne and Waychunas 1988, Perkins et al. 1991, Hasenoehrl and Griffiths 1993).

Vibrational spectra of sulfate in solids

Reviews of sulfate coordination in a variety of minerals, and their vibrational spectra, were presented by Moenke (1962) and Ross (1974). The collection of vibrational spectra reported in the "Infrared Spectra of Minerals" is extensive and has been widely used by geologists and soil scientists for the identification of a variety of minerals (Farmer 1974). Ross (1974) presented the vibrational spectra of several minerals, with their site symmetries, but did not give a detailed discussion of sulfate bonding in crystals or of the corresponding shifts in sulfate vibrational frequencies. Except for a handful of minerals, a detailed discussion of sulfate minerals is lacking even in the more recent literature. Although there are more recent reviews on the IR and Raman spectra of minerals, they do not include a large collection of data for sulfate minerals (e.g. Karr 1975, Gadsden 1975, Ferraro 1982, Pechar 1988, Salisbury 1992, Cejka 1999). The vibrational spectra in the mid infrared region of two naturally occurring sulfate minerals are shown in Figure 24. Detailed analysis of energies of sulfate vibrations, together with the complementary information from the vibrational energies of other groups in minerals, is useful to interpret the relationship between the vibrational spectra of sulfate in minerals and its chemical bonding with the neighboring cations (for examples, studies of Siedl and Knop (1969) on water in gypsum). Theoretical vibrational spectroscopy studies are also helpful in interpreting the complex vibrational spectra of solid sulfates.

Examination of cation complexes of a series of alkali sulfates, alkaline-earth sulfates, transition-metal sulfates and selected heavy-metal sulfate indicates that the symmetric

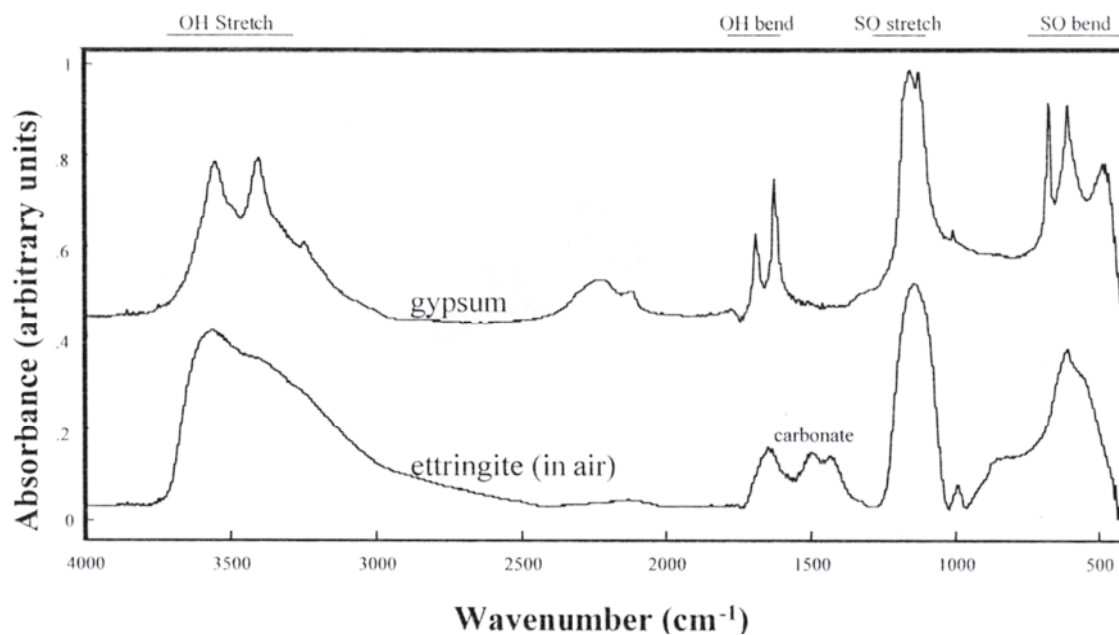


Figure 24. Infrared spectra of gypsum and ettringite (Myneni, unpublished data).

stretching $\nu_{s(S-OM)}$ ($M = \text{cation}$), vibrations do not exhibit any strong trends with the type of cation that is bonded to the SO_4^{2-} group. The $\nu_{s(S-OM)}$ vibrations (range: $960\text{--}1020\text{ cm}^{-1}$) do not shift significantly away from those of uncomplexed sulfate (e.g. as in aqueous solutions; $\sim 980\text{ cm}^{-1}$, discussed later). The largest shift is found in protonated sulfate salts, with the $\nu_{s(S-OM)}$ vibrations around 890 cm^{-1} . Although definite trends were not observed for the spectral shift of $\nu_{s(S-OM)}$ vibrations to lower energies when compared to those of uncomplexed sulfate (such as alkali sulfates; Rull and Ohtaki 1997) (Fig. 31c). Changes in cation coordination around sulfate in structurally similar compounds cause shifts in the $\nu_{s(S-OM)}$ vibrations. If spectral features are resolved and understood, they can provide important information on the environment of sulfate bonding and can offer clues on the structural environment of sulfate in unknown compounds. Using such changes in $\nu_{s(S-O)}$ vibrations, Myneni et al. (1998a) identified three different types of sulfate groups and their coordination to water in ettringite.

Although information on the vibrational spectroscopy of crystalline and well-characterized minerals is critical for understanding and interpreting the chemical bonding and molecular chemistry of sulfate in complex, heterogeneous geological samples, few recent attempts have been made to correlate the crystal chemistry of sulfates with their vibrational spectral features. Some recent studies have focused on sulfate complexes in aqueous solutions, and at the mineral-water interface (as discussed later), but a majority of these studies have not used structurally similar and well-characterized minerals for interpreting the coordination chemistry of sulfate in complex systems. Detailed vibrational spectroscopic investigations of sulfate minerals can assist in interpreting the sulfate-coordination environment.

Vibrational spectra of sulfate in aqueous solutions

In dilute aqueous solutions of $\text{pH} > 3.0$, SO_4^{2-} occurs primarily as a tetrahedral species and exhibits symmetric stretching (ν_1) and bending (ν_2), and asymmetric stretching (ν_3) and bending (ν_4) at 983 , 450 , 1105 , and 611 cm^{-1} , respectively (Nakamoto 1986; Table 5). Of these, the asymmetric stretching and bending vibrations are IR active

Table 5. Normal vibrational modes of SO_4^{2-} and its protonated forms in aqueous solutions. Subscripts: IR: Infrared spectra, R: Raman spectra; s: symmetric stretching or bending vibrations, as: asymmetric stretching or bending vibrations.

<i>Chiral Spis</i>	ν_1	ν_2	ν_3	ν_4
	(cm^{-1})			
SO_4^{2-}				
Nakamoto (1986)	983	450	1105	611
Myneni et al. (1998a)	980 _{IR}	--	1098	--
Hug (1997)	--	--	1100 _{IR}	--
Persson & Lövgren (1996)	--	--	1100 _{IR}	--
Max et al. (2000)	982 _{IR}		1099	---
Degenhardt & Mcquillan (1999)	977 _{IR}		1099	
Rull & Ohtaki (1997)				
Rudolph (1998a)				
Faguy et al. (1996)	980.8 _R	--	--	--
	981.4 _R	452	1110	617
	980 _R	--	1100	--
HSO_4^-				
Ataka & Osawa (1998)	876 _{IR (S-OH)}	--	1050 _{(S-O)s} , 1090 _{(S-O)as}	--
Hug (1997)	891 _{IR (S-OH)}	--	1051 _{(S-O)s}	--
Max et al. (2000)	887 _{IR (S-OH)}	--	1194 _(S-O)	--
Faguy et al. (1996)	885 _{R (S-OH)s}	--	1051 _{(S-O)s}	--
Rudolph (1996)	898 _{R (S-OH)}	422 _(S-OH)	1198 _{(S-O)as} , 1050 _{(S-O)s} , 1200 _{(S-O)as} , 1052 _{(S-O)s} , 1202 _{(S-O)as}	--
$\text{H}_2\text{SO}_4^\circ$				
Horn & Sully (1999)	902 _{IR (S-OH)s}		1158 _{(S-O)s}	--
	957 _{(S-OH)as}		1359 _{(S-O)as}	--

(because of changes in dipole moment), and appear as strong bands in the IR spectrum. However, moderately concentrated (several mM) aqueous solutions of SO_4^{2-} exhibit a weak absorption feature corresponding to the $\nu_{s(S-O)}$ vibrations at about 980 cm^{-1} (e.g. Myneni et al. 1998a). Appearance of the $\nu_{s(S-O)}$ band in the vibrational spectrum of SO_4^{2-} suggests that its symmetry may not be perfectly tetrahedral. If the structure of water around SO_4^{2-} is also considered in symmetry analysis, aqueous SO_4^{2-} may not be tetrahedral because of the differences in water solvation and H-bonding at the O atoms of SO_4^{2-} . The sulfate-solvated water is continuously exchanged with the bulk water, and the water-exchange rates should also be considered and compared with the time scale of vibrational transitions ($\sim 10^{-12}$ s). The sample holder used to collect the spectrum of aqueous SO_4^{2-} can also cause symmetry distortions at the interfaces of the IR crystal and water.

In the case of Raman spectra, all of the fundamental modes of SO_4^{2-} are active in tetrahedral geometry and the $\nu_{\text{s(S-O)}}$ vibrations produce an intense band when compared to the other sulfate vibrations (because of changes in polarizability). Hence, several researchers studying aqueous complexes of SO_4^{2-} have focused on the intensity, asymmetry, and energies of this band. The Raman spectra of dilute aqueous solutions of SO_4^{2-} show a strong feature corresponding to the $\nu_{\text{s(S-O)}}$ band of SO_4^{2-} , without changes in other band positions. This suggests T_d symmetry for sulfate (Faguy et al 1996, Rull and Ohtaki 1997, Rudolph 1998a,b). It should also be noted that small changes in H-bonding of water around solvated sulfate (such as those discussed above) might not cause significant differences in the degenerate (ν_2 , ν_3 , ν_4) vibrations. Although these studies indicated that the symmetry of sulfate in aqueous solutions is debatable, the symmetry can be considered close to T_d geometry.

The vibrational spectra of SO_4^{2-} have been described by several researchers, but only selected results are cited in Table 5 to illustrate the small variation in reported values. It should be noted that these spectra were collected under different experimental conditions, a range of SO_4^{2-} concentrations, and in the presence of different counter-ions (e.g., Na^+ , K^+ , NH_4^+).

Natnef slfatesbutd wate. When ions are added to aqueous solutions, they disturb the H-bonding environment in liquid water, and form either H-bonds or strong complexes with water molecules (Pauling 1960, Ohtaki and Radnai 1993). However, ionic charge dissipates away from the ions, and theoretical studies indicate that the first two solvation shells of water may neutralize more than 90% of the ionic charge. Water in the solvation shell of sulfate can be probed directly by studying its OH vibrations (Myneni et al. 1998b; Fig. 25). The water molecules exhibit symmetric and asymmetric stretching vibrations above 3000 cm^{-1} , and bending vibrations around 1640 cm^{-1} (Nakamoto 1986). The studies of Myneni et al. (1998b) on a series of tetrahedral oxoanions (SO_4^{2-} , CrO_4^{2-} , MoO_4^{2-} , SeO_4^{2-} , HAsO_4^{2-} , HPO_4^{2-}) showed that vibrational spectral features of water (after subtracting the bulk water contributions) shift to different energies in accordance with the type of oxoanion and its protonation state in water. The results indicate that the oxoanions with the strongest H-bonding between the oxoanions and water exhibit weak OH vibrations and thus shift to lower wavenumbers. The strongly hydrating ions also have high pK_a values and narrower metal-O vibrational bands. The sulfate ion has a low pK_a compared to those of other examined oxoanions (Brookins 1988), and the OH stretching vibrations are at relatively high wavenumbers (Fig. 25). Similar results were also reported for sulfate at different pH values, and for several monovalent anions in HDO (Bergström et al. 1991, Brooker and Tremaine 1992, Ataka and Osawa 1998).

Protonation ffets a slfate vbrations. Protonation and cation complexation of aqueous SO_4^{2-} can modify its vibrational spectral features and these are useful in identifying the SO_4^{2-} coordination and bonding environment. If carefully evaluated, the vibrational spectra can be used to obtain the stability constants of proton-sulfate and cation-sulfate complexes (Rudolph et al. 1998 a,b; Max et al. 2000 and references therein).

Addition of a proton to SO_4^{2-} modifies the symmetry of sulfate from T_d to C_{3v} (considering the proton is along the axis of the SO bond). The addition of a proton to SO_4^{2-} also distorts the molecule significantly, and the SO bond length increases from 1.473 \AA in uncomplexed SO_4^{2-} , to 1.58 \AA for SOH in HSO_4^{2-} (Cruickshank and Robinson 1966, Taesler and Olovsson 1969, Hawthorne et al., Chapter 1, this volume). Accordingly, the bond length of uncomplexed SO shortens to 1.46 \AA . These changes modify the SO_4^{2-} vibrational spectra completely, and the $\nu_{\text{s(S-OH)}}$ vibrations appear around

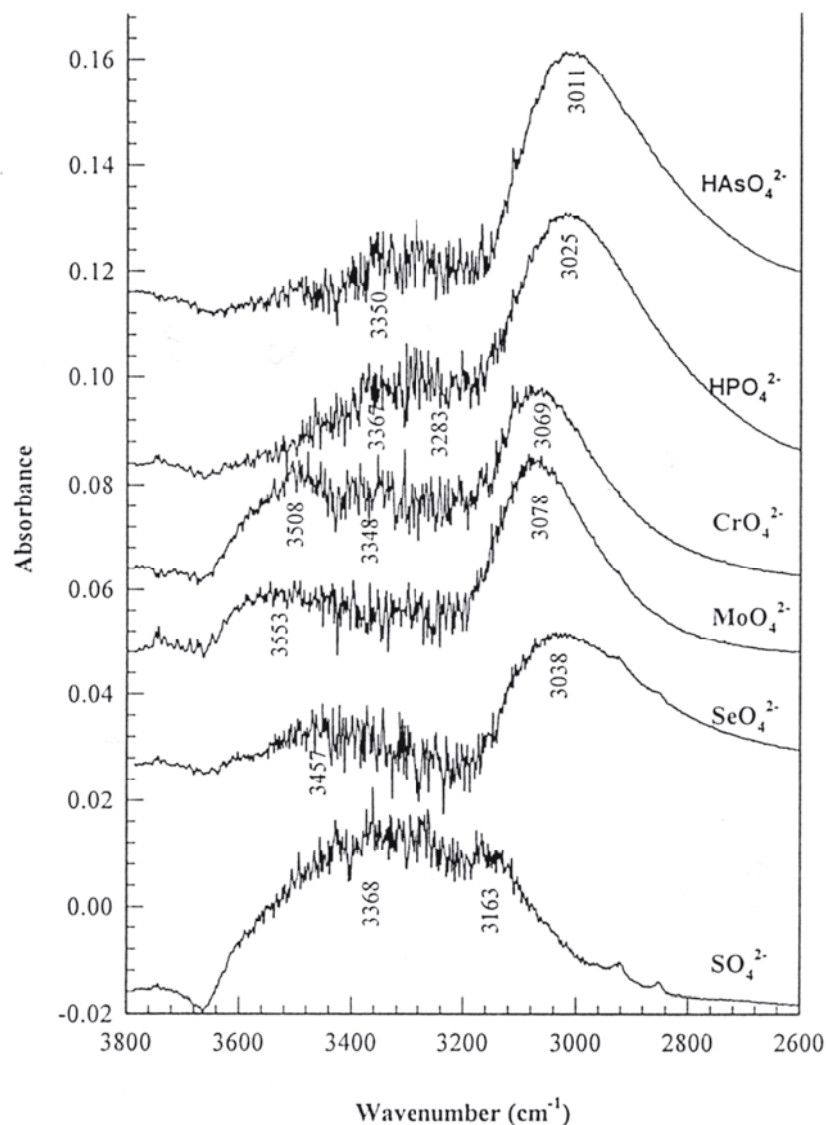


Figure 25. OH stretching vibrations of water coordinated in different aqueous oxoanions (Myneni et al. 1998b). The spectra were collected using ZnSe ATR-FTIR spectroscopy.

890 cm^{-1} (Table 5, Fig. 26). The corresponding $\nu_{\text{s(S-O)}}$, $\nu_{\text{as(S-O)}}$ vibrations of the SO_3 group appear at about 1050 and 1200 cm^{-1} , respectively. These vibrations originate from the splitting of triply-degenerate asymmetric stretching vibration (Tables 4 and 5; Fig. 26). In association with these changes, the degenerate bending of vibrations also split accordingly (Table 4; Rudolph 1996, Max et al. 2000). A detailed titration of sulfuric acid by Max et al. (2000) showed these spectral variations clearly (Fig. 26). Max et al. used the spectral energies and intensities to estimate the distribution of HSO_4^- and SO_4^{2-} in aqueous solutions at different pH values and the corresponding pK_a value, which is in close agreement with the experimental values. Proton association with sulfate also changes dramatically with a change in temperature, and the $\nu_{\text{s(S-OH)}}$ band shifts to lower energy with increases in temperature (Rudolph 1996; Fig. 27). Based on Raman spectral changes, Rudolph calculated changes in the pK_a of HSO_4^- with temperature, which showed an increase with an increase in temperature (Fig. 27).

Addition of another proton to HSO_4^- and $\text{H}_2\text{SO}_4^\circ$ results in the relaxation of the

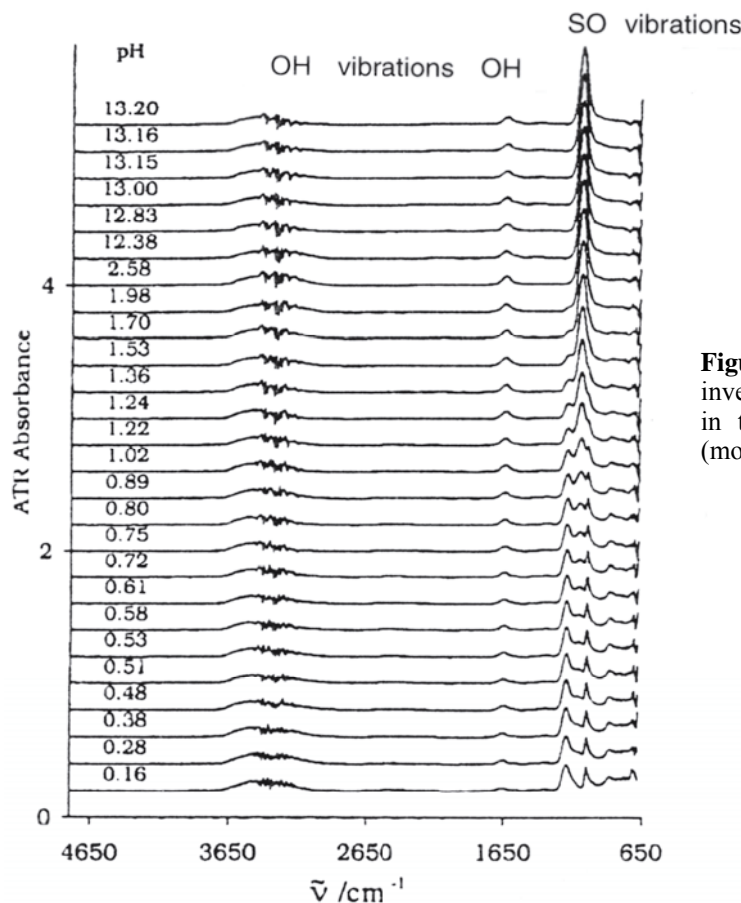


Figure 26. ATR-FTIR spectral investigation of sulfuric acid titration in the pH range of 0.16 to 13.20 (modified after Max et al. 2000).

first SOH bond to 1.54 Å (from 1.58 Å in HSO_4^-) and in further shortening of the uncomplexed SO bond lengths to 1.43 Å (Cruickshank and Robinson 1966, Myneni et al. 1998b). The symmetry of $\text{H}_2\text{SO}_4^\circ$ is considered to be C_{2v} , provided that the H atoms are along the SO bond-axis. The degenerate vibrations split accordingly and the IR-inactive bands become active (Table 5). Note that the $\nu_{s(\text{S-OH})}$ vibrations of $\text{H}_2\text{SO}_4^\circ$ shift to higher energies (relative to HSO_4^-) with the addition of protons to HSO_4^- (and with reduction in the SOH bond length). Such bond length and vibrational spectral changes have been observed for other oxoanions such as AsO_4^{3-} , SeO_4^{2-} , and PO_4^{3-} (Cruickshank and Robinson 1966, Myneni et al. 1998a,b; Persson et al. 1996). Theoretical vibrational spectral calculations of H_2SO_4 molecules using the 6-31G** basis set showed an excellent agreement with the experimental results discussed above (Lindsay and Gibbs 1988). Although previous studies focused on gas phase molecules, calculations on solvated species of protonated and metal-complexed sulfates would be useful in understanding the vibrational spectral changes with changes in chemical bonding.

The differences in the vibrational spectra of SO_4^{2-} and HSO_4^- have been used by geochemists in interpreting paleoenvironmental conditions. For example, micro-Raman spectroscopic investigation of fluid inclusions in halite were used by Benison et al. (1998) to infer the depositional environment of red beds in Permian age. The spectra of sulfate in the fluid inclusions showed two distinct features, which were assigned to the $\nu_{s(\text{S-O})}$ vibrations of SO_4^{2-} and HSO_4^- . The chemistry of fluids in inclusions is assumed to represent the chemical conditions of the formation waters, and the study by Benison et al. suggested that the pH of these solutions may have been <1.0 (Fig. 28).

Cation complexation effects

on sulfate vibrations.

Examination of cation

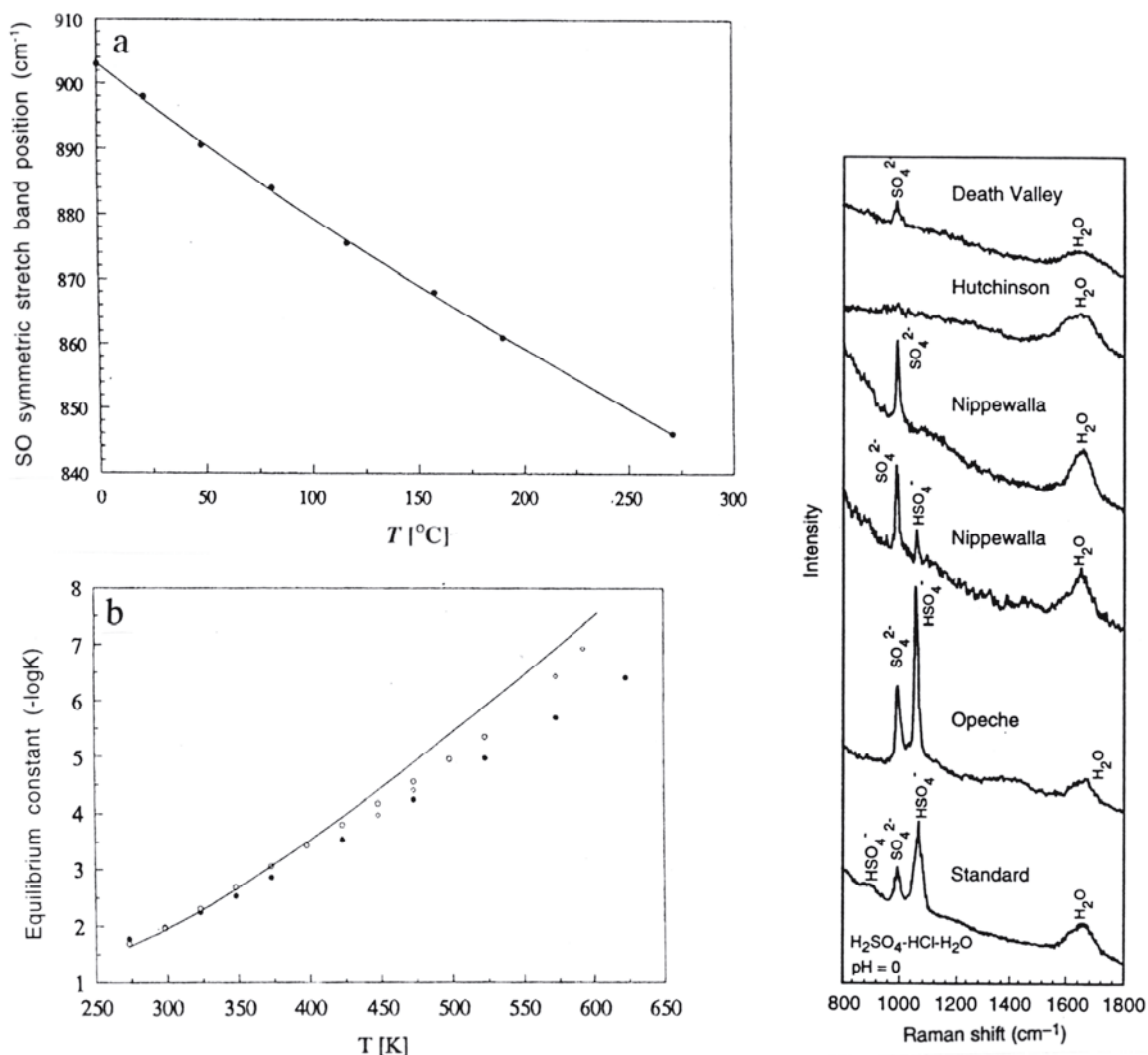


Figure 27. (a) Spectral energies of $\nu_{s(S-O)}$ vibrations of sulfuric acid as a function of temperature; (b) the second pK (K = dissociation constant) of H_2SO_4 . (modified from Rudolph 1996)

Figure 28. (right). Micro-Raman spectra of sulfate in fluid inclusions in Permian halite samples (Hutchinson, Nippewalla and Opeche formations) and modern Death Valley halite (modified from Benison et al. 1998)

complexation of sulfate in aqueous solutions, primarily using Raman spectroscopy since the 1960s, has indicated that the $\nu_{s(S-O)}$ vibrations are sensitive to cation complexation. These changes are similar to those reported in the case of protonated sulfates, but the spectral differences between cation-complexed sulfates and aqueous sulfate are much smaller. The cation complexation to sulfate polyhedra does not cause significant changes in the SOM (M = cation) bond distances (relative to the protonated complexes), and this is evident for several of the sulfate salts discussed by Hawthorne et al. (Chapter 1, this volume). Correspondingly, the $\nu_{s(S-OM)}$ vibrations of cation-complexed sulfates are close to those of uncomplexed SO_4^{2-} , and are at a higher wavenumber compared to that of protonated sulfates (Tables 5, 6). Fortunately, this makes it easier to distinguish the vibrational spectral features of protonated- and cation-complexed sulfates. However, the unequivocal identification of uncomplexed and cation-complexed sulfates is difficult.

Another problem with the identification of cationic complexes is related to the presence of several different types of cation-sulfate complexes and uncomplexed SO_4^{2-} in

Table 6. Vibrational modes of different aqueous cation sulfate complexes

<i>Cationic</i> <i>Complex</i> $\text{M}^n\text{SO}_4^{2-}$	ν_1	ν_2	ν_3	ν_4	<i>Source</i>
	(cm^{-1})				
Na^+	980 _R	450	1105	625	a
NH_4^+	985 _R	460	1120	620	a
Tl^+	985 _R	452	1100	625	a
Mg^{2+}	985 _R	455	1120	618	a
	982 _R				
	995 _R ^(S-O-Mg)	450	1115	616	b,c
	985 _{ir}				b,c
Ca^{2+}	978 _{ir}		1107		h
Fe^{2+}	981, 989 _R		1104, 1164		d
Cu^{2+}	980 _R	450	1100	620	a
	985 _R	455	1112	618	a
	990.8 _R	monoden			e
Zn^{2+}	1053 _R	bident.			a
	985 _R	451	1105	615	a
Cd^{2+}	983, 990 _R				f, g
	980 _{ir}		1042, 1126		i
Al^{3+}	985 _R	455	1100	625	a
Ga^{3+}	985 _R	475	1200	600	a
In^{3+}	980 _R	450	1105	620	a
	1000 _R ^(S-O-In)		1125		

The subscripts IR and R indicate that the data were collected using IR or Raman systems, respectively. Sources of data: a, Hester and Plane (1964); b, Frantz et al. (1994); c, Davis and Oliver (1973); d, Rudolph et al. (1997); e, Rudolph et al. (1999); f, Rudolph et al. (1994); g, Rudolph (1998a); h, Myneni et al. (1998a); i, Hug (1997).

aqueous solutions (Smith and Martell 1976). The nature of sulfate interactions with cations may also change with time, such as SO_4^{2-} in the cationic complexes changing between outer-sphere and inner-sphere complexes (Stumm and Morgan 1982, Stumm 1992). Solutions of sulfate-salts may contain a variety of these species, and the vibrational spectra of each of the component species may overlap each other and produce broad spectral features (if the species are closely related). It is very challenging to distinguish different cationic complexes based on their vibrational spectral features. If the cation-sulfate complexes are understood well, then information can be obtained on the water-exchange rates of cation- SO_4^{2-} complexes and the residence time of SO_4^{2-} in the inner- and outer-sphere complexes.

The spectral contributions of aqueous inner-sphere cation-sulfate complexes in Raman spectra are identified primarily from the asymmetry in the intense peak around 983 cm^{-1} , which corresponds to the $\nu_{\text{s(S-O)}}$ vibrations of uncomplexed or outer-spherically bound SO_4^{2-} (Davis and Oliver 1973, Rudolph and Irmer 1994, Rudolph et al. 1997,

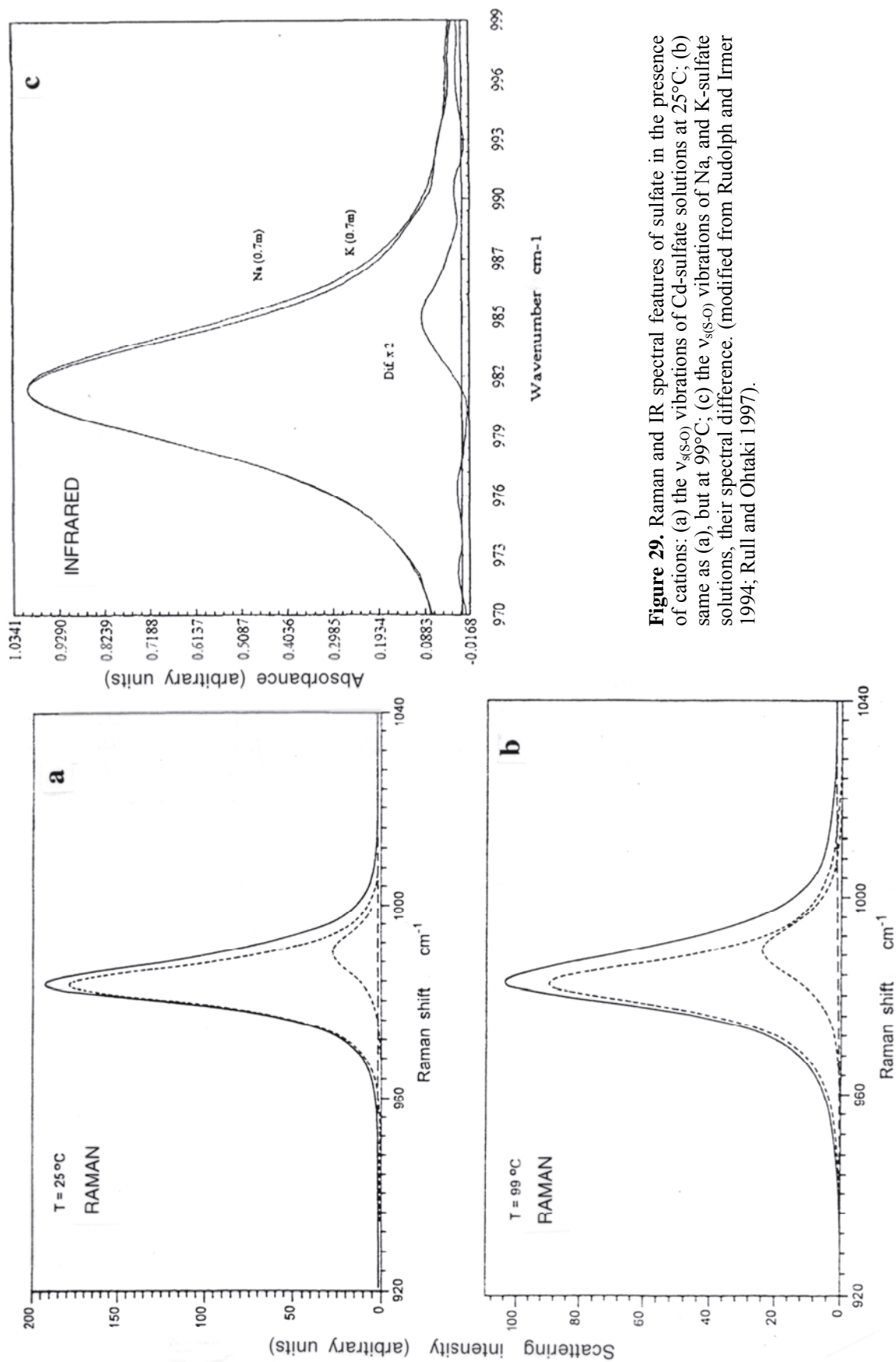


Figure 29. Raman and IR spectral features of sulfate in the presence of cations: (a) the $\nu_{s(s-o)}$ vibrations of Cd-sulfate solutions at 25°C; (b) same as (a), but at 99°C; (c) the $\nu_{s(s-o)}$ vibrations of Na, and K-sulfate solutions, their spectral difference. (modified from Rudolph and Inner 1994; Rull and Ohtaki 1997).

Rudolph 1998 a,b; and references therein) (Fig. 29). Rudolph (1998 a,b) observed that this peak asymmetry increases with increases in temperature and cation concentration (Figs. 29, 30). Rudolph and his coworkers used the increases in peak asymmetry to identify the nature of the sulfate-metal aqueous complex and its fraction in aqueous solutions (Fig. 30).

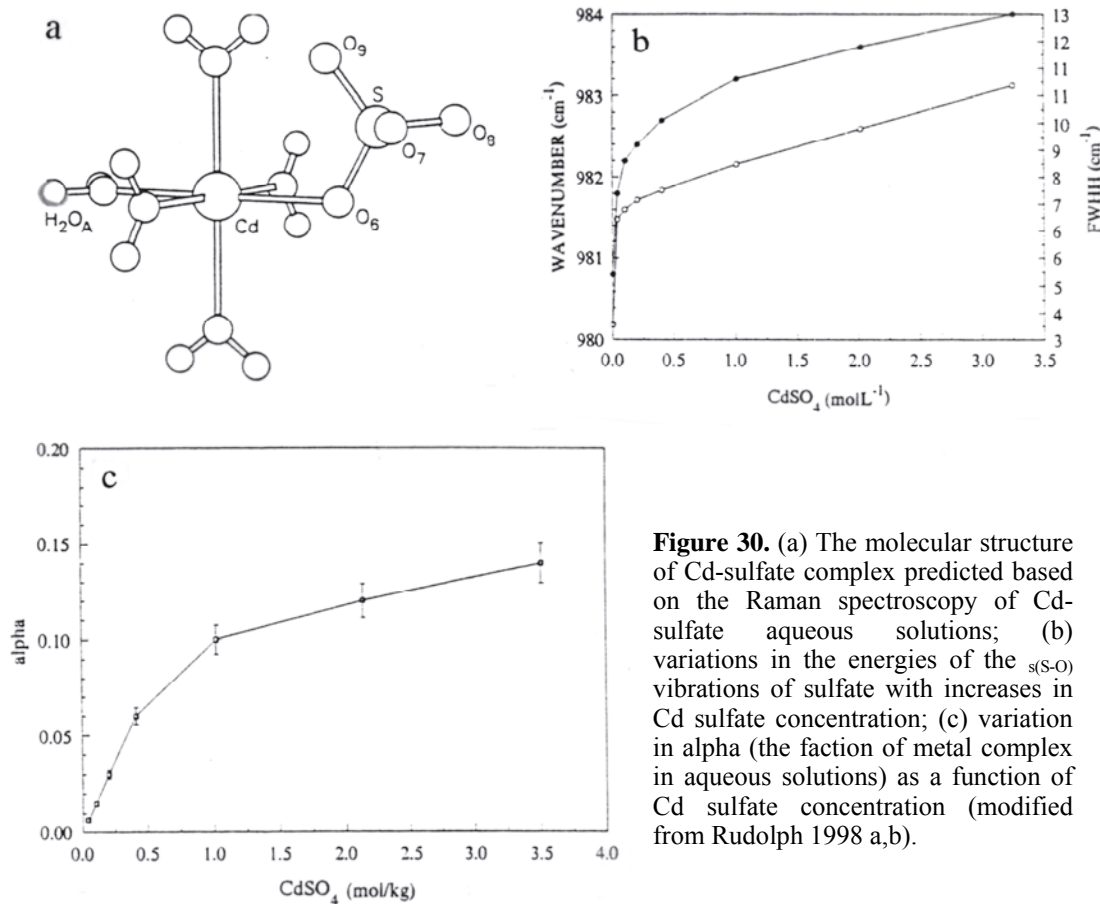


Figure 30. (a) The molecular structure of Cd-sulfate complex predicted based on the Raman spectroscopy of Cd-sulfate aqueous solutions; (b) variations in the energies of the $\nu_{s(S-O)}$ vibrations of sulfate with increases in Cd sulfate concentration; (c) variation in alpha (the fraction of metal complex in aqueous solutions) as a function of Cd sulfate concentration (modified from Rudolph 1998 a,b).

Although Rudolph and others have attributed the asymmetry in the Raman peak at 983 cm^{-1} to an inner-sphere cation-sulfate complex, this interpretation has been questioned (Nomura et al. 1980, Rull and Ohtaki 1997). One of the primary reasons is that the solutions of Cu^{2+} - and Al^{3+} -sulfate salts exhibit direct cation-sulfate inner-sphere complexes but have very a symmetric $\nu_{s(S-O)}$ band; moreover, the presence of inner-sphere complexes in these solutions is also supported by neutron and X-ray scattering studies. By contrast inner-sphere cation-sulfate complexes were not detected (by X-ray scattering) in Na^{+} - and K^{+} -salt solutions, but Na-sulfate solutions exhibit distinct asymmetry in the peak at 983 cm^{-1} (Fig. 29). Rull and Ohtaki (1997) suggested that the high asymmetry may be caused by solvation and ionic strength effects rather than by complex formation. Their results support the earlier findings of Nomura et al. (1980), who linked this high-energy asymmetry to the differences between the rotational correlation time of water molecules around cations and sulfate. Complementary spectroscopic information from other techniques is needed to understand the nature of aqueous complexes and the origin of the vibrational spectral features discussed above.

The studies by Rull and Ohtaki (1997) on Li^{+} , Na^{+} , K^{+} , Rb^{+} , and Cs^{+} sulfate solutions and solids suggest that the $\nu_{s(S-O)}$ vibrations shift linearly with changes in salt concentration (Fig. 31, Table 7). Whereas the slope of the lines plotted for $\nu_{s(S-O)}$ and salt

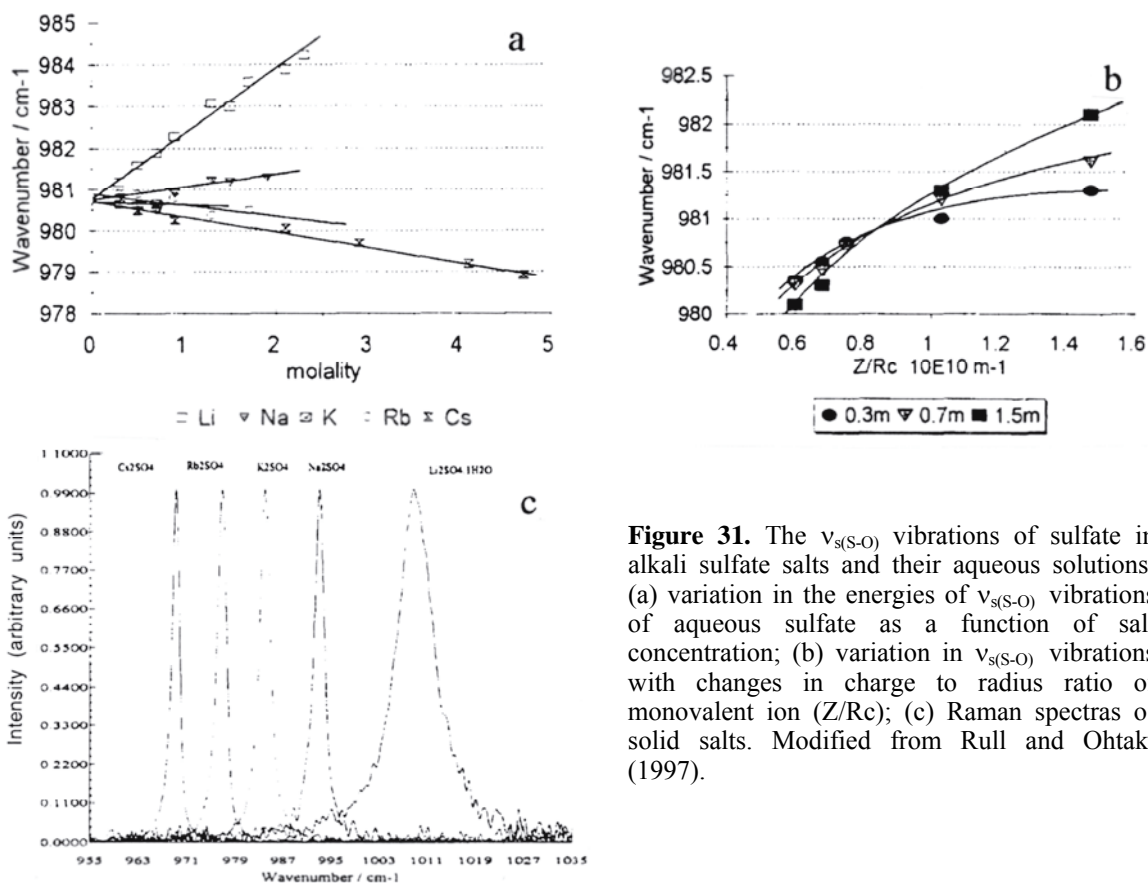


Figure 31. The $\nu_{s(S-O)}$ vibrations of sulfate in alkali sulfate salts and their aqueous solutions: (a) variation in the energies of $\nu_{s(S-O)}$ vibrations of aqueous sulfate as a function of salt concentration; (b) variation in $\nu_{s(S-O)}$ vibrations with changes in charge to radius ratio of monovalent ion (Z/Rc); (c) Raman spectra of solid salts. Modified from Rull and Ohtaki (1997).

Table 7. Raman spectra of alkali salt solutions at room temperature (modified from Rull and Ohtaki 1997). The energies of symmetric stretching S-O vibrations are shown.

Salt	Concentration (m)	ν_{mc} (cm ⁻¹)	ν_{av} (cm ⁻¹)
Li ₂ SO ₄	0.3	981.2	981.1
	0.7	981.6	981.7
	1.5	982.1	982.4
	2.0	982.6	983.4
Na ₂ SO ₄	0.3	980.8	980.8
	0.7	980.9	980.5
	1.5	981.3	981.6
	2.0	981.4	981.8
K ₂ SO ₄	0.3	980.8	980.8
	0.7	981.0	980.7
Rb ₂ SO ₄	0.3	980.9	980.8
	0.7	980.8	980.7
	1.5	980.6	980.6
Cs ₂ SO ₄	0.3	980.7	980.4
	0.7	980.6	980.3
	1.5	980.4	980.3
	2.0	980.1	979.7

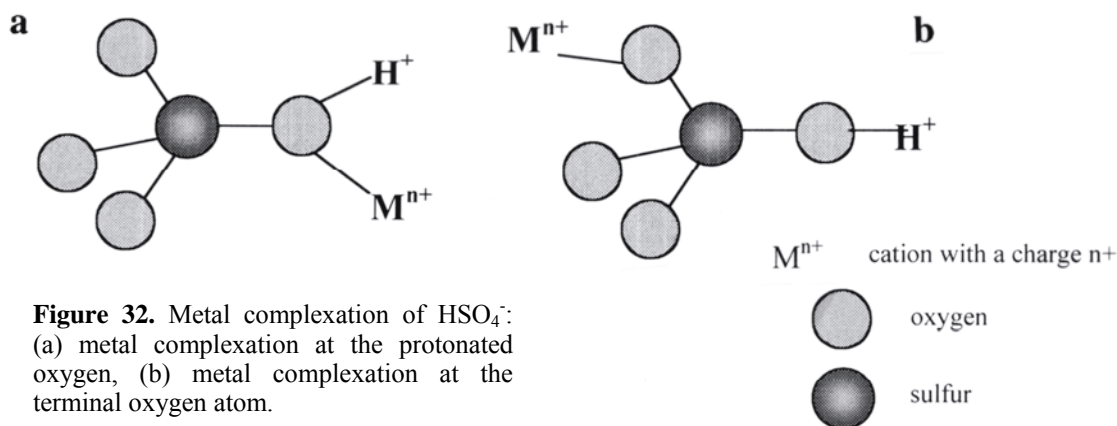


Figure 32. Metal complexation of HSO_4^- : (a) metal complexation at the protonated oxygen, (b) metal complexation at the terminal oxygen atom.

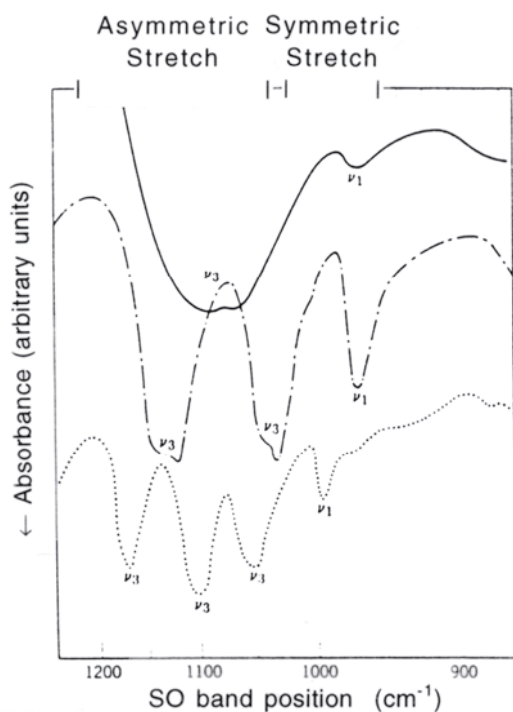


Figure 33. IR spectra of Co-sulfate complexes in different coordination environments (modified from Nakamoto 1986).

concentration showed a positive trend for Li^+ and Na^+ and a negative trend for Rb^+ and Cs^+ , the slope was relatively flat for K^+ . One of the notable features is that increases in aqueous salt concentration shifted the $\nu_{\text{s(S-O)}}$ vibrations of sulfate in the direction as the peaks corresponding to the respective solids (Fig. 31). This suggests that the cation directly influences the sulfate vibration, either through inner-sphere or outer-sphere complex formation. The significant difference between the energies of $\nu_{\text{s(S-O)}}$ vibrations in salts and their aqueous solutions indicate that the cation-anion interactions are relatively weak in aqueous solution. Another notable result from this study is that the $\nu_{\text{s(S-O)}}$ band shifts to lower energy with an increase in the cation size in concentrated solutions (Table 7, Fig. 31)

Cation complexation of HSO_4^- ions at low pH has not been investigated thoroughly. Raman studies of $\text{FeSO}_4\text{-H}_2\text{SO}_4$ systems by Rudolph et al. (1997) indicated that Fe^{2+} does not form inner-sphere complexes with the HSO_4^- ion in the temperature range of 25 to 303°C. The vibrational features of the HSO_4^- ion were not perturbed when Fe^{2+} ions were

added to the system. Similar results have been reported for arsenate complexes (Myneni et al. 1998b). Based on bond-valence calculations, Myneni et al. (1998a) predicted that the protonated As-OH/S-OH/P-OH groups of $\text{HAsO}_4^{2-}/\text{HSO}_4^-/\text{HPO}_4^{2-}$, respectively, cannot form cation complexes in the form shown in Figure 32. This is because of the excessive charge at the bonding O atoms (>2.0 , from bond-valence estimates, Brown and Altermatt 1985, Myneni et al. 1998a). However, cations can bind to free-terminal O atoms of HSO_4^- . As discussed above, protonation-induced perturbations in sulfate polyhedron have more effect than the complexation of sulfate to cations. For this reason, small changes in bond length that are associated with cation complexation of HSO_4^- may not be sufficient to cause changes in the vibrational modes of the HSO_4^- ion. Hence, an absence of changes in the HSO_4^- vibrational spectra does not completely rule out the existence of cation- HSO_4^- complexes. Thus, complexation of cations with HSO_4^- ions in solutions or at mineral-water interface should be approached with caution.

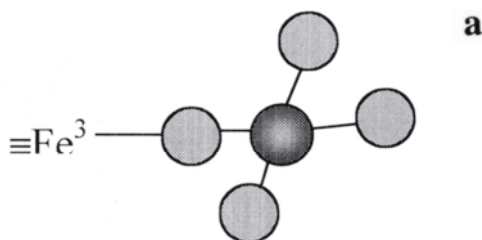
Whereas studies of Raman spectra have focused on the $\nu_{s(S-OM)}$ vibrations, infrared studies have focused on spectral splitting in the $\nu_{as(S-O)}$ vibrations. This spectral splitting in IR spectra was demonstrated by Nakamoto (1986) for Co-sulfate complexes, in which sulfate exhibits T_d , C_{3v} and C_{2v} symmetries (also refer to Hezel and Ross 1968). Based on the number of bands displayed by the $\nu_{as(S-O)}$ vibrations of these samples. Nakamoto assigned different symmetries for sulfate in these compounds (Fig. 33, Table 4). For example, tetrahedral symmetry was assigned to sulfate in $[Co(NH_3)_6(SO_4)] \cdot 5H_2O$ because the bands corresponding to $\nu_{as(S-O)}$ vibrations are not split, and $\nu_{s(S-O)}$ vibrations are weak.

However, the $\nu_{as(S-O)}$ vibrations shift to higher energy by 30-40 cm^{-1} relative to aqueous sulfate. Such shifts may be caused by strong H-bonding of sulfate with the ligands in the coordination shell. Similar results were also reported for sulfate interactions in ettringite, and on goethite surfaces (Persson and Lövgren 1996, Myneni et al. 1998a). For the molecules in C_{2v} symmetry, Nakamoto (1986) suggested that splitting in $\nu_{as(S-O)}$ vibrations is greater in a chelate than a bridging-bidentate complex. Several researchers have used the number of bands, and their relative energies, to identify the coordination complex of sulfate in unknown samples. Although such assignments are valid, some of the problems associated with such assignments are discussed in the next section.

Vibrational spectra of sulfate at the interfaces

For several years, soil chemists and geochemists have used the results of adsorption measurements to predict the nature of sulfate molecular interactions with different minerals to determine partition coefficients and to develop surface complexation theories (see Nordstrom and Bigham, this volume). As pointed out by Sposito (199), Brown (1990), and Brown et al. (1999), molecular information on the sorption complex cannot be deduced from macroscopic results alone. For the past two decades, vibrational spectroscopy (primarily IR spectroscopy) has been used extensively to study the nature of sulfate complexes on mineral surfaces, specifically on Fe oxides and oxyhydroxides. The differences in sample preparation, data collection, and interpretation by various authors have led to controversies on the nature of sulfate interactions with mineral surfaces. Although *in situ* studies have been conducted on selected mineral surfaces recently, several critical questions remain unanswered. These are related to: (1) the nature of sulfate coordination on mineral surfaces: i.e. inner- versus outer-sphere complexes, (2) variations in the nature of the surface complex with changes in solution chemistry, and (3) the types of all sorbed complexes and their concentrations. A summary of vibrational spectral information of sulfate interactions at mineral-water, metal-water, and other interfaces is presented below.

Sulfate coordination on Fe-oxide surfaces.



Many of the early vibrational

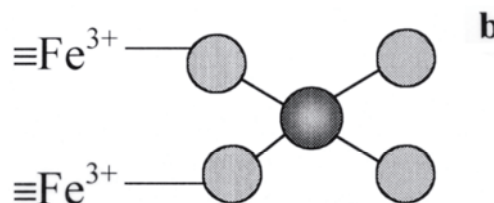
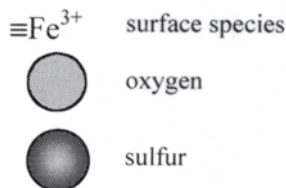


Figure 34. Coordination environment of inner-sphere sulfate on Fe-oxide surfaces: (a) monodentate complex; (b) bidentate complex.



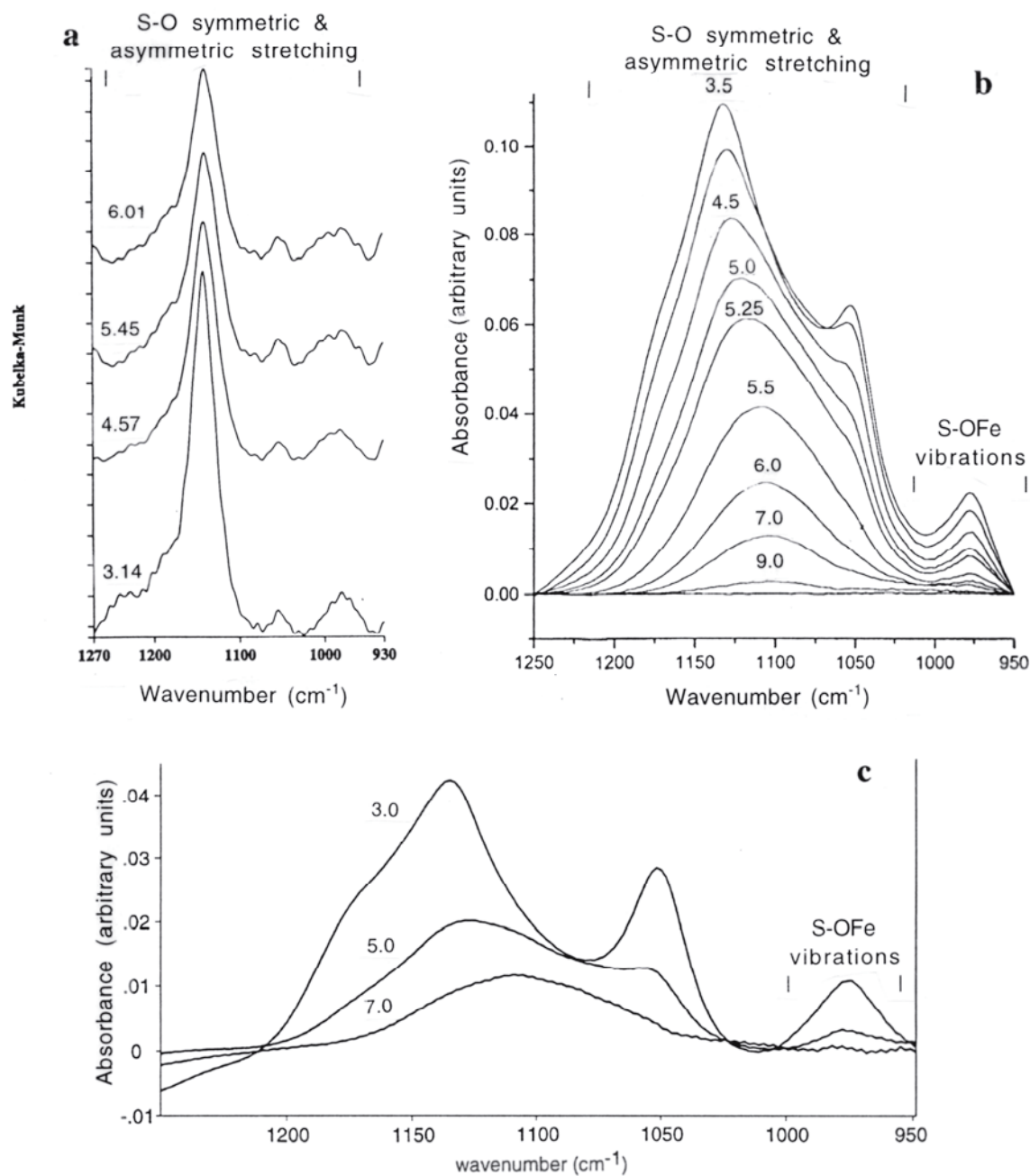


Figure 35. IR spectra of sulfate sorbed on goethite: (a) diffuse-reflectance spectroscopic investigation (modified from Persson and Lövgren 1996); (b) ATR-FTIR spectra (modified from Peak et al. 1999); (c) ATR-FTIR spectra (modified from Ostergren et al. 2000).

spectroscopy studies where done on pellets or powder samples (prepared by mixing with KBr) using transmission, diffuse-reflection and external-reflection sampling geometry (Parfitt and Smart 1978, Harrison and Berkheiser 1982, Turner and Kramer 1991, Watanabe et al. 1994, Persson and Lövgren 1996) (Figs. 35-37). These *ex situ* studies indicated that the asymmetric stretching vibrations of sulfate are split into more than two peaks, and it was therefore suggested that sulfate formed inner-sphere complexes on the surfaces of Fe oxides. All these researchers, with the exception of Persson and Lövgren (1996), suggested that the sorbed sulfate is in the C_{2v} symmetry and forms a bidentate bridging complex (Nakamoto 1986), as shown in Figure 34. A summary of these

observations are reported in Table 8.

Splitting in the asymmetric stretching frequencies was more pronounced when the samples were kept in vacuum or heated (Fig. 37). The observations of Li et al. (1993) on sulfate reactions with hematite surfaces at high temperatures are in support of these results. The XPS results of sulfate on hematite and maghemite also indicated that sulfate interacts with two chemically distinct sites (Watanabe et al. 1994; Fig. 21).

Table 8. Molecular chemistry of sulfate adsorbed on Fe oxide surfaces.

<i>Athos</i>	<i>Sapnfontin</i>	<i>Cats n Sifatnteactins with FeOxideSurfacs</i>
Sulfate on Goethite		
Parfitt & Russell (1977)	Changes in OH/OD vibrations; Sampling on dry systems	H ₂ SO ₄ reactions on goethite surface; Bidentate-bridging complexes.
Persson & Lövgren (1996)	Diffuse reflectance; 1145, 1045, 970 cm ⁻¹ ; 1220 for samples with pH<5	Sample pH>3.0, outer-sphere, HSO ₄ ⁻ on surfaces above the pK _a of H ₂ SO ₄ ^o .
Peak et al. (1999)	pH > 6.0: 1104, 975; pH < 6.0: 1170 (wk), 1133, 1055 976 cm ⁻¹ ; sampling on wet systems	Outer-sphere complex at pH > 6.0. Inner-sphere complex at pH < 6.0, monodentate, some of the sorbed complexes may be present as HSO ₄ ⁻
Ostergren et al. (2000)	pH = 3.0; ~1180, ~1140, ~1050 cm ⁻¹ ; pH = 5.0; 1123, 1057 cm ⁻¹ ; pH = 7.0; 1105 cm ⁻¹ ; sampling on wet systems	Outer-sphere complex at pH > 5.0. Inner-sphere complex at pH < 5.0, “combination of complexes with less than C _{3v} symmetry”.
Sulfate on Hematite		
Parfitt & Russell (1978)	Dry: 1200, 1128, 1040, 970 cm ⁻¹ Vacuum: 1245, 1131, 1030, 950 cm ⁻¹	Inner-sphere; bidentate bridging complex
Turner & Kramer (1991)	Dry: 1255, 1130, 1030, 950 cm ⁻¹ ; Interpretation is based on IR, and titration of released surface hydroxyls	Inner-sphere; mononuclear & bidentate bridging; mononuclear increases with a decrease in pH
Watanabe et al. (1994)	FTIR and XPS of sulfate on hematite & maghemite; data collection on dry samples	Inner-sphere, bidentate-bridging, sulfate binds at two non-equivalent sites
Hug (1997)	Wet: 1128, 1060, 978 cm ⁻¹ Dry: 1195, 1135, 1047, 970 cm ⁻¹	Sample pH 3-5 monodentate. Bidentate- bridging complex/HSO ₄ ⁻ in dried samples
Eggleston et al. (1998)	FTIR and STM Observations	FTIR: same as Hug (1997) STM: inner-sphere; spectrum of inner- & outer-sphere; bidentate or bisulfate sorption. Lifetimes are similar to that of aqueous FeSO ₄ ⁺ complexes.
Sulfate on Hematite		
Parfitt & Russell (1978)	Amorphous Fe-oxides, data collection on dry samples	Bidentate-bridging
Harrison & Berkheiser (1982)	On Freshly prepared Fe-oxides Dry: 1170, 1125, 1050, 970 cm ⁻¹ Vacuum: 1215, 1125, 1040, 970 cm ⁻¹	Bidentate-bridging

Persson and Lövgren (1996) used diffuse-reflectance spectroscopy to examine the nature of sulfate complexes on goethite surfaces. On the basis of the absence of splitting in sulfate $\nu_{\text{as(S-O)}}$ vibrations, they proposed that sulfate formed outer-sphere complexes with goethite surfaces in the pH range of 3-8 (Fig. 35). They also suggested that goethite surfaces stabilize outer-sphere HSO_4^- on solid surfaces in the acidic pH range (for stability of goethite, see Bigham and Nordstrom, Chapter 7, this volume). It should be noted that their spectral features show that the $\nu_{\text{as(S-O)}}$ vibrations of sulfate on goethite are shifted to wavenumbers approximately 40 cm^{-1} above those of aqueous sulfate (Fig. 35). Small peaks are also found at low and high energies of this band. Recent *in situ* ATR-FTIR spectroscopic studies have shown the same spectral features, which suggests that the structure of sorbed sulfate deviates from T_d symmetry even above pH 5.0 (Peak et al. 1999, Ostergren et al. 2000). Although Persson and Lövgren (1996) suggested outer-sphere complexation for sulfate sorbed on goethite, in this author's opinion, sulfate sorbed on goethite is not similar to aqueous sulfate. It is in a different configuration such as a H-bonded complex, as indicated by the shift in the $\nu_{\text{as(S-O)}}$ vibrations (Myneni et al. 2000b). Hug (1997) and Peak et al. (1999) criticized the sample-preparation and data-collection techniques used by previous researchers in studying the nature of sulfate complexes at Fe-oxide-water interfaces. Conversion of wet samples into powder and pellets for IR investigations may alter the sulfate coordination in solids. Drying and diluting the samples with KBr may also cause problems with the water content of the samples. Examination of samples in vacuum condition was also questioned because of the potential loss of structural water and corresponding changes in sulfate coordination (Fig. 37), as has been shown in recent studies (Hug, 1997, Peak et al. 1999).

Hug (1997) conducted a detailed examination of the shifts in vibrational spectra of

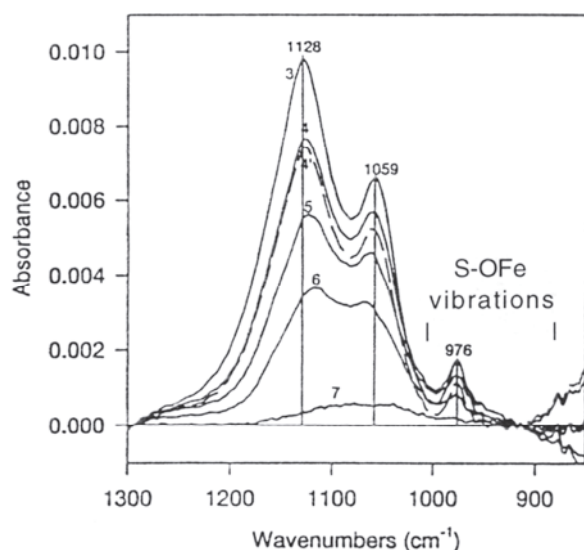


Figure 36. ATR-FTIR spectra of sulfate sorbed on hematite. The pH conditions are shown on each of the spectra (modified from Hug 1997).

aqueous Fe^{3+} -complexed sulfate and HSO_4^- and suggested that sulfate forms inner-sphere, monodentate complexes on hematite surfaces in the pH range of 3-5. The proposed structure for sulfate on hematite surfaces is shown in Figure 34a. Although the work of Hug (1997) was on hematite, these results are not consistent with the model of tetrahedral outer-sphere sulfate complexes on goethite surfaces as proposed by Persson and Lövgren (1996). The ATR-FTIR spectra of Hug (1997) showed that the $\nu_{\text{as(S-O)}}$ vibrations of sulfate exhibit two bands, which are indicative of C_{3v} symmetry and not C_{2v} as reported in earlier studies (Fig. 36). The spectra of air-dried samples showed a third peak around 1200 cm^{-1} ; based on the number of peaks Hug (1997) suggested that the symmetry of sorbed sulfate in these samples may be C_{2v} and that sulfate may be in the

form of either bidentate-bridging complex or HSO_4^- (Fig. 36). Recent studies by Eggleston et al. (1998), Peak et al. (1999), and Ostergren et al. (2000) are in support of Hug's interpretations. However, Peak et al. (1999) and Ostergren et al. (2000) reported that sulfate forms outer-sphere complexes on goethite surfaces at relatively high pH and forms an inner-sphere complex at pH values less than 5.0 (Fig. 35). By analyzing the scanning tunneling microscope scan frequency, Eggleston et al. (1998) concluded that the lifetimes of sulfate complexes on hematite surfaces vary from several tens to hundreds of milliseconds. Based on such a large variation in the lifetimes, it was suggested that characterization of adsorbates into inner- and outer-sphere complexes on the basis of macroscopic studies may be an oversimplification.

A summary of these studies indicates that: (1) sulfate coordination on mineral surfaces is affected by sample drying, and studies on dry samples may not represent the coordination chemistry of sulfate in wet conditions, (2) sulfate forms inner-sphere complexes on hematite at $\text{pH} < 5$, and (3) sulfate on goethite forms inner-sphere complexes in the acidic pH range, and outer-sphere complexes at near-neutral pH.

Some critical issues have not been considered by previous researchers in evaluating the nature of sulfate complexes on surfaces. These issues are: (1) all of the previous *in situ* studies had shown similar spectral features with small variations in energies of the $\nu_{\text{as(S-O)}}$ vibrations, and the pH at which splitting $\nu_{\text{as(S-O)}}$ vibrations begins is different for goethite and hematite (Hug 1997, Peak et al. 1999); (2) the energy of the $\nu_{\text{s(S-O)}}$ mode, which is a strong indicator of the presence of bisulfate complexes, was not considered in the previous studies (Myneni et al. 1998b); (3) the simultaneous occurrence of more than one type of surface complex, such as inner- and outer-sphere complexes, was not considered; (4) spectral comparisons of Fe-sulfate salts, in which sulfate forms bidentate-bridging complexes with ferric iron, has not been conducted; and (5) occurrence of Fe sulfate precipitates (such as jarosite) in samples of acidic pH also has not been considered. Such detailed comparisons or theoretical studies will help in identifying the nature of sulfate surface complexes.

Sulfate coordination on Cr-oxide surfaces. The insoluble Cr^{3+} oxides and oxyhydroxides are common in Cr-rich soil profiles, waste environments, and radioactive-waste-disposal sites. Cr-bearing steel is used extensively in industry because of its high resistance to corrosion. Recent IR studies of sulfate interactions with Cr-hydroxide colloids indicate that sulfate geometry changes after its adsorption on Cr-oxide surfaces (Degenhardt and McQuillan 1999). However, the $\nu_{\text{as(S-O)}}$ vibrations at $\sim 1100 \text{ cm}^{-1}$ did not exhibit distinct splitting, and the $\nu_{\text{s(S-O)}}$ vibrations appeared at 982 cm^{-1} for sulfate sorbed on Cr-oxide surfaces in the pH range of 3.2 to 8.0 (Fig. 38). Sulfate sorption at $\text{pH} < 4.0$ showed a distinct shoulder to the peak corresponding to the $\nu_{\text{as(S-O)}}$ vibrations, and the peak maximum shifted from 1099 to 1116 cm^{-1} . Drying of sulfate-sorbed samples enhanced the peak asymmetry and showed two distinct features with increases in drying time (Fig. 38). Based on these changes Degenhardt and McQuillan (1999) concluded that sulfate forms an outer-sphere complex on Cr-hydroxide surfaces in wet conditions, and that the peak asymmetry is caused by electrostatic interactions between the surface and interfacial sulfate. For dry samples, the formation of inner-sphere monodentate sulfate complexes was proposed. The formation of weak outer-sphere complexes of sulfate on Cr oxides may contribute to pitting on stainless-steel surfaces.

Sulfate coordination on metal surfaces. Sulfate interactions on metal surfaces (e.g. Cu, Ag, Pt, Au) of different orientation have been examined by several researchers because of the importance of these metals in electrochemistry and batteries (for a review, see Bockris and Khan 1993). Several investigations have used Raman and IR spectroscopy for exploring sulfate reaction with metal surfaces at different pH values.

The results indicate that some metal surfaces interact with sulfate through three of its oxygen atoms, and do not interact with bisulfate, e.g. on Au(111) and Cu surfaces (Brown and Hope 1995, Ataka and Osawa 1998). In other cases, e.g. Pt(111) (Faguy et al. 1996), the sulfate- H_3O^+ ion pair interacts with metal surfaces, and the nature of the surface

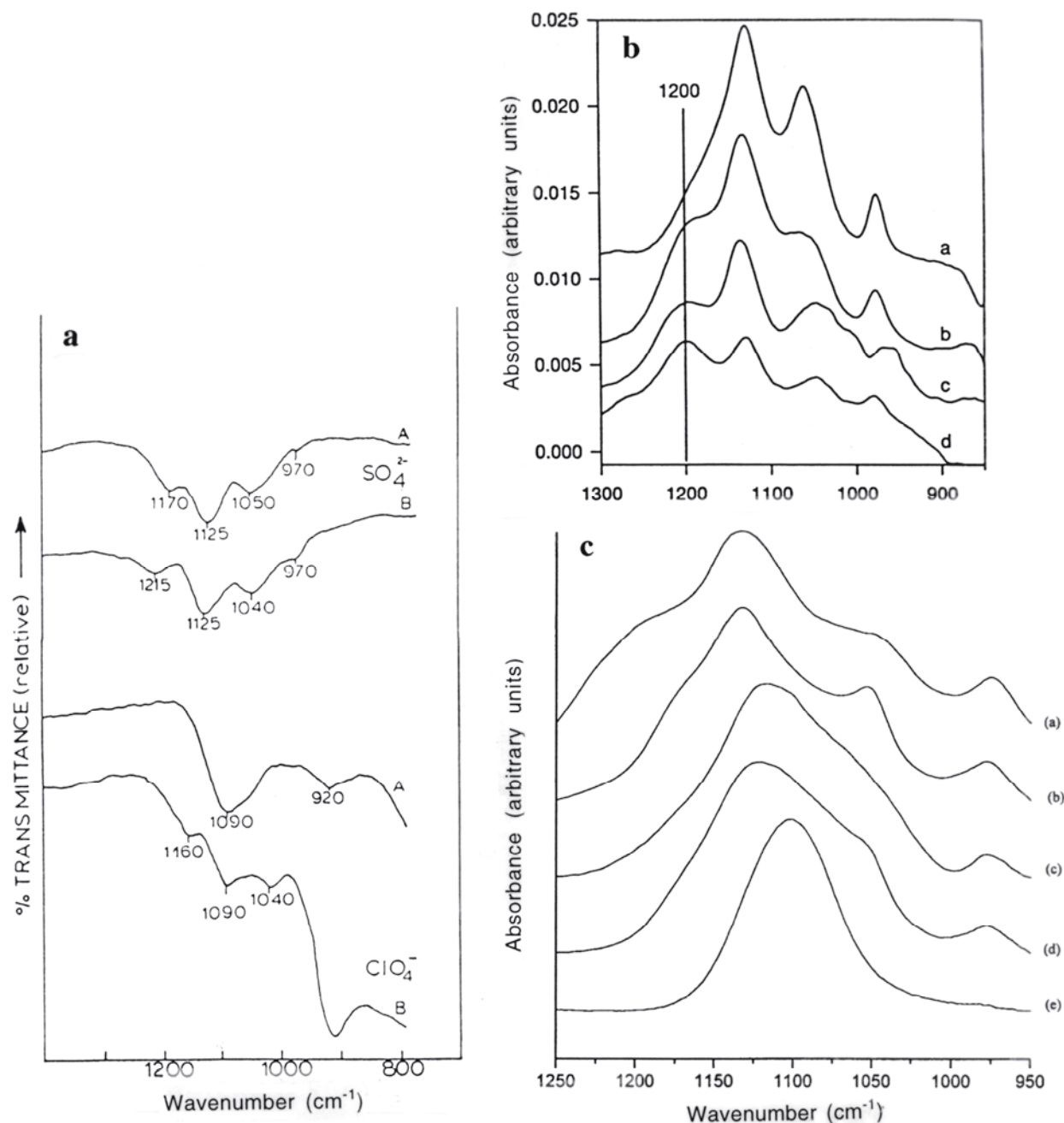


Figure 37. IR spectra of sulfate sorbed on Fe oxides, showing the influence of drying of sample on the vibrational spectra of sulfate: (a) sulfate and perchlorate sorbed on freshly prepared Fe-oxhydroxides; spectra were collected using the transmission of IR beam through the dried samples; A: air dried samples, and B: evacuated samples (modified from Harrison and Berkheiser 1982); (b) FTIR spectra of sulfate sorbed on hematite. a: sulfate-reacted hematite in wet conditions (ATR-FTIR spectra), b: the same sample without water and after drying in air, c: after drying with N_2 , and d: after reaction with water and 0.1 M HCl (modified from Hug 1997); (c) FTIR spectra of sulfate. a: schwertmannite in diffuse reflectance mode (air-dried), b: sulfate sorbed on goethite, pH 3.5, c: schwertmannite in ATR mode (wet), d: sulfate sorbed on goethite, pH 5.0, and e: 100mM aqueous sulfate (modified from Peak et al. 1999).

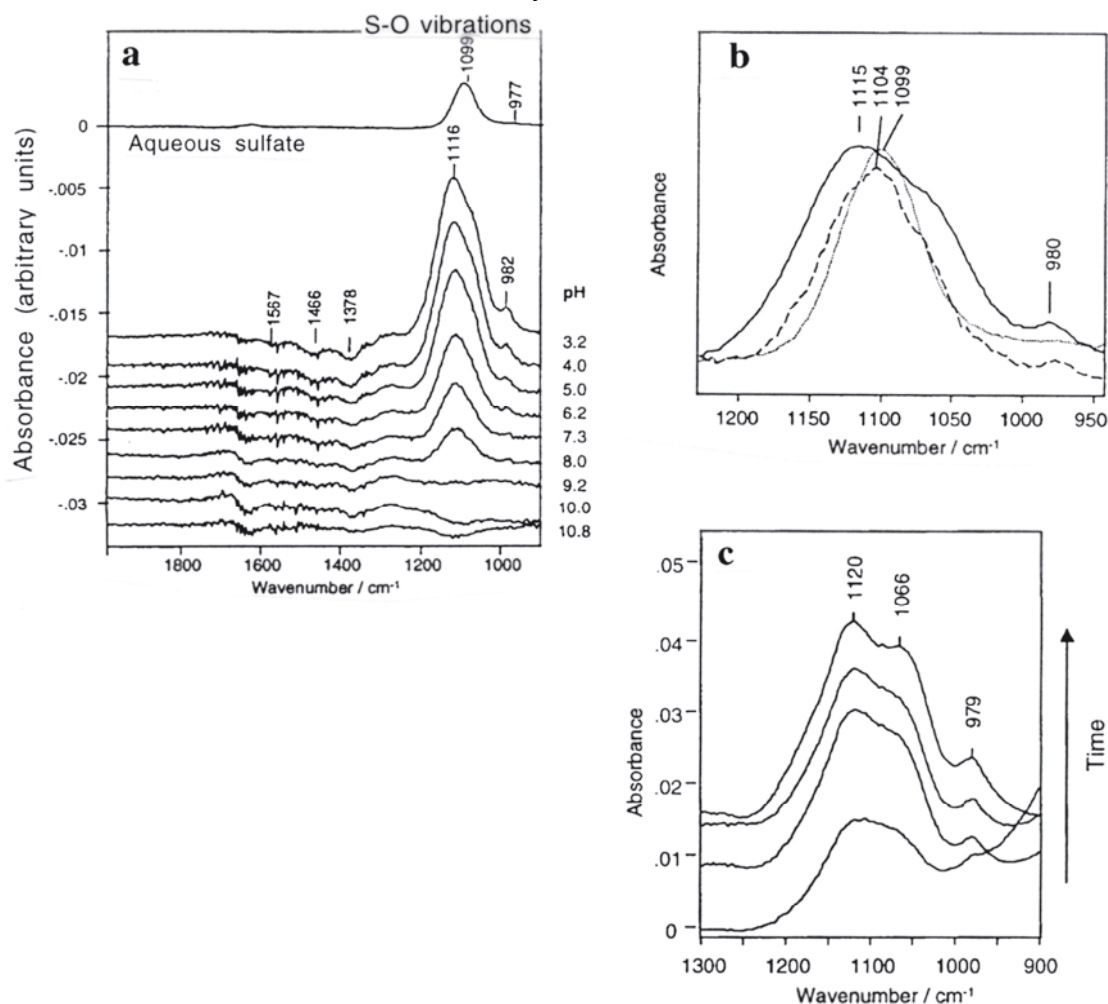


Figure 38. FTIR spectra of sulfate sorbed on Cr oxide: (a) ATR-FTIR spectra of sulfate sorbed on Cr oxide at different pH values; (b) spectral difference between aqueous sulfate (...), and Cr oxide reacted with sulfate at low (----) and high (—) coverages; (c) spectra showing the influence of sample drying on changes in the environment of sulfate coordination. The lowermost spectrum is that of wet sample, and the upper curves are for progressively dried samples. (modified from Degenhardt and McQuillan 1999).

complex is intermediate between sulfate and bisulfate with the H_3O^+ species stabilizing the surface complex. Although these systems are not directly relevant to geological environments, important information on the vibrational modes of sulfate and their changes associated with metal-surface interactions are useful for interpreting samples of geochemical importance.

Spectromicroscopy of sulfates

Although specific spectromicroscopy investigations have not been conducted on sulfate in minerals or other geological materials, such studies are possible. Using laboratory-based micro-IR facilities, a spatial resolution of a few tens of micrometers can be achieved. The synchrotron-based IR spectromicroscopy facilities at the ALS and NSLS can offer a spatial resolution of less than $5\ \mu\text{m}$ because of the higher brightness of the synchrotron beams relative to the beams from the glowbar-source in commercially available IR instruments. In addition, surface-sensitive micro-FTIR studies can be conducted using grazing incidence and ATR objectives. The laboratory-based micro-Raman facilities can offer a resolution of less than one micrometer. Melendres (1998) provides more information on these techniques.

COMPLEMENTARY SPECTROSCOPIC METHODS

Scattering methods

Scattering or diffraction of neutrons, X-rays, and electrons by materials has been widely used for studying the structure of sulfate in various forms. The application of X-ray diffraction in studying crystalline sulfates is discussed by Hawthorne et al. (Chapter 1, this volume). X-ray and neutron scattering methods are also used in studying the coordination chemistry of sulfates in aqueous solutions. These methods are most applicable for concentrated systems, and they have provided important information on the solvation of sulfate in aqueous solutions. Because a neutron beam is scattered by the atomic nuclei, and X-rays are scattered by the electron cloud around nuclei, these methods offer complementary information (Bats 1976, Bacon 1977). In X-ray scattering, the scattering power of atoms is a function of momentum transfer and the atomic number of the elements (electron density), whereas neutron scattering is dependent on the composition of the nucleus of the atom (isotope). The applications of these methods to the study of sulfate solutions summarized by Magini et al. (1988), Ohtaki and Radnai (1993) and references therein.

The previous studies have indicated that it is difficult to evaluate the solvation of anions because the distance of $\text{SO}_4^{2-}\text{H}_2\text{O}_w$ overlaps strongly with that of $\text{H}_2\text{O}_w\text{H}_2\text{O}$ (O_w : oxygen of water molecules; subscript 'w' is used to distinguish the O of water molecules from that of sulfate). For metalsulfate inner-sphere complexes, this problem is even worse because SM ($M = \text{cation}$) distances overlap with those of SO_w . The average SO_w distances in concentrated NH_4^+ , Mg^{2+} , Mn^{2+} , Ni^{2+} , Zn^{2+} , Cd^{2+} , Cr^{3+} , and In^{3+} sulfate solutions is approximately 3.80 nm (range: 3.70-3.93 nm; Ohtaki and Radnai 1993), and the hydration number (number of water molecules in the first solvation shell) is about 8.0 (range: 7-12). Correlations among these bond distances and the cation size, charge, and coordination number are not observed (Ohtake and Radnai 1993).

Infrared emission spectroscopy

Compared to other infrared spectroscopy methods described above, infrared emission spectroscopy has been used infrequently, but it can offer information on *in situ* dehydration and high-temperature phase transitions in minerals. The IR emission spectra are collected by heating the samples to different temperatures, and the IR radiation emitted by the samples is analyzed by IR detectors. Vassallo and Finnie (1992) examined a few sulfate minerals using this technique, and the results indicated that the emission and transmission spectra of these minerals are similar.

Optical spectroscopy

Optical spectroscopy [ultraviolet-visible (UV-VIS) spectroscopy, sum-frequency generation spectroscopy] is not widely used in probing the molecular chemistry of sulfates in geological materials. The studies of Gaft et al. (1985) indicate that anhydrite, barite, celestite, and anglesite are luminescent and exhibit a distinct band around 360 nm. The luminescence was suggested to originate from the crystal structure rather than from physical impurities. However, when luminescent centers (e.g. Mg^{2+} , Gd^{3+}) were added to the crystal in the form of impurities, the luminescence disappeared. Several Fe^{3+} sulfates and other sulfate salts have also been investigated using the optical properties of cations that associate with sulfates (e.g. Rossman 1975, 1976; Wan et al. 1978, and references therein). Similarly, probe molecules have been used to examine the molecular orientation and bonding interactions of organosulfates on clean metal or oxide substrates (Huang et al. 2000, and references therein). Although they give indirect information on sulfate interactions with optically active centers in crystals, these methods do not provide direct

information on sulfate coordination and bonding. Sum-frequency generation spectroscopy has been used recently to investigate the nature of water and organic molecules at the interfaces (Miranda and Shen 1999, and references therein). In the past, the non-availability of lasers of low energies has limited the applications of this technique to studies on sulfates. But the availability of tunable lasers and the broad-band synchrotron beamlines optimized for infrared spectroscopy should assist in these studies in the near future.

SUMMARY AND FUTURE DIRECTION

- (1) Vibrational spectroscopy has been used extensively in studying crystalline sulfates, but very few studies have compared the spectral features of sulfate with its coordination environment. Many previous studies have cited the energies of vibrations without proper band assignments. This has severely limited the identification of sulfate molecular chemistry in unknown crystalline samples and aqueous solutions, and at interfaces. Theoretical studies combined with a detailed investigation of different crystalline sulfates would be useful for researchers in several disciplines.
- (2) The number of synchrotron X-ray spectroscopic studies on sulfates and other related S compounds is increasing. The lack of synchrotron beamlines optimized for studying sulfate and other S compounds in geological materials and beamline oversubscription have limited the use of these methods. Availability of suitable multi-element solid-state detectors together with the beamline facilities will make the XANES and EXAFS studies possible on a variety of extremely dilute geological samples. These techniques could provide new and complementary information on the molecular chemistry of sulfates at low concentrations.
- (3) Sulfate reactions on the mineral-water interfaces of Fe oxides and certain hydrous Fe oxides in aqueous solutions have been well explored using X-ray and vibrational spectroscopic methods. Such information on other minerals and airwater interfaces is absent. Molecular information on such systems would be useful to predict the nature of redox transformations, trace-element mobility in soil and sediment systems, and gas transfer at the interfaces.
- (4) Theoretic studies of sulfate in different coordination environments and calculated electronic and vibrational spectra are useful in interpreting the spectral features of unknown samples. Such studies have been conducted for only a few selected species. Theoretical XANES calculations at the S-absorption edge have not yet been performed.
- (5) Because of inconsistencies regarding the nature of aqueous complexation on sulfate in the published literature, detailed studies are necessary to evaluate the nature of complex formation between sulfate and cations and their stability in aqueous solutions. Such information is essential in evaluating the relevant thermodynamic information data that are used extensively in geochemistry.

ACKNOWLEDGMENTS

I thank Dr. C.N. Alpers for putting together this volume and providing valuable comments at every state in preparation of this manuscript, and Dr. P.H. Ribbe for helping with the preparation of the final document. Reviews by Drs. G.R. Rossman, P. O'Day and J.L. Jambor helped improve the presentation and technical discussions. I thank Ms. R. Reina and Ms. Jyothi for editorial comments, and Ms. Mayuri for helping with the figures. This work is supported by funding from the Basics Energy Sciences, DOE (Geosciences) and a faculty start-up grant from Princeton University.

REFERENCES

- Anders SA, Padmore HA, Duarte RM, Renner T, Stammler T, Scholl A, Scheifein MR, Stöhr J (1999) Photoemission electron microscope for the study of magnetic materials. *Rev Sci Instruments* 70: 3973-3981
- Ataka K, Osawa M (1998) In situ infrared study of water-sulfate coadsorption on gold(111) in sulfuric acid solutions. *Langmuir* 14:951-959
- Bacon GE (1977) *Neutron Scattering in Chemistry*. Butterworths, Boston
- Baker AD, Betteridge D (1972) *Photoelectron Spectroscopy: Chemical and Analytical Aspects*. Pergamon Press, New York
- Bats JW (1976) *Diffraction and Chemical Bonding*. Twente University of Technology, Enschede
- Benison KC, Goldstein RH, Wopenka B, Burruss RC, Pasteris JD (1998) Extremely acid Permian lakes and ground waters in North America. *Nature* 392:911-914
- Bergström P, Lindgren J, Kristiansson O (1991) An IR study of ClO_4^- , NO_3^- , I^- , Br^- , Cl^- , and SO_4^{2-} anions in aqueous solution. *J Phys Chem* 95:8575-8580
- Bhagavantam S, Venkataraidu T (1969) *Theory of Groups and Its Application to Physical Problems*. Academic Press, New York, 279 p
- Bockris JOM, Khan SUM (1993) *Surface Electrochemistry: A Molecular Level Approach*. Plenum Press, New York
- Briggs D (1977) *Handbook of X-ray and Ultraviolet Photoelectron Spectroscopy*. Heyden, London
- Briggs D, Seah MP (1983) *Practical Surface Analysis by Auger and X-ray Photoelectron Spectroscopy*. Wiley, New York
- Brooker MH, Tremaine PR (1992) Raman studies of hydration of hydroxy complexes and the effect on standard partial molar heat capacities. *Geochim Cosmochim Acta* 56:2573-2577
- Brookins DG (1988) *Eh-pH Diagrams for Geochemistry*. Springer-Verlag, New York
- Brown GE Jr (1990) Spectroscopic studies of chemisorption reaction mechanisms at oxide-water interfaces. *In Mineral-Water Interface Geochemistry*. Hochella MF, White AF (eds) *Rev Mineral* 23:309-363
- Brown GE Jr, Calas G, Waychunas GA, Petiau J (1988) X-ray absorption spectroscopy and its applications in mineralogy and geochemistry. *In Spectroscopic Methods in Mineralogy and Geology*. Hawthorne FC (ed) *Rev Mineral* 18:431-512
- Brown GE Jr, Henrich VE, Casey WH, Clark DL, Eggleston C, Felmy A, Goodman DW, Gratzel M, Maciel H, McCarthy MI, Neelson KH, Sverjensky DA, Toney MF, Zachara JM (1999) Metal oxide surfaces and their interactions with aqueous solutions and microbial organisms. *Chem Rev* 99:77-174
- Brown GM, Hope GA (1995) *In situ* spectroscopic evidence for the adsorption of SO_4^{2-} ions at a copper electrode in sulfuric acid solution. *J Electroanal Chem* 382: 179-182
- Brown GS, Doniach S (1980) The principles of X-ray absorption spectroscopy. *In Synchrotron Radiation Research*. Winick H, Doniach S (eds) Plenum Press, New York
- Brown ID, Altermatt D (1985) Bond-valence parameters obtained from a systematic analysis of the inorganic crystal structure database. *Acta Crystallogr B* 41:244-247
- Calas, Manceau A (1986) X-ray absorption spectroscopy of geologic materials. *J Physique* 47:813-818
- Cejka J (1999) Infrared spectroscopy and thermal analysis of uranyl minerals. *In Uranium: Mineralogy, Geochemistry and the Environment*. Burns PC, Finch R (eds) *Rev Mineral* 38:521-622
- Colthup NB, Daly LH, Wiberly SE (1990) *Introduction to infrared and Raman spectroscopy*. Academic Press, Boston
- Cotton FA (1971) *Chemical Applications of Group Theory*. Wiley Eastern Ltd., New York.
- Cruikshank DWJ, Robinson EA (1966) Bonding in orthophosphates and orthosulfates. *Spectrochim Acta* 22:555-563
- Davis AR, Oliver BG. (1973) Raman spectroscopic evidence for contact ion pairing in aqueous magnesium sulfate solutions. *J Phys Chem* 77:1315-1316
- Degenhardt J, McQuillan AI (1999) *In situ* ATR-FTIR spectroscopic study of adsorption of perchlorate, sulfate, and thiosulfate ions onto chromium(III) oxide hydroxide thin films. *Langmuir* 15:4595-4602
- Eggleston CM, Hug S, Stumm W, Sulzberger B, Afonso MDS (1998) Surface complexation of sulfate by hematite surfaces: FTIR and STM observations. *Geochim Cosmochim Acta* 62:585-593
- Fadini A, Schnepel F-M (1989) *Vibrational Spectroscopy*. Ellis Horwood Ltd., New York
- Faguy PW, Marinkovic NS, Adzic RR (1996) An *in situ* infrared study on the affect of pH on anion adsorption at Pt(111) electrodes from acid sulfate solutions. *Langmuir* 12:243-247
- Farmer VC (1974) *The Infrared Spectra of Minerals*. Mineralogical Society, London
- Fateley WG, McDevitt NT, Bentley FF (1971) Infrared and Raman selection rules for lattice vibrations: The correlation method. *Appl Spectr* 25: 155-173

- Fernandez-Ramos A, Cabaleiro-Lago E, Hermida-Ramon JM, Martinez-Nunez E, Pena-Gallego A (2000) DFT conformational study of cysteine in gas phase and aqueous solution. *J Mol Structure (Theochem)* 498: 191-200
- Ferraro JR (1982) *The Sadder Infrared Spectra Handbook of Minerals and Clays*. Sadder, Philadelphia
- Ferraro JR, Nakamoto K (1994) *Introduction to Raman Spectroscopy*. Academic Press, Boston
- Frank P, Hedman B, Carlson RMK, Tyson TA, Roe AL, and Hodgson KO (1987) A large reservoir of sulfate and sulfonate residues within plasma cells from *Ascidia ceratodes*, revealed by X-ray absorption near-edge structure spectroscopy. *Biochemistry* 26:4975-4979
- Frank P, Hedman B, Carlson RMK, Hodgson KO (1994) Interaction of vanadium and sulfate in blood cells from the tunicate *Ascidia ceratodes*: Observations using X-ray absorption edge structure and EPR spectroscopies. *Inorg Chem* 33:3794-3803
- Frank P, Hedman B, Hodgson KO (1999) Sulfur allocation and vanadium-sulfate interactions in whole blood cells from the tunicate *Ascidia ceratodes*, investigated using X-ray absorption spectroscopy. *Inorg Chem* 38:260-270
- Franz JD, Dubessy J, Mysen BO (1994) Ion-pairing in aqueous $MgSO_4$ solutions along an isochore to 500°C and 11 kbar using Raman spectroscopy in conjunction with the diamond anvil cell. *Chem Geol* 116:181-188
- Gadsden JA (1975) *Infrared spectra of minerals and related inorganic compounds*. Butterworths, London
- Gaft ML, Bershov LV, Krasnaya AR, Yaskoko VY (1985) Luminescence centers in anhydrite, barite, celestite and their synthetic analogs. *Phys Chem Minerals* 11:255-260
- George GN, Gorbaty ML (1989) Sulfur K-edge X-ray absorption spectroscopy of petroleum asphaltenes and model compounds. *J Am Chem Soc* 111:3182-3186
- George GN, Gorbaty ML, Kelemen SR, Sansone M (1991) Direct determination and quantification of sulfur forms in coals from the Argonne Premium Sample Program. *Energy & Fuels* 5:93-97
- George WO, Steele D (ed) (1995) *Computing Applications in Molecular Spectroscopy*. The Royal Society of Chemistry, Cambridge, UK
- Gillette PC, Lando JB, Koenig JL (1982) Band shape analysis of Fourier transform infrared spectra. *Appl Spectr* 36:401-404
- Gorbaty ML, George GN, Kelemen SR (1990) Direct determination and quantification of sulfur forms in heavy petroleum and coals: 2. The sulfur K edge X-ray absorption spectroscopy approach. *Fuel* 69:945-950
- Harrick NJ (1987) *Internal Reflection Spectroscopy*. Harrick Scientific Corporation, New York
- Harrison J.B, Berkheiser V (1982) Anion interactions with freshly prepared hydrous iron oxides. *Clays and Clay Minerals* 30:97-102
- Hasenoehrl EJ, Griffiths PR (1993) Classification of condensed-phase infrared spectra by structures using principal component analysis. *Appl Spectrosc* 47:643-653
- Hawthorne FC (00) (1988) *Spectroscopic Methods in Mineralogy and Geology*. Reviews in Mineralogy, Vol 18
- Hawthorne FC, Waychunas GA (1988) Spectrum fitting methods. *In Spectroscopic Methods in Mineralogy and Geology*. Hawthorne FC (ed) *Rev Mineral* 18:63-96
- Hester RE, Plane RA (1964) A Raman spectrophotometric comparison of interionic association in aqueous solutions of metal nitrates, sulfates and perchlorates. *Inorg Chem* 3:769-770
- Hezel A, Ross SD (1968) Forbidden transitions in the infra-red spectra of tetrahedral anions: IV. The vibrational spectra ($4000-400\text{ cm}^{-1}$) of some cobalt(III) sulphato- and phosphato-complexes. *Spectrochim Acta* 24A:985-992
- Hibble SJ, Walton RI, Feavioir MR, Smith AD (1999) Sulfur-sulfur bonding in the amorphous sulfides WS₃, WS₅, and Re₂S₇ from sulfur K-edge EXAFS studies. *J Chem Soc, Dalton Trans* 2877-2883
- Hitchcock AP, Horseley JA, Stohr J (1986) Inner-shell excitation of thiophene and thiolane: Gas, solid, and monolayer states. *J Chem Phys* 85:4835-4848
- Hochella MF Jr (1988) Auger electron and photoelectron spectroscopies. *In Spectroscopic Methods in Mineralogy and Geology*. Hawthorne FC (ed) *Rev Mineral* 18:573-630
- Hochella MF Jr, White AF (eds) (1990) *Mineral-Water Interface Geochemistry*. Reviews in Mineralogy Vol 23, Mineral Soc Am, Washington, DC
- Horn AB and Sully KJ (1999) ATR-FTIR spectroscopic studies of the formation of sulfuric acid and sulfuric acid monohydrate films. *Phys Chem Chem Phys* 1:3801-3806
- Huang MH, Dunn BS, Zink JI (2000) *In situ* luminescence probing of the chemical and structural changes during formation of dip-coated lamellar phase dodecyl sulfate sol-gel thin films. *J Am Chem Soc* 122:3739-3745
- Huffman OP, Mitra S, Huggins FE, Shah NS, Vaidya N, Lu F (1991) Quantitative analysis of all major forms of sulfur in coal by X-ray absorption fine structure spectroscopy. *Energy & Fuels* 5:574-581

- Huffman GP, Shah NS, Huggins FE, Stock LM, Chatterjee K, Kilbane JJ, Chou M, Buchanan DH (1995) Sulfur speciation of desulfurized coals by XANES spectroscopy. *Fuel* 74:549-555
- Hug S (1997) In situ Fourier transform infrared measurements of sulfate adsorption on hematite in aqueous solutions. *J Colloid Interface Sci* 188:415-422
- Jirsak T, Rodriguez JA, Hrbek J (1999) Chemistry of SO₂ on Mo(110), MoO₂/Mo(110) and Cs/Mo(110) surfaces: effects of O and Cs on the formation of SO₃ and SO₄ species. *Surface Science* 426:319-335
- Johnston CL (1990) Fourier transform infrared and Raman spectroscopy. *In Instrumental surface analysis of geologic materials*, Perry DL (ed), VCH Publishers, New York.
- Karr C (1975) Infrared and Raman spectroscopy of lunar and terrestrial minerals. Academic Press, New York
- Kasrai M, Bancroft GM, Brunner RW, Jonasson RG, Brown JR, Tan KH, Feg X (1994) Sulfur speciation in bitumens and asphaltenes by X-ray absorption fine structure spectroscopy. *Geochim Cosmochim Acta* 58:2865-2872
- Kasrai M, Lennard WN, Brunner RW, Bancroft GM, Bardwell JA, Tan KH (1996) Sampling depth of total electron and fluorescence measurements in Si L- and K-edge absorption spectroscopy. *Appl Surf Sci* 99:303-312
- Koningsberger DC, Prins R (eds) (1988) X-ray Absorption: Principles, Applications, Techniques of EXAFS, SEXAFS, and XANES. John Wiley & Sons, New York
- Lee PA, Pendry JB (1975) Theory of extended X-ray absorption fine structure. *Phys Rev B* 11:2795-2811
- Li RS, Chen JF, Yang H, Zhang WY, Wei Q, Jin MZ, Zheng YG (1993) Interaction between ammonium sulfate-iron oxide shown by ESR and Mössbauer spectroscopy. *Catal Lett* 18:317-322
- Li D, Bancroft GM, Kasrai M, Fleet ME, Yang BX, Feng XH, Tan K, Peng M (1994) Sulfur K-, and L-edge X-ray absorption spectroscopy of sphalerite, chalcopyrite and stannite. *Phys Chem Minerals* 20:489-499
- Li D, Bancroft GM, Kasrai M, Fleet ME, Feng XH, Tan K (1995) S K- and L-edge X-ray absorption spectroscopy of metal sulfides and sulfates: Applications in mineralogy and geochemistry. *Can Mineral* 33:949-960
- Lindsay CG, Gibbs GV (1988) A molecular orbital study of bonding in sulfate molecules: Implications for sulfate crystal structures. *Phys Chem Minerals* 15:260-270
- Lytle FW, Sayers DE, Stern EA (1982) The history and modern practice of EXAFS spectroscopy. *In Advances in X-ray Spectroscopy*. Bonnelle C, Mande C (eds) Pergamon, Oxford
- Lytle FW, Greigor RB, Sandstrom DR, Marques EC, Wong J., Spiro CL, Huffman GP, and Huggins FE (1984) Measurement of soft X-ray absorption spectra with a fluorescent ion chamber detector. *Nucl Instrum Meth* 226:542-548
- Maddams WF (1980) The scope and limitations of curve fitting. *Appl Spectr* 34:245-267
- Magini M, Licheri G, Paschina G, Piccaluga G, Pinna G (1988) X-ray Diffraction of Ions in Aqueous Solutions: Hydration and Complex Formation. CRC Press, New York
- Masion A, Rose J, Bottero JY, Tchoubar D, Elmerich P (1997) Nucleation and growth mechanisms of iron oxyhydroxides in the presence of PO₄ ions: 3. Speciation of Fe by small angle X-ray scattering. *Langmuir* 13:3882-3885
- Max JJ, Menichelli C, Chapados C (2000) Infrared titration of aqueous sulfuric acid. *J Phys Chem* 104:2845-2858
- McMillan PF, Hess AC (1988) Symmetry, group theory and quantum mechanics. *In Spectroscopic Methods in Mineralogy and Geology*. Hawthorne FC (ed) *Rev Mineral* 18:11-61
- McMillan PF, Hofmeister AM (1988) Infrared and Raman spectroscopy. *In Spectroscopic Methods in Mineralogy and Geology*. Hawthorne FC (ed) *Rev Mineral* 18:99-159
- Melendras CA (1998) Synchrotron infrared spectromicroscopy of electrode surfaces and interfaces. *Synch Rad News* 11:39-46
- Miranda PB, Shen Y-R (1999) Liquid interfaces: A study by sum-frequency vibrational spectroscopy. *J Phys Chem B* 103:3292-3307
- Mochizuki Y, Agren H, Pettersson LGM, Carravetta V (1999) A theoretical study of sulphur K-shell X-ray absorption of cysteine. *Chem Phys Lett* 309:241-248
- Moenke H (1962) *Mineralspektren I*. Akademie-Verlag, Berlin
- Morra MJ, Fendorf SE, Brown PD (1997) Speciation of sulfur in humic and fulvic acids using X-ray absorption near-edge structure (XANES) spectroscopy. *Geochim Cosmochim Acta* 61:683-688
- Myer-Ilse W, Warwick T, Attwood D (2000) X-ray Microscopy. *Proc 6th Intern Conf*, Berkeley, California (1999), American Institute of Physics, New York
- Myneni SCB, Martinez GA (1999) P and S functional group chemistry of humic substances. *SSRL Activity Reports-1998*, 364-368
- Myneni SCB, Traina SJ, Waychunas GA, Logan TJ (1998a) Vibrational spectroscopy of functional group chemistry and arsenate coordination in ettringite. *Geochim Cosmochim Acta* 62: 3499-3514

- Myneni SCB, Traina SJ, Waychunas GA, Logan TJ (1998b) Experimental and theoretical vibrational spectroscopic evaluation of arsenate coordination in aqueous solutions, solids and at mineral-water interfaces. *Geochim Cosmochim Acta* 62:3285-3300
- Myneni SCB, Luo Y, Naslund LA, Ojamae L, Ogasawara H, Pelmenchikov A, Vaterlain P, Heske C, Pettersson LGM, Nilsson A (2000a) Spectroscopic evidence for unique hydrogen bonding structures in water (unpublished data, submitted for publication)
- Myneni SCB, Waychunas GA, Traina SJ, Brown GA (2000b) Molecular structure of sulfate on Fe-oxide surfaces (unpublished data, manuscript to be submitted)
- Nakamoto K. (1986) *Infrared and Raman Spectra of Inorganic and Coordination Compounds*. John Wiley & Sons, New York
- Natoli CR (1995) XAS, MCD, and PED interpreted in the unifying framework of effective MS theory. *Physica B* 208 & 209:5-10
- Nefedov VI and Formichev VA (1968) *J Struct Chem* 9:107 (cited by Sekiyama et al. 1986).
- Nomura H, Koda S, Miyahara Y (1980) Water and metal cations in biological systems. *In Proc Symp 1978*, Pullman B, Yuji K (eds) Scientific Societies Press, Tokyo.
- Ogletree DF (2000) Photoelectron spectroscopy at ten torr. Abstracts of the 8th Intern Conf on Electron Spectroscopy and Structure (conference proceedings will appear in a special issue of *J Electron Spectr Relat Phenom*), Berkeley, CA
- Ohtaki H, Radnai T (1993) Structure and dynamics of hydrated ions. *Chem Rev* 93: 1157-1204
- Okude N, Nagoshi M, Noro H, Baba Y, Yamamoto H, Sasaki TA (1999) P and S K-edge XANES of transition-metal phosphates and sulfates. *J Electron Spectrosc Relat Phenom* 101-103:607-610.
- Ostergren JD, Brown GE, Parks GA, Persson P (2000) Inorganic ligand effects on Pb(II) sorption on goethite (-FeOOH). *J Colloid Interface Sci* 225:483-493
- Parfitt RL, Smart RStC (1978) Mechanism of sulfate adsorption on iron oxides. *Soil Soc Am J* 42:48-50
- Pauling L (1960) *The Nature of the Chemical Bond*. Cornell Univ Press, Ithaca, NY
- Peak D, Ford RG, Sparks DL (1999) An *in situ* ATR-FTIR investigation of sulfate bonding mechanisms on goethite. *J Colloid Interface Sci* 218:289-299
- Pechar F (1988) *Infrared Reflection Spectra of Selected Minerals*. Academia, Praha
- Perkins JH, Hasenoehrl EJ, Griffiths PR (1991) *Anal Chem* 63:1738
- Perry DL (ed) (1990) *Instrumental Surface Analysis of Geologic Materials*. VCH Publishers, New York
- Persson P, Lövgren L (1996) Potential and spectroscopic studies of sulfate complexation at the goethite-water interface. *Geochim Cosmochim Acta* 60:2789-2799
- Persson P, Nilsson N, Sjöberg S (1996) Structure and bonding of orthophosphate ions at the iron oxide-aqueous interface. *J Colloid Interface Sci* 177:263-275
- Pickering IJ, Prince RC, Divers T, George GN (1998) Sulfur K-edge X-ray absorption spectroscopy for determining the chemical speciation of sulfur in biological systems. *FEBS Letters* 441: 11-14
- Pingitore NE, Meitzner G, Love KM (1995) Identification of sulfate in natural carbonates by X-ray absorption spectroscopy. *Geochim Cosmochim Acta* 59:2477-2483
- Rehr JJ, Booth CH, Bridges F, Zabinsky SI (1994) X-ray absorption fine structure in embedded atoms. *Phys Rev* 49:12347-12350
- Rehr J and Albers RC (2000) Theoretical approaches to X-ray absorption fine structure. *Rev Mod Phys* 72:621-654.
- Ressler T, Wong J, Roos J, Smith I (2000) Quantitative speciation of Mn-bearing particles emitted from autos burning (methylcyclopentadienyl) manganese tricarbonyl-added gasolines using XANES spectroscopy. *Environ Sci Technol* 34:950-958
- Rodriguez JA, Jirsak T, Chaturvedi S, Kuhn M (1999a) Reaction of SO₂ with ZnO (000-1)-O and ZnO powders: Photoemission and XANES studies on the formation of SO₃ and SO₄. *Surf Sci* 442:400-412
- Rodriguez JA, Chaturvedi S, Hanson J, Brito JL (1999b) Reaction of H₂ and H₂S with CoMoO₄ and NiMoO₄: TPR, XANES, time-resolved XRD, and molecular orbital studies. *J Phys Chem B* 103: 770-781
- Rompel A, Cinco RM, Latimer MJ, McDermott AB, Guiles RD, Quintanilha A, Krauss RM, Sauer K, Yachandra V, Klein MP (1998) Sulfur K-edge X-ray absorption spectroscopy: A spectroscopic tool to examine the redox state of S-containing metabolites in vivo. *Proc Natl Acad Sci* 95:6122-6127
- Rose Williams K, Hedman B, Hodgson KO, Solomon EI (1997) Ligand K-edge X-ray absorption spectroscopic studies: metal-ligand covalency in transition metal thiolates. *Inorg Chim Acta* 263:315321
- Ross SD (1974) Phosphates and other oxy-anions of group V. *In The Infrared Spectra of Minerals*. Farmer VC (ed) Mineral Soc London, p 383-422
- Rossman GR (1975) Spectroscopic and magnetic studies of ferric iron hydroxy sulfates: Intensification of color in ferric iron clusters bridged by a single hydroxide ion. *Am Mineral* 60:698-704
- Rossman GR (1976) Spectroscopic and magnetic properties of ferric iron hydroxy sulfates: The series Fe(OH)SO₄·nH₂O and jarosites. *Am Mineral* 61:398-404

- Rudolph WW (1994) Raman and infrared spectroscopic investigation of contact ion pair formation in aqueous cadmium sulfate solutions. *J Soln Chem* 23:663-683
- Rudolph WW (1996) Structure and dissociation of the hydrogen sulfate ion in aqueous solution over a broad temperature range: A Raman study. *Z Phys Chemie* 194:73-95
- Rudolph WW (1998a) Hydration and water-ligand replacement in aqueous cadmium (II) sulfate solution. A Raman and infrared study. *J Chem Soc Faraday Trans* 94:489-499
- Rudolph WW (1998b) A Raman spectroscopic study of hydration and water-ligand replacement reaction in aqueous cadmium(II) sulfate solution: Inner-sphere and outer-sphere complexes. *Ber Bunsenges Phys Chem* 102:183-196
- Rudolph WW, Inner G (1994) Raman and infrared spectroscopic investigation of contact ion pair formation in aqueous cadmium sulfate solutions. *J Soln Chem* 23:663-683
- Rudolph WW, Brooker Tremaine PR (1997) Raman spectroscopic investigation of aqueous FeSO₄ in neutral and acidic solutions from 25°C to 303°C: Inner-and outer-sphere complexes. *J Soln Chem* 26:757-777
- Rudolph WW, Brooker MH, Tremaine PR (1999) Raman spectroscopy of aqueous ZnSO₄ solutions under hydrothermal conditions: Solubility, hydrolysis, and sulfate ion pairing. *J Soln Chem* 28:621-630
- Rull F, Ohtaki H (1997) Raman spectral studies on ionic interaction in aqueous alkali sulfate solutions. *Spectrochim Acta* 53A:643-653
- Salisbury JW (1992) Infrared (2.1-25mm) spectra of minerals. Johns Hopkins University Press, Baltimore
- Sarret G, Connan J, Kasrai M, Bancroft GM, Charrie-Duhaut A, Lemoine S, Adam P, Albrecht P, Eybert-Berard L (1999) Chemical forms of sulfur in geological and archaeological asphaltenes from the Middle East, France, and Spain determined by sulfur K-, and L-edge X-ray absorption near-edge structure spectroscopy. *Geochim Cosmochim Acta* 63:3767-3779
- Sayers DE (1975) Extended X-ray absorption fine structure technique: III. Determination of physical parameters. *Phys Rev B* 11: 4836-4845
- Sayers DE, Lytle FW, Stern EA (1970) Point scattering theory of X-ray K absorption fine structure. *Advan X-ray Anal* 13:248-271
- Schulze DG, Stucki JW, Bertsch PM (eds) (1999) Synchrotron X-ray Methods in Clay Science. The Clay Minerals Society, Boulder, Colorado
- Seeger DM, Korzeniewski C, Kowalchuk W (1991) Evaluation of vibrational force fields derived by using semiempirical and *ab initio* methods. *J Phys Chem* 95:6871-6879
- Sekiyama H, Kosugi N, Kuroda H, Ohta T (1986) Sulfur K-edge absorption spectra of Na₂SO₄, Na₂SO₃, Na₂S₂O₃, and Na₂S₂O_x (x = 5-8). *Bull Chem Soc Jpn* 59:575-579
- Shadle SE, Hedman B, Hodgson KO, Solomon EI (1995) Ligand K-edge X-ray absorption spectroscopic studies: Metal-ligand covalency in a series of transition metal tetrachlorides. *J Am Chem Soc* 117: 2259-2272
- Siedl V, Knop O (1969) Infrared studies of water in crystalline hydrates: Gypsum, CaSO₄·2H₂O. *Can J Chem* 47:1362-1368
- Smith R, Martell AE (1976) Critical Stability Constants: Vol 4. Inorganic Complexes. Plenum Press, New York
- Spiro CL, Wong J, Lytle FW, Greigor RB, Maylotte DH, Lamson SH (1984) X-ray absorption spectroscopic investigation of sulfur sites in coal: Organic sulfur identification. *Science* 226:48-50
- Sposito G (1989) The Chemistry of Soils. Oxford University Press, New York
- Sposito G (1990) Molecular models of ion adsorption on mineral surfaces. *In Mineral-Water Interface Geochemistry*. Hochella MF, White AF (eds) *Rev Mineral* 23:261-279
- Sposito G (1994) Chemical Equilibria and Kinetics in Soils. Oxford University Press, New York
- Stern EA (1974) Theory of extended X-ray absorption fine structure. *Phys Rev B* 10:3027-3037
- Stevenson FJ (1994) Humus Chemistry. John Wiley, New York
- Stewart JJP (1989a) Optimization of parameters for semiempirical methods: 1. Method, *J Comp Chem* 10:209-220
- Stewart JJP (1989b) Optimization of parameters for semiempirical methods: II. Applications, *J Comp Chem* 10:221-264
- Stöhr J (1984) Surface crystallography by means of SEXAFS and NEXAFS. *In Chemistry and Physics of Solid Surfaces*. Vanselow VR, Howe R (eds) Springer-Verlag, New York
- Stöhr J (1992) NEXAFS Spectroscopy. Springer-Verlag, Berlin
- Stumm W (1992) Chemistry of the Solid-Water Interface. John Wiley, New York
- Stumm W, Morgan II (1982) Aquatic Chemistry, 2nd edn. Wiley Interscience, New York
- Suetaka W (1995) Surface infrared and Raman spectroscopy: Methods and applications. Plenum Press, New York
- Taesler I, Olovsson I (1969) Hydrogen bond studies. XXXVII. The crystal structure of sulfuric acid dihydrate (H₃O⁺)₂SO₄²⁻ *J Chem Phys* 51:4213-4219

- Teo BK (1986) EXAFS: Basic principles and data analysis. Inorganic chemistry concepts 9. Springer-Verlag, Berlin
- Tossell JA, Vaughan DJ (1992) Theoretical Geochemistry: Application of Quantum Mechanics in the Earth and Mineral Sciences. Oxford University Press, New York
- Turner LJ, Kramer JR (1991) Sulfate ion binding on goethite and hematite. *Soil Sci* 152:226-230
- Tyson TA, Roe AL, Frank P, Hodgson KO, Hedman B (1989) Polarized experimental and theoretical K-edge X-ray absorption studies of SO_4^{2-} , ClO_3^- , $\text{S}_2\text{O}_3^{2-}$, and $\text{S}_2\text{O}_6^{2-}$. *Phys Rev B*. 39:6305-6315
- Urban MW (1993) Vibrational spectroscopy of molecules and macromolecules on surfaces. John Wiley & Sons, New York
- Vairavamurthy A (1998) Using X-ray absorption to probe sulfur oxidation states in complex molecules. *Spectrochim Acta* 54A:2009-2017
- Vairavamurthy A, Manowitz B, Zhou W, Jeon Y (1994) Determination of hydrogen sulfide oxidation products by sulfur K-edge X-ray absorption near edge structure spectroscopy. *In Environmental Geochemistry of Sulfide Oxidation*. Alpers CN, Blowes DW (eds) Am Chem Soc Symp Series 550:412-430, Am Chem Soc, Washington, DC
- Vairavamurthy A, Maletic D, Wang S, Manowitz B, Eglinton T, Lyons T (1997) Characterization of sulfur-containing functional groups in sedimentary humic substances by X-ray absorption near-edge structure spectroscopy. *Energy Fuels* 11:546-553
- Vassallo AM, Finnie KS (1992) Infrared emission spectroscopy of some sulfate minerals. *Appl Spectrosc* 46:1477-1482
- Vaughan D (1986) X-ray Data Booklet. Lawrence Berkeley Laboratory Publication, Berkeley, CA
- Vaughan DJ, Patrick RAD (eds) (1995) Mineral Surfaces. Mineralogical Society Series, Chapman & Hall, New York
- Waldo GS, Carlson RMK, Moldowan JM, Peters KE, Penner-Hahn JE (1991) Sulfur speciation in heavy petroleum: Information from X-ray absorption near-edge structure. *Geochim Cosmochim Acta* 55:801-814
- Wan C, Ghose S, Rossman GR (1978) Guildite, a layer structure with a ferric hydroxy-sulfate chain and its optical absorption spectra. *Am Mineral* 63:478-483
- Warburton DR, Purdie D, Muryn CA, Prakash NS, Prabhakaran K, Thronton G, Patrick RAD, Norman D (1992) Transferability of phase shifts for extended X-ray absorption fine structure studies of metal sulfides and sulfur on nickel surfaces. *Phys Rev B* 45:12043-12049
- Warneck P (1988) Chemistry of the Natural Atmosphere. Academic Press, San Diego
- Warwick T, Ade H, Cerasari S, Denlinger J, Franck K, Gracia A, Hayakawa A, Hitchcock A, Kikuma J, Kortright J, Meigs G, Moronne M, Myneni SCB, Rightor E, Rotenberg E, Seal S, Shin H-J, Steele R, Tyliczszak T, Tonner B (1998) A scanning transmission X-ray microscope for materials science spectromicroscopy at the Advanced Light Source. *Rev Sci Instr* 69:2964-2973
- Wasserman SR, Allen PG, Shuh DK, Bucher JJ (1999) EXAFS and principal component analysis: A new shell game. *J Sync Radiation* 6:284-284
- Watanabe H, Gutleben CD, Seto J (1994) Sulfate ions on the surface of maghemite and hematite. *Solid State Ionics* 69:29-35
- Waychunas GA, Brown GE (1984) Applications of EXAFS and XANES spectroscopy to problems in mineralogy and geochemistry. *In EXAFS and Near-Edge Structure: III*. Hodgson KO et al. (eds) Springer-Verlag, New York
- Waychunas GA, Brown GE Jr., Apter MJ (1986) X-ray K-edge absorption spectra of Fe minerals and model compounds: II. EXAFS. *Phys Chem Minerals* 13:31-47
- Wu ZY, Ouvrard G, Moreau P, Natoli CR (1997) Interpretation of pre-edge features in the Ti and S K-edge X-ray absorption near edge spectra in the layered disulphides TiS_2 , and TaS_2 . *Phys Rev B* 55: 9508-9513
- Xia K, Weesner F, Bleam W, Bloom PR, Skyllberg UL, Helmke PA (1998) XANES studies of oxidation states of sulfur in aquatic and soil humic substances. *Soil Sci Soc Am J* 62: 1240-1246